THEORETICAL AND EXPERIMENTAL STUDY OF HYDROGEN PRODUCTION THROUGH PEM WATER ELECTROLYSIS

MYAT YU SOE

A THESIS REPORT SUBMITTED IN PARTIAL FULFILLMENT
OF THE REQUIREMENTS FOR THE DEGREE OF
MASTER OF ENGINEERING IN AUTOMOTIVE ENGINEERING
SCHOOL OF ENGINEERING
KING MONGKUT'S INSTITUTE OF TECHNOLOGY LADKRABANG
2024

KMITL-2024-EN-M-277-291

THESIS TITLE	Theoretical and experimental study of hydrogen production through PEM water electrolysis
STUDENT NAME	Ms. Myat Yu Soe
STUDENT ID	64601178
DEGREE	Master of Engineering
PROGRAM	Automotive and Advanced Transportation Engineering
YEAR	2024
ADVISOR	Assoc. Prof. Dr. Jarruwat Charoensuk
CO-ADVISOR	Prof. Dr. Katsunori Hanamura

ABSTRACT

The majority of the world's transportation systems are controlled by combustion vehicles that have a greater impact than the other types of vehicles on air pollution and emissions greenhouse gas. When the electricity power is generated from renewable resources, switching from convectional fuel cars to electric vehicles can reduce greenhouse gas emissions. In the energy transition, electric vehicles are anticipated to become even more significant. There are many challenges to manage the electric power consumption rate. This thesis mainly dealt with hydrogen production in which solar energy is used to drive the proton exchange membrane electrolysis. The electrochemical fundamentals of hydrogen production and the impact of temperature and flow rate of water on the efficiency are investigated. Together with the atmospheric hydrogen storage tank, the electrical equivalent circuit for the proton exchange membrane electrolyzer was created and put into practice using MATLAB/Simulink. To compare the simulated and experimental results, the voltage (2 volt) and current (1 ampere) were supplied in a similar way. The electrolysis is tested under the temperature of 20 – 60 degrees Celsius and water feeding flow rate of 20 – 60 ml/min. The reversible potential relating to the temperature is calculated with the MathCAD software. Results from the simulation and experiment agree, it is observed. Moreover, the onset potential is decreased with the temperature increased and the efficiency decreases for the higher currents.

Keywords: Solar energy, Hydrogen, Proton exchange membrane (PEM) electrolysis, Efficiency, Temperature, MATLAB/Simulink

ACKNOWLEDGEMENT

I would like to sincerely thank everyone who helped me to complete my thesis and for their assistance. This thesis would not have been feasible without their priceless help, direction, and support.

Firstly, I am grateful to TAIST-Tokyo Tech committee for choosing me as a full scholarship recipient and allowing me to study Master of Automotive and Advanced Transportation Engineering at King Mongkut's Institute of Technology Ladkrabang.

I would like to express my deep and sincere gratitude to my research main advisor, Assoc. Prof. Dr. Jarruwat Charoensuk from King Mongkut's Institute of Technology Ladkrabang for allowing me the chance to do this research and for your essential advice during this process.

I wish to extend sincere thanks to Dr. Chaiyuth Saekung from National Science and Technology Development Agency, Thailand who helped and gave me a lot of support throughout my research period. His expertise, patience, and insightful feedback have been instrumental in shaping this thesis and refining my research skills. I consider myself extremely lucky to have had the chance to work under his guidance.

I also would like to thank Prof. Dr. Katsunori Hanamura from School of Engineering, Tokyo Institute of Technology and Dr. Min Thu San from Yangon Technological University for their insightful advice and recommendations, which have significantly improved the caliber of the thesis research. Their expertise and thorough review of my work have significantly contributed to its overall improvement.

I would also like to acknowledge to all the friends from A2TE15 batch for their useful help and all those who were directly or indirectly involved in the successful completion of this research work. Moreover, I would like to thank the National Science and Technology Development Agency (NSTDA) of Thailand for the scholarship that I have received over the years.

Finally, my heart-felt and sincere gratitude goes to my parents who have nurtured a love of learning in me and allowed me to study in Thailand for making education accessible.

Myat Yu Soe

TABLE OF CONTENTS

Chapter **Page**

LIST OF TABLES

Table **Page**

LIST OF FIGURES

Figure **Page**

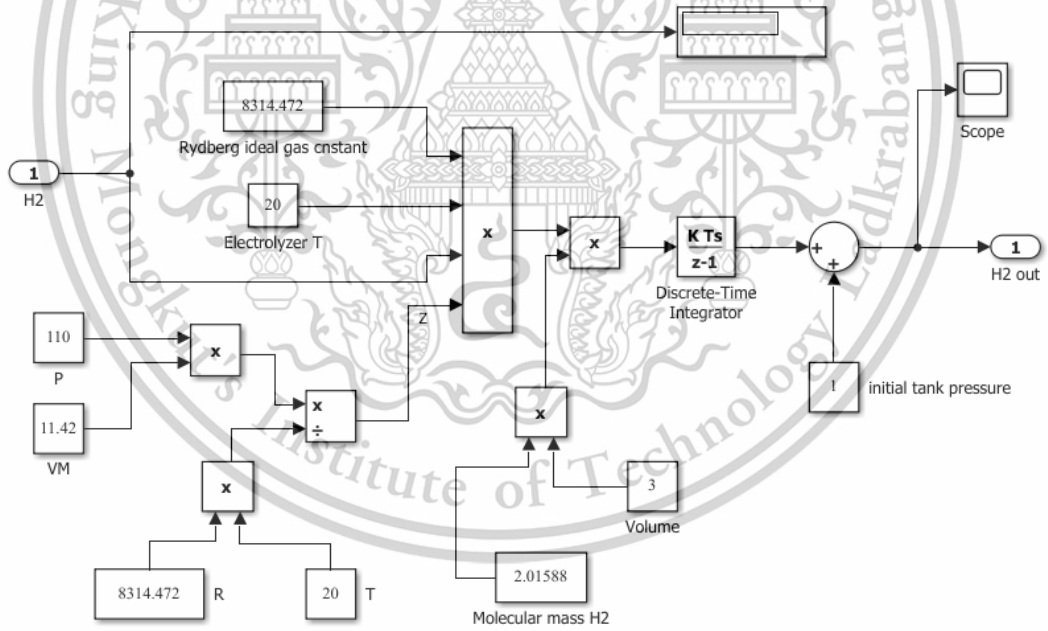

LIST OF SYMBOLS

E	Electromagnetic energy
λ	Wavelength
f	Frequency
Φ	Tilt angle
δ	Declination angle
n	Number of days
β	Altitude angle
I	Current of solar module
I_{ph}	Photo current
I_0	Saturation current
I_{sh}	Shunt current
I_{sc}	Short circuit current
I_{rr}	Solar irradiation
I_{rs}	Reverse saturation
q	Elementary charge on electron
V	Voltage
R_s	Series resistance
K	Boltzmann's constant
N_s	Number of solar cells connected in series
T	Operating temperature

E_g	Band gas energy of the semiconductor
V_o	Output voltage
V_s	Input voltage
D	Duty cycle
I_o	Output current
I_s	Input current
e_{rev}	Reverse voltage
R_i	Initial PEM cell resistance
k	Derived curve fitting parameter
P	Pressure
P_0	Reference pressure
F	Faraday constant
dR_t	Resistance coefficient of temperature
R	Universal gas constant
G	Gibbs free energy
ΔG	Change in Gibbs free energy
$\Delta \bar{G}_f$	Change in molar Gibbs free energy of formation
H	Enthalpy
ΔH	Change in enthalpy
$\Delta \bar{H}_f$	Change in molar enthalpy of formation
S	Entropy

ΔS	Change in entropy
$\Delta \bar{S}$	Change in molar entropy of formation
$\bar{c}_p$	Molar heat capacity
V_i	Optimal voltage or ideal voltage
V_m	Molar volume determined by the ideal gas
V_H	Rate of hydrogen production
V_b	Tank volume
P_b	Tank pressure
P_{bi}	Initial pressure of the storage tank
Z	Compressibility factor
N_a	Avogadro's number
e	Charge of an electron
n	Number of moles of electrons per mole of product
V_{rev}	Reversible voltage
V_{TN}	Thermo-neutral voltage or enthalpy voltage
V_{actual}	Actual applied voltage
n_{H_2}	Total moles of hydrogen generated
$\eta_{Voltage}$	Voltage efficiency
$\eta_{Faraday}$	Faradaic efficiency
$\eta_{Overall}$	Overall efficiency

STH	Solar to hydrogen efficiency
η_{act}	Activation overpotential
η_{ohm}	Ohmic overpotential
η_{conc}	Concentration overpotential
α	Charge transfer coefficient
i	Actual current density
i_o	Exchange current density
R_{total}	Total resistance of the cell
$R_{electrode}$	Resistance associated with the electrodes
$R_{electrolye}$	Resistance by ions passing through the electrolyte
$R_{interfacial}$	Resistance between electrodes and electrolyte
$R_{external}$	Resistance in the external circuit

LIST OF ABBREVIATIONS

PEM	Proton Exchange Membrane Polymer Electrolyte Membrane
CCS	Carbon Capture and Storage
ICE	Internal Combustion Engine
DC	Direct Current
AC	Alternating current
H_2O	Water
H_2	Hydrogen gas
O_2	Oxygen gas
KOH	Potassium hydroxide
NaOH	Sodium hydroxide
l	Liquid
g	Gas
aq	Aqueous solution
SOE	Solid oxide electrolysis
PV	Photovoltaic
OH^-	Hydroxide ion
e^-	Electron
H^+	Hydrogen ion or proton
O^{2-}	Oxygen ion
LSM	Lanthanum strontium manganite
UV	Ultraviolet
PID	Proportional integral derivative
MEA	Membrane electrode assembly

CHAPTER 1
INTRODUCTION

1.1 Research background

Nowadays, transportation is one of the essential activities which has the effect on the accelerating the economic and social advancement [1] .The main energy source for transport industry is fossil fuels which are hydrocarbon sources made from decomposing plants and animals. Burning fossil fuels releases massive amounts of carbon dioxide and other greenhouse gases. Fossil fuel consumption has had a number of detrimental effects on the environment, including air pollution and global warming. According to the WHO statement, around 7 million people die each year as a result of breathing uncleaned air which affects 90% of the world's population [2].

Air pollution, emissions and energy issues related to transportation are serious difficulties throughout the world. It is impossible to forgo transportation demands for environmental quality and public health. The Center for Community Health, Environment, and Transportation conducts research and finds the new ways to facilitate the mobility system for people and to be sustainable environment, enhancing the public health [3].

The development of renewable energy is becoming an attractive solution. However renewable energy is not suitable in vehicles like fossil fuels. Searching for alternate renewable energy sources that are conveniently obtainable through the use of wind, sun, and waves has become imperative. Based on statistical data, switching to fuel cell technology may result in annual fuel savings of over one million dollars per ship [4].

Hydrogen can be mainly used in the transport industry as an energy for fuel cell vehicles and will be one of the solutions for the storage of renewable energy. Hydrogen is an energy carrier that can be created from other energy sources, unlike fossil fuels. Hydrogen is one of the most abundant elements in the universe. It does not exist alone because it easily reacts with other elements. It is the lightest gas and the fastest growing industrial gas [5]. The importance of hydrogen in the energy transition is expected to grow more. The UN and many governments are attempting to attain net zero emissions by 2050 to combat climate change [6].

Currently most hydrogen is produced from hydrogen resources like fossil fuels and clean technology is needed for hydrogen production. Numerous non-fossil fuel-based methods exist for producing hydrogen, including thermochemical cycles, photocatalysis, and water electrolysis. Numerous non-fossil fuel-based methods exist

for producing hydrogen, including thermochemical cycles, photocatalysis, and water electrolysis.[7]. Among them, water electrolysis is an interesting technology for hydrogen production. Since water is a clean resource that is widely available, it is possible to produce enormous amounts of hydrogen using water electrolysis.

According to other studies, Solar-powered hydrogen generation is becoming more and more popular as a vital part of the renewable energy landscape due to the growing demand for clean and sustainable energy sources. However, several significant challenges hinder the widespread adoption of this technology. Efficient conversion of solar energy into hydrogen through Proton Exchange Membrane (PEM) electrolysis is impeded by issues such as low conversion efficiency, high capital costs, and limited scalability. Additionally, the intermittent nature of solar radiation makes it difficult to produce hydrogen continuously and steadily. Further research is essential to optimize the integration of solar photovoltaic or concentrated solar power systems with PEM electrolysis, addressing technical, economic, and environmental considerations. In order to fully realize the potential of solar-powered hydrogen production as a feasible and sustainable route for clean energy generation and storage, it is imperative that these obstacles be overcome.

1.2 Objectives

This research aimed to achieve the following objectives.

- To analyze the nature of hydrogen, electrochemical fundamentals and address the intermittent nature of solar energy by developing effective and economical storage solution for the hydrogen production.
- To construct a MATLAB/Simulink simulation model of a solar-powered PEM electrolyzer system.
- To compare experimental results of the rate of hydrogen production and efficiency when the different levels of water temperature and water flow rate are applied.

1.3 Scope of works

This research was structured into three main components: analyzing the behavior of hydrogen, the solar energy and electrochemical fundamentals, building the PEM electrolyzer powered by a solar panel system in MATLAB/Simulink and experimentally increasing the efficiency and hydrogen production rate with the influence of water temperature and water flow rate.

First and foremost, the behavior of hydrogen and hydrogen production is investigated through the color spectrum and solar energy was examined and tilt angle of the solar panel is determined based on the sun orientation and sun path. The concepts and fundamentals of water electrolysis are classified. The electrochemical fundamentals of water electrolysis is investigated based on the first law of Thermodynamics.

The simulation model of the proton exchange membrane powered by a solar panel along with the atmospheric hydrogen storage tank is built in MATLAB/Simulink. It consists of a discrete number of sub models and blocks. There are the main four subsystems which are PV array, buck converter which is used to step down the DC-Dc voltage, electrolyzer which is the core of the water electrolysis system to produce hydrogen and hydrogen tank.

Furthermore, the experimental components are set up. The reversible potential was investigated through the heat energy corresponding to Gibb's free energy for electrochemical decomposition of water with the help of MathCAD software. To evaluate the effects of water temperature and water flow rate, it was conducted on the temperature of 20-60 degree Celsius and flow rate of 20-60 ml/min. The electrolyzer efficiency was investigated by using higher heating value. Irreversibility is investigated in order to characterize the losses in thermodynamic and electrochemical systems.

CHAPTER 2
LITERATURE REVIEW

2.1 Hydrogen

Understanding why hydrogen is a crucial element in advancing the energy revolution involves focusing on its molecular composition. Hydrogen, represented by the chemical symbol H and derived from the Latin hydronium, stands as the first element in the periodic table and is a fundamental component of nearly all organic compounds [8]. The most basic element in the family of chemical elements is hydrogen, a colorless, odorless, tasteless, and combustible gaseous material. The hydrogen atom comprises a nucleus containing a proton with a positive electrical charge of one unit, and an electron carrying a negative electrical charge of one unit is also linked to this nucleus.

Under normal conditions, hydrogen gas is a diffuse mixture of hydrogen molecules, each consisting of two atoms, which is referred to as a diatomic molecule and is symbolized by the symbol H_2. The earliest recognized significant chemical characteristic of hydrogen is tis combustion with oxygen, resulting in the formation of water symbolled by H_2O. Hydrogen, being combustible, serves as an energy carrier akin to fossil nature gas and methane. Notably, unlike the combustion of fossil fuels, instead of producing carbon, carbon monoxide, sulfur oxides, or other hazardous pollutants for the environment, burning hydrogen produces water vapor. [9].

Hydrogen is labeled as an energy carrier since it is not typically found in a free state in nature and is instead generated from alternative energy sources. It serves as a clean-burning fuel, and when it undergoes a reaction with oxygen in a fuel cell, it generates heat and electricity, producing only water vapor as a by-product [10] [11].

2.2 Hydrogen Color Spectrum

Though it is sometimes described in colorful ways, hydrogen is an invisible gas. The various forms of hydrogen do not appear to differ from one another. The colors are white, green, pink, or purple, yellow, blue, turquoise, gray and brown or black. In the energy business, they serve as essentially color-coded or nicknamed systems for distinguishing between various forms of hydrogen. Hydrogen is given distinct color codes based on the type of manufacturing [12]. The color spectrum of hydrogen with the various production pathway is described in

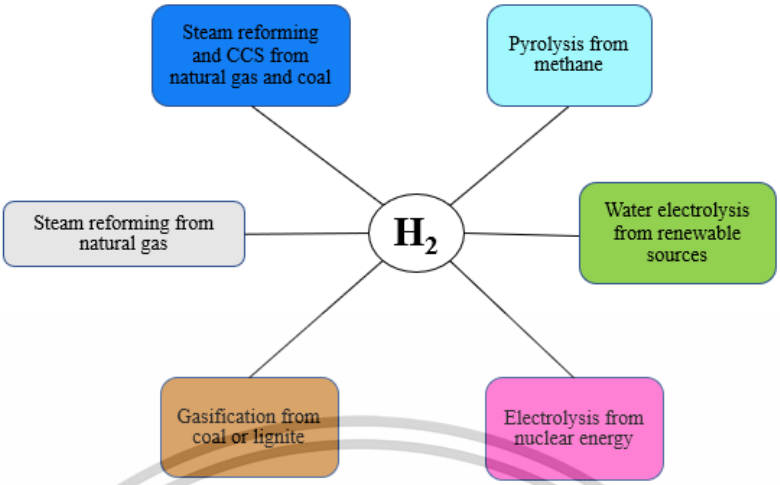

Figure 2.1 Hydrogen color spectrum

Green hydrogen is created by electrolyzing water with clean electricity obtained from excess renewable energy sources like solar, wind, or hydropower. Water is divided into hydrogen and oxygen by an electrochemical reaction in electrolyzers; no carbon dioxide is released during this process.

Natural gas and heated water in the form of steam are combined in a process known as steam reforming to produce blue hydrogen, which is mostly produced from natural gas. Although carbon dioxide is created as a byproduct, hydrogen is the end product. This carbon is captured and stored using carbon capture and storage, or CCS. Since some greenhouse gas is still created during the steam reforming process, blue hydrogen is also referred to as low-carbon hydrogen.

The most popular method of producing hydrogen from natural gas or methane without absorbing greenhouse gases is steam methane reforming, which produces grey hydrogen. Green hydrogen is the opposite of black and brown hydrogen. The most harmful method to the environment is gasification, which is used to consume coal, lignite, or other fossil fuels.

Pink hydrogen is produced from nuclear energy through electrolysis. Red or purple hydrogen are other names for this kind of hydrogen. The method of methane pyrolysis is used to create turquoise hydrogen. Hydrogen generated using solar-powered electrolysis is referred to as yellow hydrogen. It is comparable to green hydrogen. The exact renewable energy sources that are employed are what make a difference. White hydrogen is a naturally occurring form of geological hydrogen produced by fracking and found in subterranean deposits. At this time, it cannot be used.

2.3 Hydrogen Production

In molecules where it exists, hydrogen can be created by separating from the other elements. For use as a fuel, hydrogen can be created in a variety of methods from a wide range of sources. Hydrogen production processes can be broadly divided into four groups.

1. Thermochemical process
2. Electrolytic process
3. Water splitting process using direct sun radiation
4. Biological process

Hydrogen is liberated from the molecular structure of a variety of materials, including biomass, coal, and natural gas, through thermochemical processes. The thermochemical process is detailly divided into four categories.

1. Steam methane reforming or natural gas reforming
2. Gasification of biomass
3. Liquid reforming generated from biomass
4. Solar thermochemical hydrogen

A reputable and advanced production method that makes use of the natural gas pipeline network already in place is natural gas reforming. Currently, this pathway accounts for 95% of the hydrogen produced in the United States. This is an important technological avenue for producing hydrogen on-demand. Methane from natural gas is utilized in thermal processes like partial oxidation and steam-methane reforming to create hydrogen. In this process, high temperature steam (700-1000 degree Celsius) is used. Together with carbon monoxide and a negligible quantity of carbon dioxide, hydrogen is generated. Hydrogen can be produced by steam reforming alternative fuels such as gasoline, propane, and ethanol. For the time being, one practical way to produce hydrogen for fuel cell electric vehicles and other uses is by reforming natural gas.

Biomass is a plentiful domestic resource, and biomass gasification is an established technology that uses heat, steam, and oxygen in a controlled process to convert biomass into hydrogen and other byproducts without burning. Working biofuel gasification plants provide important information and best practices for producing hydrogen.

Liquids obtained from biomass resources, such as ethanol and bio-oils, can undergo a reforming process akin to natural gas reforming to generate hydrogen. These liquids provide easier transportation than their biomass feedstocks, which may allow for semi-centralized production or even distributed hydrogen generation at filling

stations. Mid-term potential exists for the technological pathway of reforming liquids obtained from biomass.

Thermochemical water splitting produces hydrogen and oxygen from water by using chemical reactions in combination with high temperatures from concentrated solar power or waste heat from nuclear power operations. This technology pathway is considered long-term and has the potential for minimal to no greenhouse gas emissions. This approach is taken into consideration because it uses water and either solar or nuclear electricity to power high-temperature thermochemical water-splitting cycles, which produce hydrogen with nearly no greenhouse gas emissions [13].

In electrolytic process, electrolyzer uses electrical energy to separate water into oxygen and hydrogen. This technology is mature and commercially available. There are ongoing developments in creating systems that can effectively harness intermittent renewable energy [14].

Water is divided into hydrogen and oxygen using light in the direct solar water splitting process. It is also called photolytic process. Even though research on this technique is still in its very early stages, the long-term potential for sustainable hydrogen production with no environmental impact is encouraging. It can be divided into two methods.

1. Photoelectrochemical
2. Photobiological

Hydrogen is produced from water using photoelectrochemical water splitting, which uses sunlight and specific semiconductors called photoelectrochemical materials. These materials immediately convert water molecules into hydrogen and oxygen by the use of light energy. This technological route is thought to be a long-term fix because it has the ability to produce little to no greenhouse gas emissions. By using semiconductor materials, the photoelectrochemical water splitting technology converts solar energy directly into chemical energy in the form of hydrogen. Similar semiconductors to those used in photovoltaic solar electricity generation are used in this technique, but the semiconductor is submerged in an electrolyte based on water.

Photobiological hydrogen production involves the use of microorganisms and sunlight to convert water, and occasionally organic matter, into hydrogen. This technology pathway is currently in the early stages of research, representing a longer-term approach with the potential for sustainable hydrogen production and minimal environmental impact. Researchers are actively working on developing methods to extend the duration of microbial hydrogen production and enhance the rate of hydrogen generation [15].

Microorganisms that use sunlight or organic matter, such as bacteria and microalgae, can produce hydrogen through biological reactions. Microorganisms that use photolysis, such cyanobacteria or green microalgae, use sunlight to divide water into hydrogen and oxygen ions. While this technology is still in the research and development stage, it has the potential to produce hydrogen sustainably and with low carbon emissions in the long run. In detail, there are two forms of technology.

1. Microbial biomass conversion
2. Photobiological

By using microorganisms' ability to consume and break down biomass, microbial biomass conversion produces hydrogen. Hydrogen is produced in fermentation-based systems by microorganisms, such as bacteria, breaking down organic matter. Refined sugars, unprocessed biomass sources such as corn stover, and wastewater are examples of this organic matter. Known as dark fermentation techniques, these procedures do not require light to function. Fermentation is a widely utilized industrial method that uses biomass, a plentiful home resource, to produce biofuels and other goods [16], [17].

2.3.1 Hydrogen Production from Solar Energy

Hydrogen production from solar energy involves harnessing sunlight through methods to generate hydrogen. These techniques include solar-driven high-temperature thermochemical water splitting, photobiological hydrogen synthesis, photoelectrochemical water splitting, and solar electrolysis. In photoelectrochemical water splitting, water molecules are directly divided into hydrogen and oxygen using semiconductor materials and solar light. Through biological processes, microorganisms like algae or cyanobacteria and sunlight are used in the photobiological hydrogen generation process to transform water and occasionally organic matter into hydrogen. With the use of high temperatures produced by concentrated solar power, the solar-driven high temperature thermochemical water splitting process offers the possibility of producing hydrogen through chemical reactions with little to no greenhouse gas emissions. Electrolysis, a clean and sustainable way of producing hydrogen from water by dividing it into hydrogen and oxygen, is powered by solar energy. Every technique has benefits and drawbacks, and continuous research attempts to maximize effectiveness, lower expenses, and support a sustainable and low-carbon future for hydrogen production [18].

Solar electrolysis has the advantage of being a well-established and commercially available technology. Powered by renewable energy sources like solar

electricity, it can be especially effective in producing hydrogen through water electrolysis in a clean and efficient manner. While considered a long-term technology pathway, high-temperature thermochemical water splitting has the possibility of emitting few or no greenhouse gases. However, it may face challenges related to infrastructure and cost. Photobiological hydrogen production leverages biological processes and sunlight, offering a sustainable pathway. However, it currently faces challenges such as low production rates and issues related to oxygen inhibition [19]. There are four production pathways from solar energy as described in Figure 2.2.

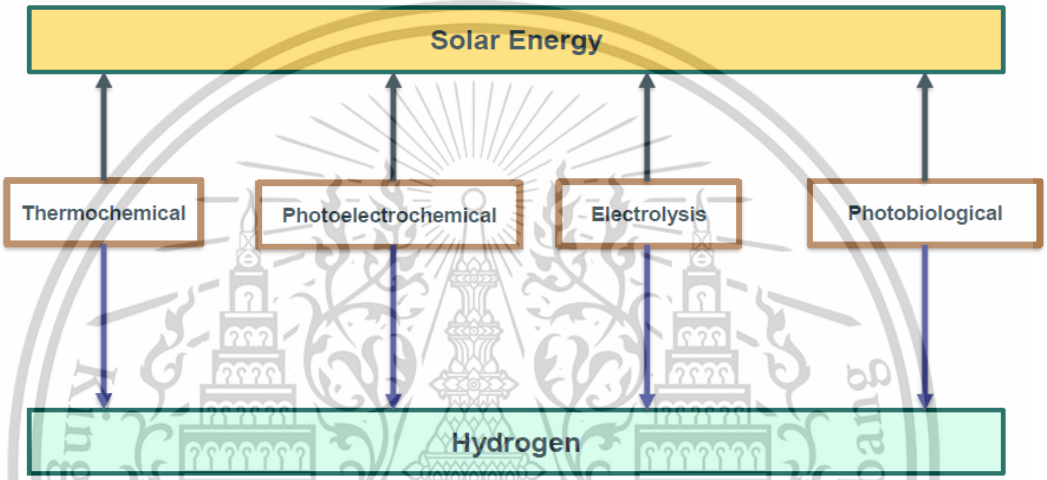

Figure 2.2 Hydrogen production technology using solar energy

2.3.2 Hydrogen from Water

hydrogen generated from water often referred to as green energy when generated using renewable energy sources, has drawn more attention as a result of its potential for low-carbon, sustainable energy. And water is the most abundant on the earth and it is renewable. There is no pollution when hydrogen is generated and only hydrogen and oxygen is produced [20] [21].

2.4 Water Electrolysis

The pressing need to combat climate change and move toward sustainable energy sources has led to a rise in interest in hydrogen as a clean, adaptable energy source on a worldwide scale in recent years. Since hydrogen has the ability to decarbonize a number of industries and sectors, including transportation, manufacturing, and power generation, it is regarded as a crucial component in the

transition to a low-carbon economy [22]. Its unique attributes, such as high energy density and the ability to produce electricity with zero emissions when used in fuel cells, make it an attractive option for clean energy applications [23] .

Green hydrogen, or hydrogen created with renewable energy sources, is produced in large part through the process of water electrolysis. Through the use of electricity produced by renewable energy sources including solar, wind, and hydropower, water is electrochemically split into hydrogen and oxygen. This method is highly sustainable and aligns with the broader goal of achieving a carbon-neutral energy landscape [24], [25].

The interest in water electrolysis is driven by several factors. The first is renewable integration. A solution to the problems of energy storage and grid balancing is offered by water electrolysis, which offers a way to store extra energy produced by intermittent renewable sources. The second is decentralized production. Electrolyzers can be deployed in various locations, enabling decentralized hydrogen production, and reducing the need for centralized hydrogen manufacturing plants. The third is green hydrogen for industry. The fourth is clean transportation. Green hydrogen, especially in fuel cell electric vehicles, has the potential to be a key component in the transportation sector's decarbonization. The last is grid flexibility. By reacting as an energy carrier and storage medium, hydrogen created by water electrolysis can increase the resilience and flexibility of the grid [26].

The process of splitting water (H_2O) into its component parts, hydrogen (H_2) and oxygen (O_2), using electrical energy is known as water electrolysis. An electrolyzer, which usually consists of two electrodes which are an anode and a cathode submerged in an electrolyte solution, usually water, is the container in which this electrochemical reaction occurs. [27]. Equation *(2.1)* represents the basic reaction that occurs during water electrolysis.

$$2H_2O(l) \rightarrow 2H_2(g) + O_2(g) \quad (2.1)$$

Depending on the electrolyte utilized in the electrolysis cell, there are three primary categories for water electrolysis as described in Figure 2.3. The first one is alkaline water electrolysis which is the use of liquid electrolyte. Th second one is proton exchange membrane or polymer electrolyte membrane electrolysis which is electrolysis in acid ionomer environment. The last one is solid oxide electrolysis or

steam electrolysis or high temperature electrolysis which is the use of solid oxide electrolyte.

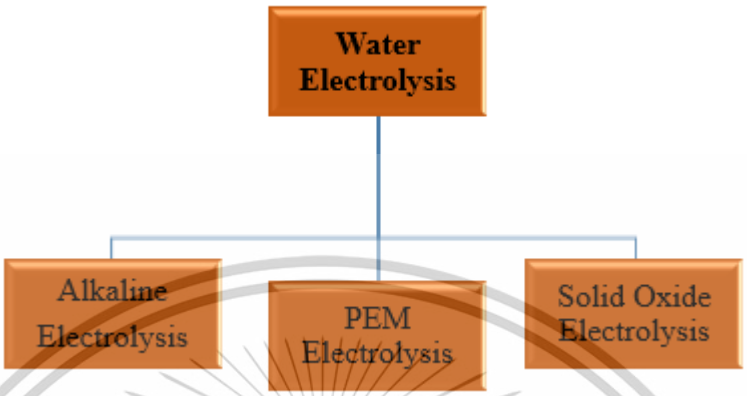

Figure 2.3 Types of water electrolysis

2.4.1 Alkaline Water Electrolysis

Alkaline electrolysis is a proven technology that has been used in industry for many years. Alkaline water electrolysis is a process that uses an alkaline electrolyte, usually potassium hydroxide (KOH) or sodium hydroxide (NaOH) to produce hydrogen and oxygen gas from water. The alkaline environment helps facilitate the ionization of water molecules. Water is broken down into its component parts using an electrolytic cell in this procedure, which applies an electric current. An anode, or positive electrode, and a cathode, or negative electrode, make up an electrolytic cell. These electrodes are typically made of like nickel or stainless steel. The cathode and anode are connected to an external power source, providing the necessary electric current for the electrolysis process. Hydroxide ions (OH^-) migrate towards the anode while hydrogen ions (H^+) move towards the cathode as described in Figure 2.4.

The reduction of hydrogen ions (H^+) to hydrogen gas (H_2) occurs at the cathode.

$$2H_2O\ (l) + 2e^- \rightarrow H_2\ (g) + 2OH^-\ (aq) \quad (2.2)$$

Water molecules undergo oxidation at the anode to produce oxygen gas (O_2) and hydroxide ions (OH^-):

$$4OH^-\ (aq) \rightarrow O_2\ (g) + 2H_2O\ (l) + 4e^- \quad (2.3)$$

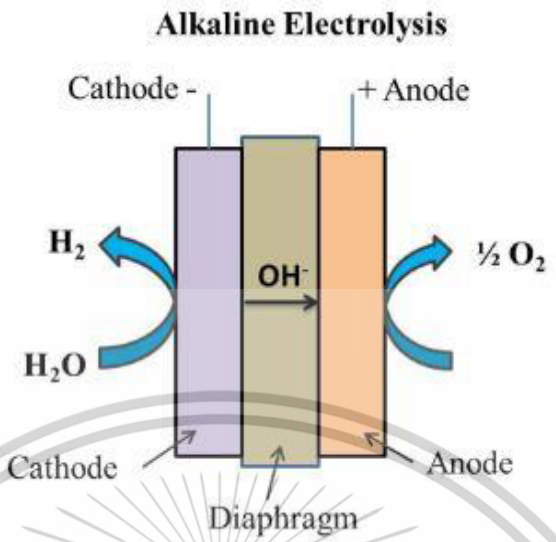

Figure 2.4 Alkaline water electrolysis

Large-scale industrial hydrogen production has been achieved by the widespread use of alkaline water electrolysis. It has a history of use in applications where the purity of hydrogen is not a critical factor. Compared to some other electrolysis technologies, alkaline electrolysis tends to have lower capital costs. For the challenges, the electrodes often contain precious metals, such as nickel, which can contribute to the overall cost. The durability of the electrodes can be a concern, and maintenance may be required to ensure long-term operation. When alkaline water electrolysis is fueled by renewable energy, it can help produce green hydrogen., making the overall process more environmentally friendly [28].

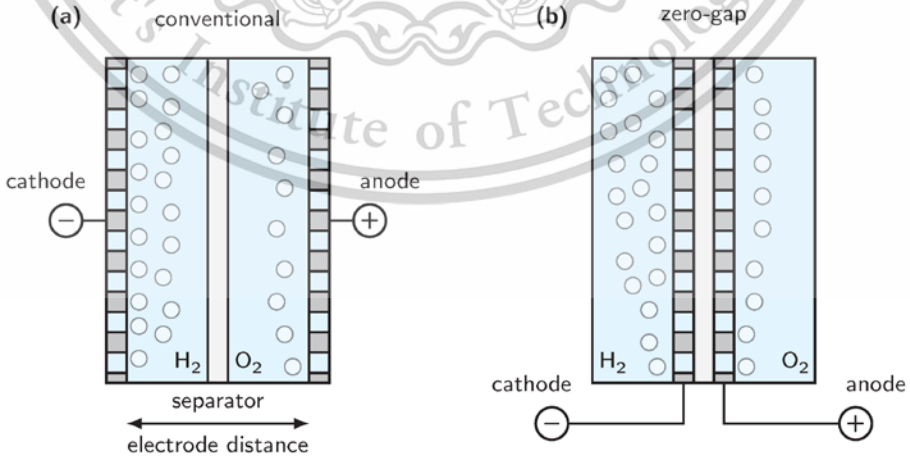

Figure 2.5 Two types of alkaline water electrolysis

2.4.2 Proton Exchange Membrane Water Electrolysis

Proton exchange membrane (PEM) water electrolysis is a state-of-the-art method that splits water electrochemically to make hydrogen. PEM electrolysis is also called polymer electrolyte membrane water electrolysis. Proton exchange membranes, or solid polymer electrolytes, are used in PEM water electrolysis as a means of conducting protons. The proton conducting membrane is an essential element that permits only protons to flow through and hinders the combination of oxygen and hydrogen gases. The anode and cathode of a PEM electrolyzer are separated by a solid polymer electrolyte membrane, which is typically composed of a perfluoro sulfonic acid polymer like Nafion. It provides good proton conductivity and chemistry stability. The anode is usually made of a catalytic material for the oxidation reaction (usually platinum-based) and the cathode facilities the reduction reaction.

When a current of electricity is applied, water molecules near the anode undergo oxidation, releasing protons (H^+) and electrons (e^-). Protons travel to the cathode via the PEM, where they mix with hydrogen gas and electrons. [29] [30].

The overall reaction can be represented as follows:

$$2H_2O(l) \rightarrow 2H_2(g) + O_2(g) \quad (2.4)$$

At the cathode (Reduction):

$$4H^+(aq) + 4e^- \rightarrow 2H_2(g) \quad (2.5)$$

At the anode (Oxidation):

$$2H_2O(l) \rightarrow O_2(g) + 4H^+(aq) + 4e^- \quad (2.6)$$

PEM electrolysis is known for its high efficiency reaching levels of 80% making it competitive for various applications. PEM electrolyzers can rapidly start and stop in response to changes in electrical input, providing flexibility for dynamic energy demands. The modular and compact nature of PEM electrolyzers makes them suitable for decentralized hydrogen production, enabling on-site generation. PEM electrolysis is ideal for integrating intermittent renewable energy sources, like wind and solar and generates hydrogen with a high purity appropriate for fuel cell vehicles, providing a clean alternative for transportation sector [31].

The cost of materials, particularly platinum catalysts, can be a challenge although ongoing research aims to reduce the costs. Maintaining the durability of the membrane and electrodes over time, especially in acidic conditions, is an ongoing focus of research [32].

2.4.3 Solid Oxide Electrolysis

Solid oxide electrolysis (SOE) is an advanced electrolysis technology that involves the direct electrochemical conversion of steam (H_2O) into hydrogen (H_2) and oxygen (O_2) using a solid oxide electrolyte. Usually operating at temperatures between 500 and 1000 degrees Celsius, this process involves extreme temperatures. To improve the solid oxide electrolyte's ionic conductivity, a high temperature is required. The key component of the SOE is the solid oxide electrolyte which is often made of ceramics such as zirconia (yttria-stablished zirconia) or ceria-based materials. This solid electrolyte allows oxygen ions (O^{2-}) to migrate from the cathode to the anode. The anode is often made of materials such as nickel cermet, which can catalyze the oxidation reaction, while the cathode is usually made of materials like lanthanum strontium manganite (LSM) or other perovskite oxides, which can catalyze the reduction reaction.

Oxygen gas is created at the anode when oxygen ions mix with electrons.

$$O^{2-} + 2e^- \rightarrow \frac{1}{2} O_2(g) \tag{2.7}$$

As electrons move via an external circuit to produce an electric current, oxygen ions move through the solid oxide electrolyte. Hydrogen gas is emitted at the cathode as oxygen ions recombine with electrons to generate oxygen gas.

$$H_2O + 2e^- \rightarrow H_2(g) + O^{2-} \tag{2.8}$$

To increase overall system efficiency, SOE can be combined with renewable energy sources like concentrated solar power or surplus heat from industrial activities. High-purity hydrogen that is appropriate for a range of uses, including fuel cells, can be produced via SOE [33] [34].

2.4.4 Advantages and Disadvantages

Alkaline electrolysis is a well-established technology with a long history of successful implementation. Alkaline electrolysis systems can achieve high efficiency at elevated temperatures. When compared to other electrolysis technologies, alkaline electrolysis usually exhibits less efficiency at lower temperatures. The use of alkaline environments can lead to corrosion of materials, potentially reducing the lifespan of the electrolyzer which may have limitations in terms of operating flexibility, especially in dynamic load conditions.

PEM electrolysis is appropriate for a variety of applications because it can function effectively at lower temperatures. PEM electrolyzers often have a more

compact design, making them suitable for small-scale applications and distributed energy system and can respond quickly to changes in electricity input, allowing for better integration with intermittent renewable energy sources. PEM electrolyzers often use expensive materials like platinum as catalysts, contributing to higher initial costs. PEM electrolysis systems are sensitive to impurities and contaminants, which can affect their performance and durability and may have limitations in terms of operating temperature range compared to other electrolysis technologies.

SOE operates at high temperatures, leading to higher efficiency and potentially lower energy input and can use various feedstocks, including natural gas and biogas, providing flexibility in hydrogen production. Combining SOE with other high-temperature processes enables the production of both heat and power. The high operating temperatures of SOE can lead to challenges in materials selection and long-term durability. SOE systems can be more complex compared to other electrolysis technologies, potentially leading to increased maintenance requirements and may have longer start-up times due to the need for high temperatures, affecting their responsiveness to changes in demand.

The summary of advantages and disadvantages is described in Table 2.1.

Table 2.1 Advantages and disadvantages of water electrolysis

	Alkaline Electrolysis	**PEM Electrolysis**	**Solid Oxide Electrolysis**
Advantages	Maturity, Low-cost catalysts, Operational flexibility	High efficiency, Fast response, Compact design	High-temperature operation, Thermochemical compatibility, Potential for syngas production
Disadvantages	Corrosion issues, KOH Electrolyte limitations, Gas purity challenges	Cost off electrodes, Durability, Sensitive to impurities	High operation temperatures, Cost, Complexity

2.4.5 Efficiency and Performance

Typically, alkaline electrolysis achieves an efficiency of 60–70%. Electrical energy consumption ranges between 4.5–5.5 kWh per cubic meter (Nm^3) of hydrogen

produced. Alkaline electrolysis uses a liquid electrolyte, often potassium hydroxide (KOH) or sodium hydroxide (NaOH), and non-precious metal catalysts like nickel. It operates at low pressures (1-30 bar) and temperatures of 60–80°C. Mature and cost-effective technology, making it well-suited for large-scale hydrogen production, but it tends to have slower startup and lower current densities compared to other methods. As advantages, it has lower capital costs compared to other technologies and proven and reliable for industrial applications. As drawbacks, it has limited dynamic operation (e.g., cannot ramp up or down quickly), which makes it less ideal for intermittent energy sources like solar or wind.

PEM electrolysis can reach an efficiency of 70–80%, making it more efficient than alkaline electrolysis. Electrical energy consumption ranges between 4.0–5.0 kWh per Nm^3 of hydrogen produced. It uses a solid polymer electrolyte and platinum-group metal catalysts. And it operates at a higher pressure (up to 70 bar) and a temperature of around 50–80°C. It has faster response to times and higher current densities, making it more suitable for dynamic, renewable energy sources. As advantage, it has higher efficiency and faster startup, capable of producing high-purity hydrogen without further purification and more compact system design. As drawback, it has higher capital costs due to expensive catalyst materials and requires more maintenance than alkaline systems.

Solid oxide electrolysis cell offers the highest efficiency, ranging from 85–90%. However, it requires external heat, so the actual electrical efficiency is lower but compensated by the heat input. Energy consumption is around 3.0–4.0 kWh per Nm^3 of hydrogen, provided that sufficient heat is supplied. It uses a ceramic electrolyte and operates at high temperatures (around 700–1,000°C) and waste heat from industrial processes or high-temperature reactors, making it ideal for integration with high-temperature sources. It has high efficiency due to the ability to use both heat and electricity for electrolysis and is ideal for large-scale hydrogen production where high temperatures are available. However, it has a complex system with high capital and operational costs, durability issues due to the high temperatures, leading to material degradation over time and still in the early stages of commercialization compared to AE and PEM electrolysis.

2.5 Solar Energy

Solar energy is a sustainable and renewable energy source that comes from solar radiation. Solar energy is divided into light energy, thermal energy, and chemical energy. We can generate electricity called electrical energy from solar cells or solar modules by using light energy.

2.5.1 Photovoltaic

The term photovoltaic (PV) describes technology that directly turns sunlight into electricity. The words foto, which means photo, and voltaic, which means electricity, are the roots of the word photovoltaic. Photovoltaic technology involves the use of solar cells, also known as photovoltaic cells, to generate electric power by harnessing the energy from the sun. Photo refers to the conversion of light (protons) into electricity (voltage) using semiconductor materials in solar cells. This process is the basis of generating solar power from sunlight. Light is a wave that consists of photons. Photons are elementary particles of light, and they are the basic units or quanta of electromagnetic radiation. Light consists of waves and light energy is considered electromagnetic energy because it exhibits the fundamental characteristics of electromagnetic waves.

Generating electrical power involves directing the movement of electrons in a specific direction. This directional movement requires applying force to an electron, and this force is derived from various energy sources.

2.5.2 Energy and Wavelength

The connection between frequency, wavelength and energy is described by the wave-particle duality of electromagnetic radiation. Light and other electromagnetic radiation have characteristics of both waves and particles. The energy of a photon, the fundamental particle of electromagnetic radiation, is directly related to its wavelength as equation (*2.9*).

$$E = \frac{1.24}{\lambda} \tag{2.9}$$

where E = electromagnetic energy and λ = wavelength of electromagnetic wave.

$$\lambda = \frac{1}{f} \tag{2.10}$$

where f = frequency of electromagnetic wave.

A wave's wavelength and frequency are inversely related. The wavelength shrinks as the frequency rises and vice versa. A photon's energy and frequency are directly correlated. Higher frequency corresponds to higher energy. A photon's energy and wavelength are negatively correlated. Higher energy is associated with shorter wavelengths, whereas lower energy is associated with longer wavelengths. Within the electromagnetic spectrum, the visible light spectrum covers a narrow range of frequencies and wavelengths. The visible light spectrum has six colors which are violet,

blue, green, yellow, orange, and red). The wavelengths of all the hues in the visible spectrum are as follows: violet has the shortest wavelength, red has the longest, and all other colors fall in between. The colors of morning and evening are red and orange. In the afternoon, the color is white which is the combination of all colors and UV. So, we can generate more energy in the afternoon.

CHAPTER 3
RESEARCH METHODOLOGY

The purpose of this study is to examine and assess the effects of experimentally changing the water's temperature and input flow rate on the efficiency of producing hydrogen. Hydrogen production implemented in this study is based on the proton exchange membrane (PEM) water electrolysis. Together with the atmospheric hydrogen storage tank, the electrical equivalent circuit for the PEM electrolyzer was designed and put into practice using MATLAB/Simulink. The amount of hydrogen in the experimental and model setups is compared. Additionally, solar model implementation is investigated based on the sun orientation and sun path.

3.1 Solar PV Placing

3.1.1 Location of Thailand

Thailand is a country located in Southeast Asia and is situated between latitudes 5.8167° N and 20.3167° N and longitude 97.3447° E and 105.6367° E. The Equator is a circle of latitude that is 0 degrees. Thailand is located entirely north of the Equator. Areas near the Equator experience a tropical climate, characterized by relatively high temperatures throughout the year [35].

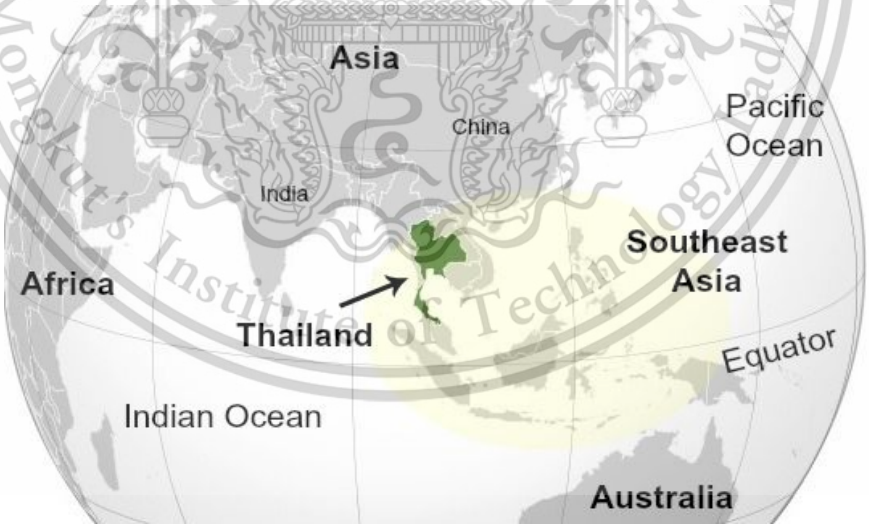

Figure 3.1 Map of Thailand

3.1.2 Sun Orientation

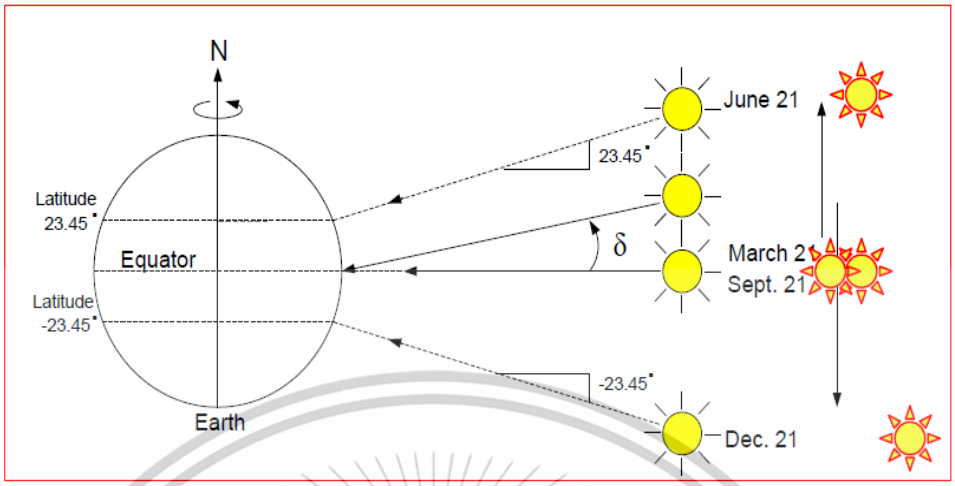

Figure 3.2 Sun orientation

The above figure is the sun orientation at noon. When the earth is fixed, the sun is orientating from Tropic of Cancer (23.45° north Latitude) to Tropic of Capricorn (23.45° South Latitude) through the equator. On March 21st, the sun is positioned directly above the Equator at solar noon. During this time, the Earth's axial tilt is such that neither the northern hemisphere nor the hemisphere of the South is inclined toward the Sun. As a result, day and night durations are approximately equal at most locations on Earth. Local solar noon is when the Sun appears at its zenith, or highest point, in the sky for sites in the Northern Hemisphere. This happens in the vicinity of 23.5 degrees north of the equator, along the Tropic of Cancer. On June 21st, observers at locations near the Tropic of Cancer experience the longest day of the year and the official start of summer. During March 21st and June 21st, the sun is shifting from the Equator to the Cancer Tropic. During June 21st and September 21st, the sun is moving backward from the Tropic of Cancer to the Equator. On September 21st, the sun is directly above the Equator again at solar noon. During September 21st and December 21st, the sun is moving from the Equator to the Tropic of Capricorn. The sun sets in the Northern Hemisphere at solar noon on December 21, marking the planet's lowest point in the sky. The Tropic of Capricorn is exactly over headed by the sun. The sun is traveling backward from the Tropic of Capricorn to the Equator on December 21 and March 21 respectively [36].

3.1.3 Sun Path

In the Northern Hemisphere, the apparent path of the sun in the sky changes throughout the year because of the earth's axis' tilt. Another name for it is the solar path. Understanding the Sun's path is crucial for various applications, including solar energy planning, agriculture, and general awareness of daylight patterns throughout the year.

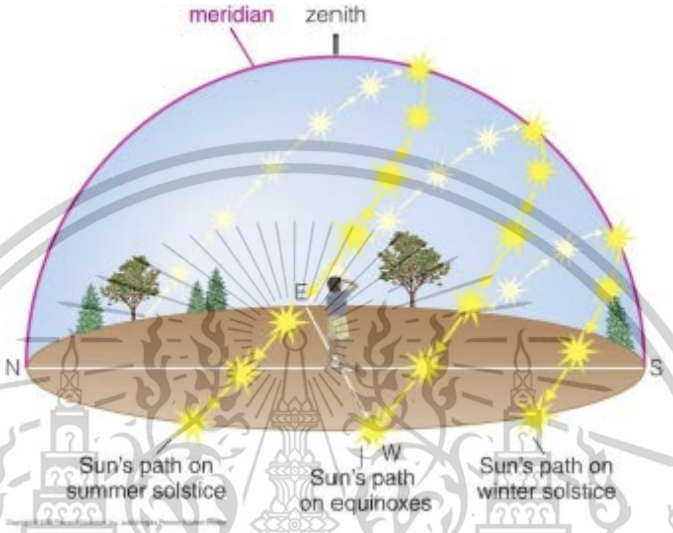

Figure 3.3 Sun path

3.1.4 Tilt Angle

The angle at which solar panels are positioned in relation to the horizontal plane is known as the tilt angle (Φ). The ideal tilt angle for solar panels varies depending on the region, season, and individual energy production objectives. Tilt angle is important to optimize power generation through the year or increase at low insolation months.

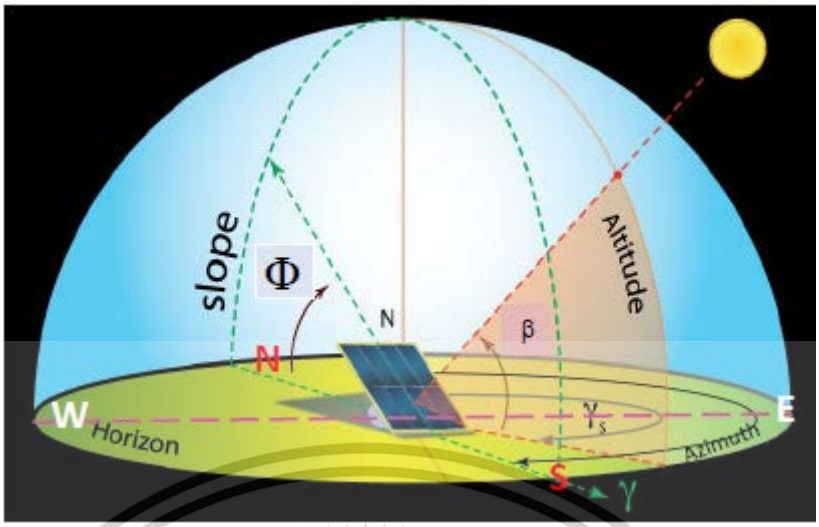

Figure 3.4 Tilt angle

Firstly, we need to know the declination angle which represents the angle formed by the sun's beams and the equator's plane on Earth. It is an essential parameter in celestial navigation and solar energy calculations. The earth's axial tilt and orbit around the sun cause the declining angle to fluctuate throughout the year. and is calculated as the equation (*3.1*).

$$\delta = 23.45 * \left(sin \frac{360}{365} * (n - 81) \right) \quad (3.1)$$

where δ = declination angle and n = day number

Table 3.1 Day number throughout the year

Month	Day Number	Month	Day Number
1st January	n = 1	1st July	n = 182
1st February	n = 32	1st August	n = 213
1st March	n = 60	1st September	n = 244
1st April	n = 91	1st October	n = 274
1st May	n = 121	1st November	n = 305
1st June	n = 152	1st December	n = 335

The angle formed by the solar panel's plane and the horizonal plane (ground level) is known as the altitude angle (β) and is calculated as the equation (*3.2*). The

altitude angle, which depends on the location and season, is a crucial factor in maximizing the efficiency of solar energy capture [37].

$$\beta = 90 - Latitude + \delta \quad (3.2)$$

Tilt angle is calculated as the equation (*3.3*).

$$\emptyset = 90 - \beta \quad (3.3)$$

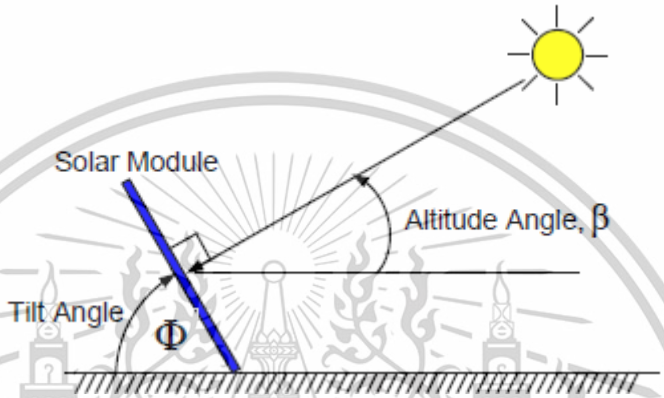

Figure 3-4 Tilt angle

3.2 Simulation Model Development

3.2.1 Photovoltaic Solar Panel Modeling

Through a basic physical process, the solar energy is directly converted within the PV panel into electrical energy. Any solar cell's operating properties are remarkably similar to those of a traditional p-n junction diode. Figure 3.5 demonstrates the solar cell's electrical equivalent circuit.

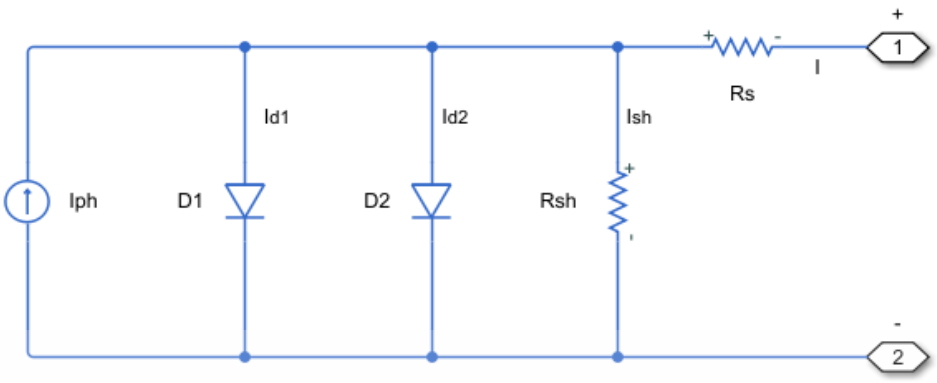

Figure 3.5 Electrical equivalent circuit of the solar cell

The solar PV module current is as the equation (*3.4*).

$$I = I_{ph} - I_0 \left\{ exp\left[\frac{q(V + I * R_s)}{n * K * N_s * T}\right]\right\} - I_{sh} \quad (3.4)$$

where I = solar PV module current, I_{ph} = photo current, I_0 = saturation current, q = elementary charge on electron, V = solar PV module voltage, I = solar PV module current, R_s = series resistance, n = empirical constant between 1 and 2, K = Boltzmann's constant, N_s = number of cells connected in series, T = operating temperature, I_{sh} = shunt resistance

The photo current is calculated as the equation (*3.5*).

$$I_{ph} = [I_{sc} + k_i(T - 298)]\frac{I_{rr}}{1000} \quad (3.5)$$

where I_{sc} = short circuit current, k_i = short circuit current off cell at 25 degrees Celsius and 1000 W/m^2 = 0.0032, I_{rr} = solar irradiation

The saturation current is calculated as the equation (*3.6*).

$$I_0 = I_{rs}\left[\frac{T}{T_n}\right]^3 exp\left[\frac{q.E_g\left(\frac{1}{T_n} - \frac{1}{T}\right)}{n.K}\right] \quad (3.6)$$

where I_{rs} = reverse saturation current, T = nominal temperature, E_g = band gas energy of the semiconductor

The reverse saturation current is calculated as the equation (*3.7*).

$$I_{rs} = \frac{I_{sc}}{exp\left[\frac{q.V_{oc}}{n.N_s.K.T}\right] - 1} \quad (3.7)$$

The reverse saturation current is calculated as the equation (*3.8*).

$$I_{sh} = \frac{V + I.R_s}{R_{sh}} \quad (3.8)$$

The photovoltaic module model in MATLAB/Simulink is displayed in Figure 3.6. The impact of temperature and irradiance on the PV array's output power is calculated by the PV array model. The PV array block receives input of desired operating temperature and irradiance. This block will include current measurement and voltage measurement to know the values. This block works under the irradiance of 1000 W/m^2 at 25 degrees Celsius. Temperature is significant in solar energy because it affects the four parameters of I_{rr}, I_0, R_s, and V_t.

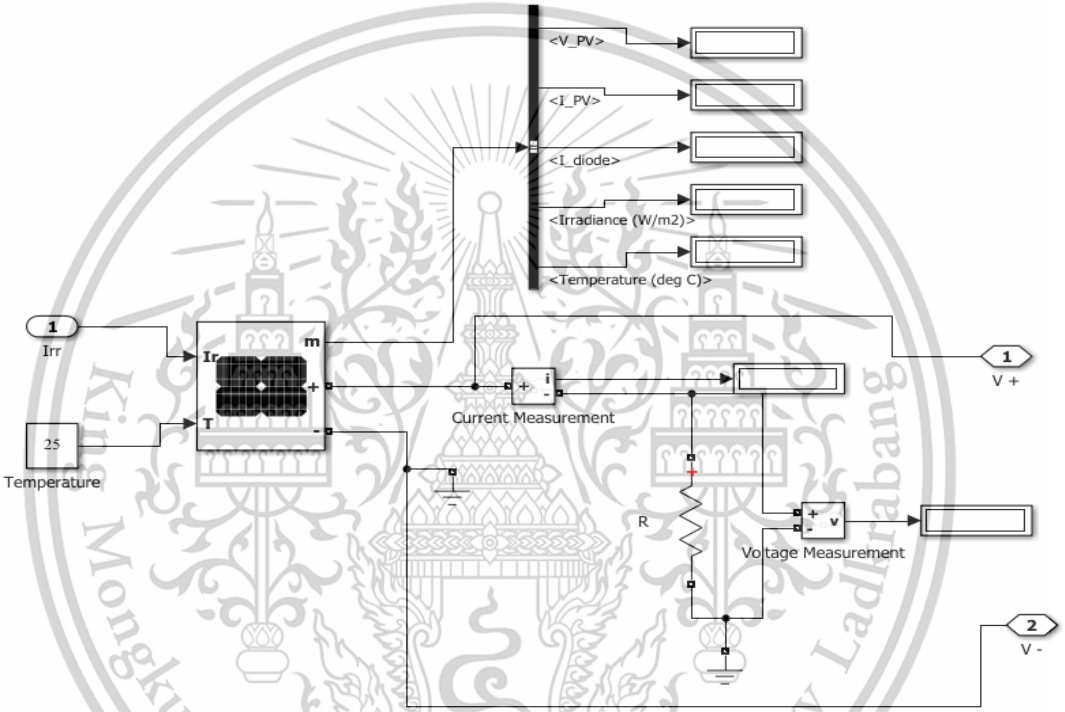

Figure 3.6 Block diagram of PV array in MATLAB/ Simulink

3.2.2 DC/DC Buck Converter Modeling

The buck converter model in MATLAB/Simulink is represented in Figure 3.7 to regulate the input and output between the electrolyzer and the solar module. The average output voltage of a back converter, a kind of step-down DC-DC voltage converter, is continuously lower than the input voltage. The buck converter is connected to two diode circuit modes. In the first mode, the energy can be stored in the inductor since the diode becomes reverse biased when the switch is turned on. In the second mode, when the switch is off, the diode becomes forward biased and receives energy from the inductor while keeping the input and output isolated. The

buck converter's main duties include controlling DC power sources and DC motor speed. The duty cycle, which can be defined as the ratio of the switch on time to its total switching time, also shows the relationship between the input and output voltages. The duty cycle is also given as the equation (*3.9*).

$$\frac{V_o}{V_s} = D = \frac{I_s}{I_o} \tag{3.9}$$

where V_o = output voltage, V_s = input voltage, I_o = output current and I_s = input current

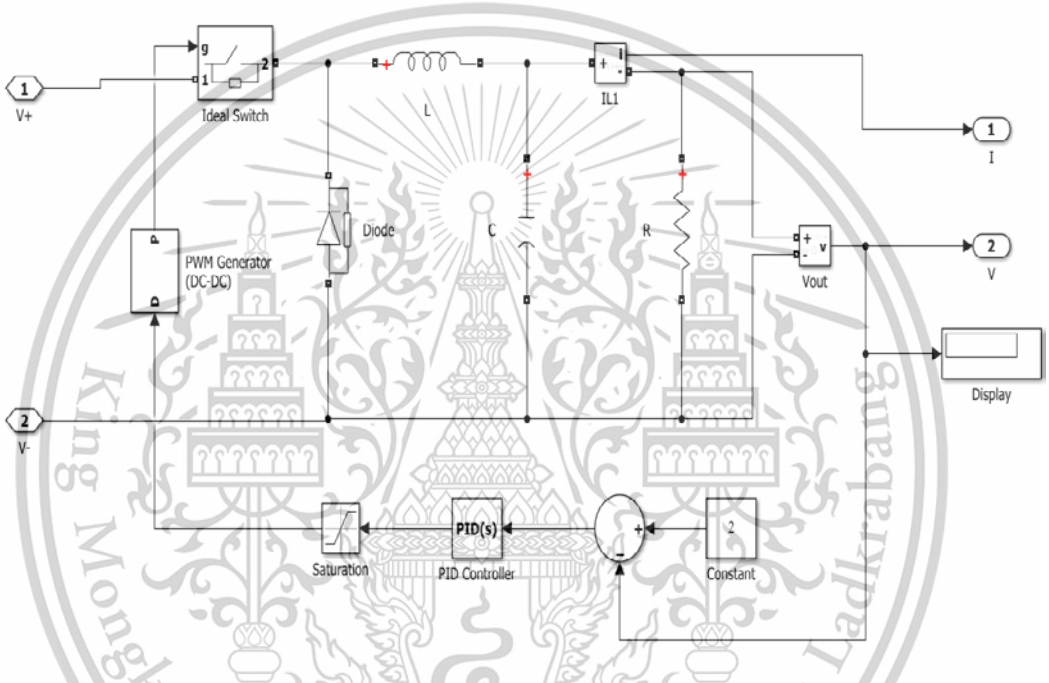

Figure 3.7 Block diagram of buck converter in MATLAB/ Simulink

The PV's output voltage and current dictate which buck converter should be used. The PV output in this investigation is set up to be 5V and 2A. Choosing a buck converter is required to control both voltage and current because the electrolyzer load is intended for 2V and 1A. The inductor, capacitor, duty cycle, and other buck converter parameters were sourced from a website that offers the required electrolyzer input values. The following Table 3.2 presents the chosen values for the buck converter. The error, or the discrepancy between the observed variable voltage and the intended set point, is monitored by the PID controller.

Table 3.2 The values of buck convertor

Item	Value
Input voltage	5 V
Output voltage	2 V
Load current	1 A
Frequency	40 kHz
Capacitor	29..17e-6 F
Inductor	87e-6 H

3.2.3 Electrolyzer Modeling

An electrolyzer is a device that separates water into its component elements, oxygen and hydrogen. The process of water electrolysis can be viewed as the opposite of supplying hydrogen to a fuel cell. In the fuel cell, an electrochemical reaction occurs, transforming DC electrical energy converted to hydrogen's chemical energy. A DC load that is voltage-sensitive can be used to represent the electrical circuit of an electrolyzer. This means that as the applied voltage increases, the circulating load current also increases, resulting in the production of more hydrogen. Figure 3.8 illustrates the circuit equivalent of a single PEM electrolyzer.

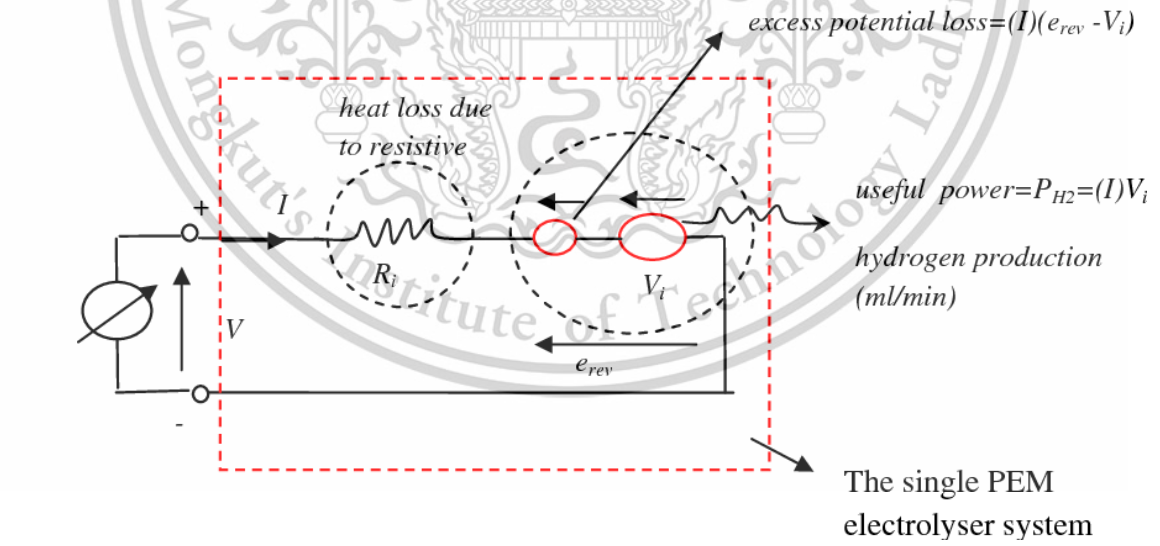

Figure 3.8 Equivalent circuit for single PEM electrolyzer

To do the simulation, a MATLAB/Simulink equivalent circuit of the PEM electrolyzer is developed as described in Figure 3.9. Certain equations representing steady state conditions have been created and incorporated into MATLAB/Simulink in order to determine the current-voltage and hydrogen generation characteristics. The I-V characteristics of a single PEM electrolysis cell can be simulated by the following equation (*3.10*) and equation (*3.11*).

$$V(T,P) = e_{rev}(T,P) - e_{rev}(T,P)e^{-\frac{5I}{0.02}} + IR_i(T,P) \tag{3.10}$$

$$I(T,P) = \begin{bmatrix} 0 & V \leq e_{rev}(T,P) \\ \dfrac{1}{R_i(T,P)} & V \geq e_{rev}(T,P) \end{bmatrix} \tag{3.11}$$

where V(T, P) = voltage at defined temperature and pressure, I(T, P) = current at defined temperature and pressure, e_{rev} (T, P) = reversal voltage under specific pressure and temperature conditions, I = input current and R_i = initial PEM cell resistance

The PEM electrolyzer's I-V characteristic curve shows the critical voltage point at which the current begins to flow. The region that represents current flow can be reasonably considered as linear, even though the characteristic is intrinsically non-linear. The PEM electrolyzer cell's internal resistance is indicated by the slope of this linear approximation. Equations (*3.10*) for non-linear features and (*3.11*) for linear modes can be used to effectively fit the I-V characteristic of the electrolyzer model to curves. The electrolyzer model can also be represented in a non-linear manner.

When the current reaches 0.02A, the second component of the equation (*3.10*) becomes insignificant. It changes the reverse voltage's linear function, erev. The active electrolysis zone is described by this linear portion of the equation.

Equation (*3.12*) defines R_i, which may be empirically modeled using temperature and pressure data.

$$R_i(T,P) = R_{i_0} + k\,ln\left(\frac{P}{P_0}\right) + dR_t(T - T_0) \tag{3.12}$$

where k = derived curve fitting parameter = 0.0395 V/A, P_0 = reference pressure = 1 atm, T_0 = reference temperature = 25 °C, dRt = resistance coefficient of temperature.

It is also possible to represent the reverse voltage, e_{rev}, empirically. The reversible potential as described in equation (*3.13*) represents the cell's minimal energy barrier.

$$e_{rev}(T,P) = e_{rev0} + \frac{kR(273+T)}{2F} ln\left(\frac{P}{P_0}\right) \quad (3.13)$$

where R = universal gas constant (J/K.mol) and F = Faraday constant (C/mol)

It is determined what the optimal voltage V_i is for electrolysis and hydrogen production by the following equation (*3.14*):

$$V_i = \frac{\Delta G}{2F} \quad (3.14)$$

where ΔG = Gibbs free energy change (J/mol)

The input I-V curve of the PEM electrolyzer cell as a function of temperature and pressure can be expressed as the equation (*3.15*) by simplifying equations (*3.10*) and (*3.11*).

$$V(T,P) = IR_i(T,P) + e_{rev}(T,P) \quad (3.15)$$

Equation (*3.16*) defines the hydrogen generation rate (ml/min), which may be computed as a function of I(T,P).

$$V_H = V_m I\left(\frac{10^3 ml}{l}\right)\left(\frac{60s}{min}\right)\left(\frac{I\left(\frac{C}{s}\right)}{2F\ (C)}\right) = \frac{6000V_m I}{2F} \quad (3.16)$$

where V_m = one molar volume as determined by the ideal gas formula as the equation (*3.17*).

$$V_m = \frac{R(273+T)}{P} \quad (3.17)$$

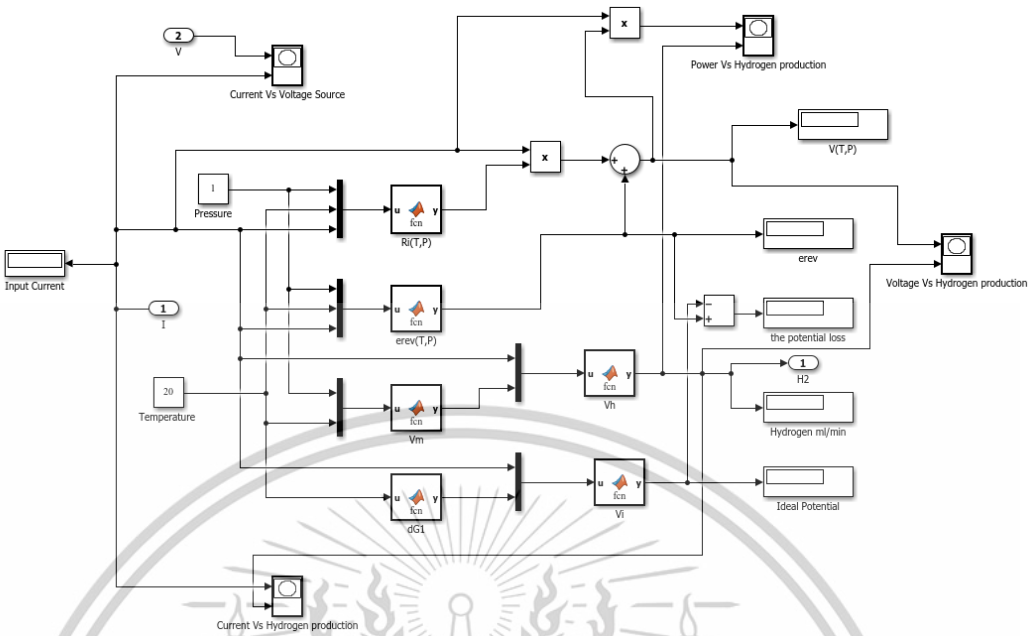

Figure 3.9 MATLAB/Simulink model for PEM electrolyzer

In this study, the reversible potential e_{rev} with relation to the ideal voltage (V_i) is computed to be 1.476V. The PEM subsystem is established at 0.326 ohms of resistance (R_i) under normal temperature and pressure conditions. These values have been verified through the MATLAB/Simulink module. Equation (*3.11*) describes the electrolyzer's input current, and equation (*3.16*) is used to calculate the rate at which hydrogen is produced (V_H).

In order to streamline and determine the PEM electrolyzer's input off I-V model as a function of temperature and pressure during steady state operation, equation (*3.10*) is applied. Figure 3.9 presents the static PEM electrolyzer model, facilitating a comparison with the experimental results.

3.2.4 Hydrogen Tank Modeling

Compressed hydrogen gas or liquid hydrogen can be stored in tanks using a variety of methods, including physical hydrogen storage. A MATLAB/Simulink dynamic module for the tank is created in order to store the hydrogen gas produced by the electrolyzer and can be represented as following equation (*3.18*).

$$P_b - P_{bi} = Z \times \frac{N_{H_2} R T_b}{P M_{H_2} V_b} \tag{3.18}$$

where P_b = the tank pressure (Pascal), P_{bi} = initial pressure of the storage tank (Pascal), Z = compressibility factor, R = universal gas constant (J/kmol. K), T_b = operating temperature (K), V_b = the tank volume (m^3) and as shown in equation (*3.19*).

$$Z = \frac{RV_m}{PT} \tag{3.19}$$

where P = pressure, V_m = molar volume and T = temperature

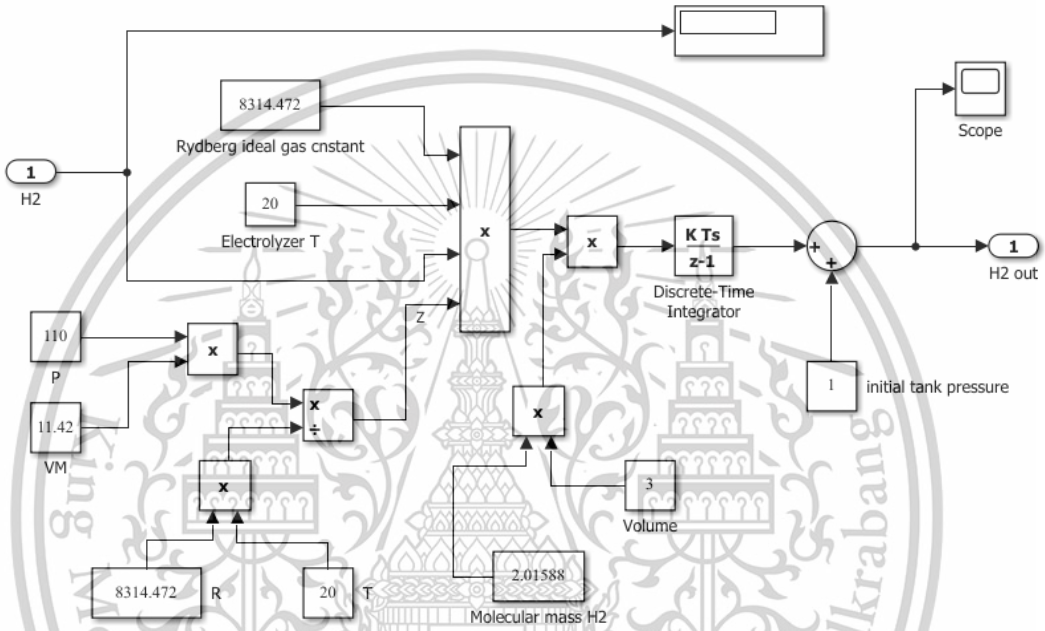

Figure 3.10 MATLAB/Simulink model for hydrogen storage system

It has been observed that the model takes into account the ratio of the hydrogen flow rate to the tank while calculating the tank pressure. To obtain the stored hydrogen supplied to the fuel cell or other uses, Equation (*3.18*) is applied in Simulink. The system for storing hydrogen is represented by its Simulink model as illustrated in Figure 3.10.

3.2.5 Renewable Energy System Modeling

The simulation is conducted within Simulink/MATLAB environment, where each component is individually created. This approach enables easy error control and debugging of simulation blocks. Every system block is implemented with precision and examined to make sure precision in running the simulation and obtaining satisfactory

results. Modules for the electrolyzer, DC/DC converter, PV solar panels, and hydrogen tank are developed and carefully coordinated. The simulation is applicable for modeling various scenarios. Figure 3.11 shows the model representing the entire system.

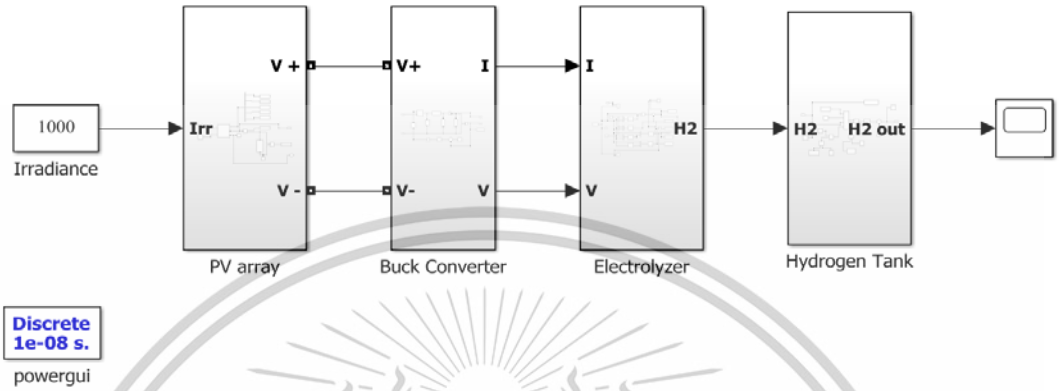

Figure 3.11 MATLAB/Simulink model for the whole renewable energy system

3.3 Experimental Setup

3.3.1 Experimental Electrolyzer Model

The experimental setup utilized in this research incorporates a rebuildable PEM (proton exchange membrane) electrolyzer which is manufactured from h-tec education. The membrane electrode assembly (MEA) is an essential part of this electrolyzer. The MEA comprises two electrodes, namely the cathode and anode, sandwiching a solid polymer electrolyte membrane. This membrane is permeable to protons while forming a barrier for electrons, featuring catalyst layers on both sides. The catalyst loading for this MEA is 2 mg/cm^3 of iridium ruthenium oxide ($IrRuO_x$) on the anode side and 0.5 mg/cm^3 of 60% platinum supported on carbon (PtC) on the cathode side. Alternative name for this type of membrane is catalyst coated membrane (CCM) and it is a backbone of the MEA. The electrolyzer has an electrode area of 16 cm^2 and incorporates two glass tubes for water and gas storage. Each of the two tubes, filled with de-ionized water, is connected to the respective sides of the two electrodes. Figure 3.12 is the PEM electrolyzer used in the experiment and Figure 3.13 shows the components of the electrolyzer.

Figure 3.12 PEM electrolyzer used in the experiment

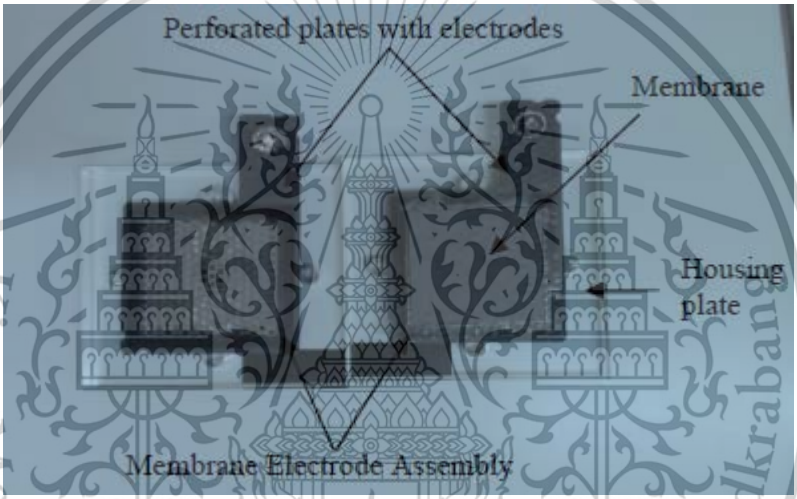

Figure 3.13 Components of PEM electrolyzer

Table 3.3 shows the parameters of the PEM electrolyzer used in the experiment.

Table 3.3 Known parameters of the electrolyzer

Parameter	Value
Electrode area	16 cm2
Membrane type	NafionTM 115
Membrane area	12.25 cm^2
Membrane thickness	127 micrometers

3.3.2 Principle of PEM Water Electrolysis

Water is separated into hydrogen and oxygen using a PEM electrolyzer in PEM water electrolysis. The PEM electrolyzer functions by applying a direct current in order

to disintegrate water molecules, generation diatomic hydrogen and oxygen. The basic equation for this process is as below.

$$2H_2O(l) + Electrical\ energy \rightarrow 2H_2(g) + O_2(g) \quad (3.20)$$

The key principle involves utilizing an electrolyte that is a proton exchange membrane which selectively conducts protons (H^+ ions) while blocking the passage of electrons. For electrolysis cell setup, anode and cathode in the electrolyzer are divided by a PEM. PEM is a solid polymer electrolyte that is usually composed of a substance called perfluorinated sulfonic acid. Electrons must travel via an external circuit, and only protons are permitted to pass through. An electrical voltage is applied across the anode and cathode, initiating the electrolysis process. Figure 3.14 demonstrates the working principle of PEM electrolyzer.

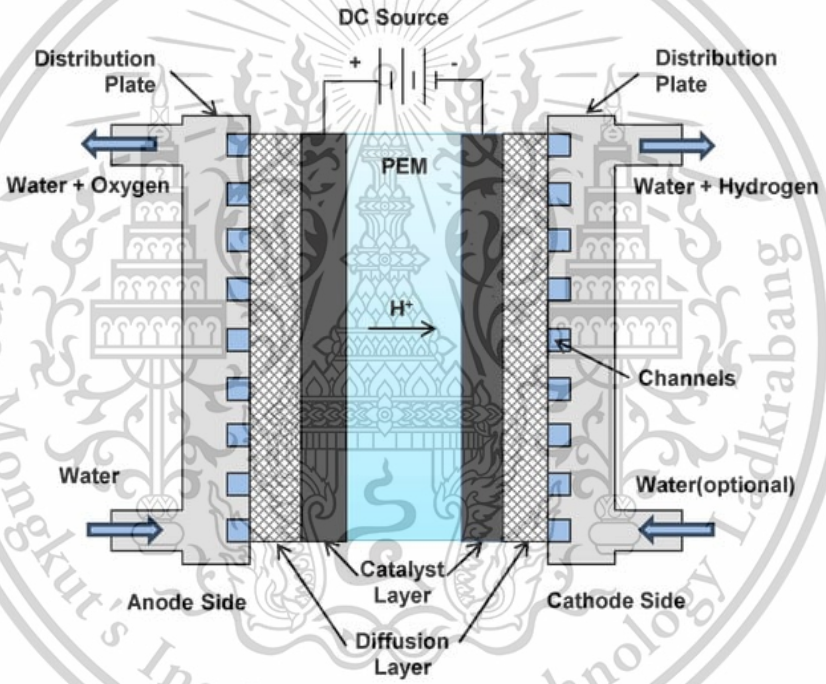

Figure 3.14 Schematics of PEM electrolyzer cell

The water is delivered to the anode side of the electrolyzer cell where it oxidizes, leading to the release of oxygen gas (O_2), hydrogen protons with a positive charge (H^+ ions) and electrons. The oxygen produced in this half-cell reaction is then eliminated along with the leftover water as the equation (*3.21*).

$$2H_2O \rightarrow O_2 + 4H^+ + 4e^- \quad (3.21)$$

Protons travel from the DC power source to the cathode via the electrolyte membrane, where they mix with electrons., resulting in the formation of hydrogen gas (H_2) as the equation (*3.22*). Water can optionally be supplied to the cathode side in order to improve the effectiveness of hydrogen extraction.

$$4H^+ + 4e^- \rightarrow 2H_2 \quad (3.22)$$

The net reaction for water electrolysis is the combination of cathode and anode reactions as the equation (*3.23*) .

$$2H_2O(l) \rightarrow 2H_2(g) + O_2(g) \quad (3.23)$$

For the electron flow, electrons generated during the water splitting reaction at the anode cannot pass through the PEM, so they produce an electric current when they pass through an external circuit.

3.3.3 Schematic diagram

The process of producing hydrogen by PV integrated water electrolysis involves two stages. First, photonic energy is transformed into electrical energy using photovoltaic panels to generate electricity. Next, water electrolysis is electrochemically transformed to produce hydrogen using electrical energy. The hydrogen production process using the PV-PEM water electrolysis device is shown in Figure 3.15.

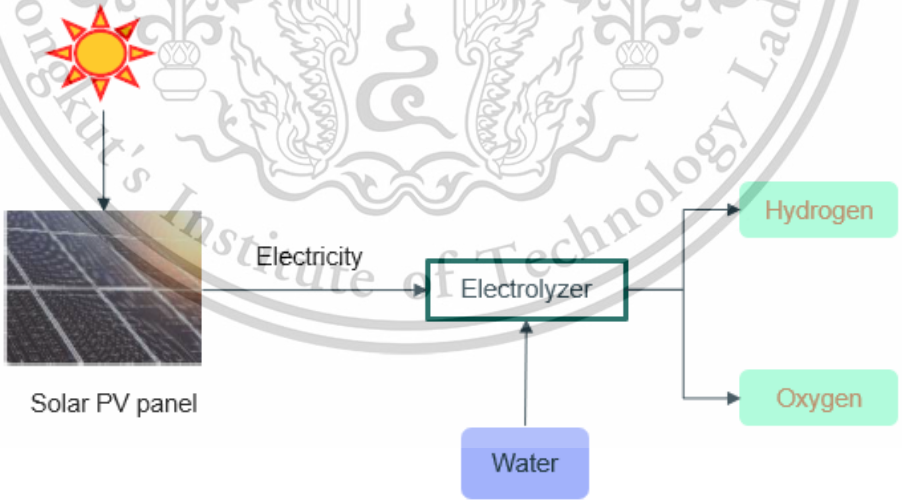

Figure 3.15 Schematic diagram of hydrogen production system

In the experiment, water molecules are broken down by an electrical current using a one-cell rebuildable PEM electrolyzer to create hydrogen and oxygen. Adjustable DC pump is used for the water input to the electrolyzer. The experiment is done with AC power supply. Therefore, AC to adjustable DC converter is utilized to provide the electrolyzer with current. Generated hydrogen is stored in storage 80 from h-tec education. The experimental hydrogen generation system using PV-PEM water electrolysis is shown in Figure 3.16.

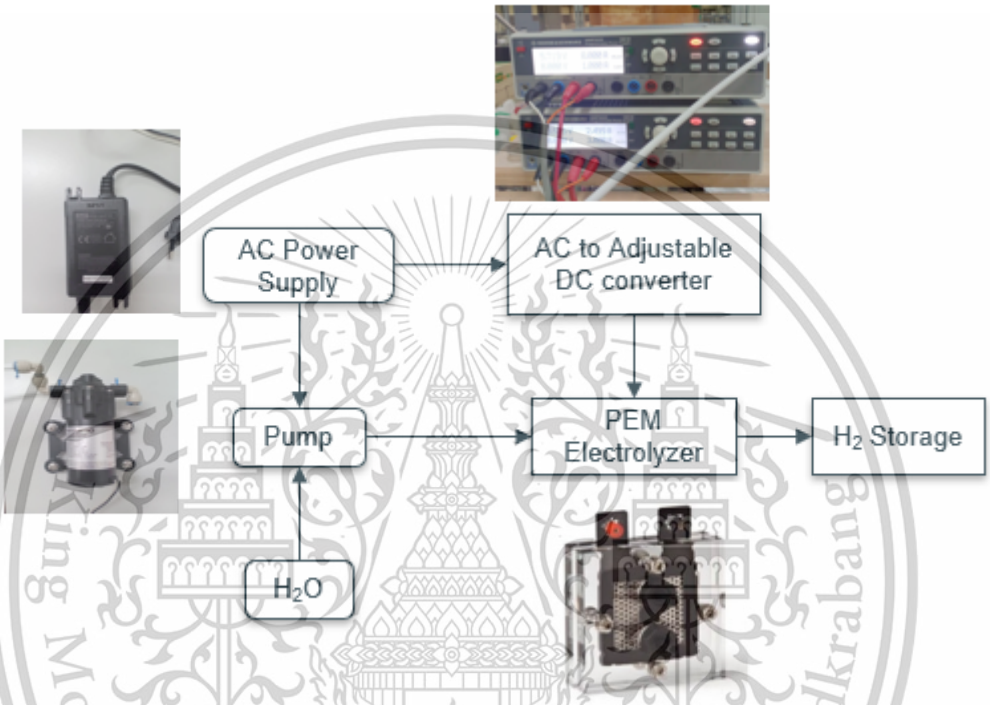

Figure 3.16 Schematic diagram of experimental hydrogen production via PEM water electrolysis

3.4 Research Computational Procedure

3.4.1 Thermodynamics

Thermodynamics plays a crucial role in understanding and analyzing PEM water electrolysis which is a procedure that turns water into hydrogen. Thermodynamic principles involved in this process help access its efficiency and feasibility. The behavior of energy and matter in the universe is governed by the fundamental principles known as the laws of thermodynamics. Whether a system is basic or complicated, these principles offer a foundation for comprehending and forecasting its behavior. There are four laws.

PEM water electrolysis operates in accordance with the laws of thermodynamics, primarily involving the first and second laws. The first law of thermodynamics is the law of energy conversation. PEM electrolysis complies with the first law, which stipulates that energy can only change forms and cannot be created or destroyed. In the context of electrolysis, electrical energy is input into the system to encourage the water's split into hydrogen and oxygen. The energy provided is used to overcome the energy required for the processes taking place at the anode and cathode to activate.

PEM water electrolysis also aligns with the second rule of thermodynamics, which addresses entropy. According to the second law, natural processes tend to become more chaotic or unpredictable. In the case of water electrolysis, the separation of water into hydrogen and oxygen involves a decrease in order (water) and an increase in disorder (individual hydrogen and oxygen molecules). This process contributes to the overall increase in entropy as required by the second law.

While PEM water electrolysis itself does not directly involve the zero law or third law of thermodynamics, these laws are fundamental to the broader understanding and application of thermodynamics. The zero law introduces the concept of temperature, and the third law sets a reference point for entropy calculations which are relevant in more extensive thermodynamic considerations[38].

3.4.2 Gibbs Free Energy

The relationship of PEM electrolysis and Gibbs free energy is fundamental in understanding the thermodynamics of the process. Gibbs free energy is a key parameter that determines the spontaneity of a reaction and provides insights into the feasibility of electrochemical processes. The thermodynamic potential known as Gibbs free energy (G), combines entropy (S) and enthalpy (H) to forecast a process spontaneity as well as the most reversible work that a system is capable of performing at constant pressure and temperature. The Gibbs free energy is defined by the following equation (*3.24*).

$$G = H - TS \tag{3.24}$$

where G = Gibbs free energy, H = enthalpy, T = temperature (K) and S = entropy

The change in Gibbs free energy (ΔG) can be used to identify a process as spontaneous or non-spontaneous when it is happening at constant temperature and pressure.

When ΔG is less than zero, the process is spontaneous, and the reaction will proceed in the forward direction.

When ΔG is greater than zero, the process is non-spontaneous as is, but it may be spontaneous in the reverse direction.

When ΔG = 0, The process is reversible and the system is in equilibrium.

The relationship between ΔG, ΔH (change in enthalpy) and Δs (change in entropy) is given by the following equation (*3.25*).

$$\Delta G = \Delta H - T\Delta S \tag{3.25}$$

The change in molar Gibbs free energy of formation ($\Delta\bar{G}_f$) specifically refers to the change under the standard conditions. Standard conditions typically imply a pressure of 1 bar and a temperature of 298K. The equation (*3.26*) shows the formation of ($\Delta\bar{G}_f$).

$$\Delta\bar{G}_f = \Delta\bar{H}_f + T\Delta\bar{S} \tag{3.26}$$

where $\Delta\bar{H}_f$is the change in molar enthalpy of formation (J/mol) and $\Delta\bar{S}$ is the change in molar entropy (J/mol) [39].

3.4.3 Enthalpy of Formation

The change in molar enthalpy of formation ($\Delta\bar{H}_f$) in PEM electrolysis refers to the enthalpy change brought about by product production from their elemental forms under standard conditions. To calculate $\Delta\bar{H}_f$, It is necessary to consider the enthalpies of formation for the reactants and products and is calculated as the equation (*3.27*).

$$\Delta\bar{H}_f = \sum\left(\Delta\bar{H}_f\ of\ products\right) - \sum\left(\Delta\bar{H}_f\ of\ reactants\right) \tag{3.27}$$

For the PEM electrolysis, the primary products are hydrogen gas and oxygen gas, and the reactant is water. Therefore, the change in molar enthalpy of formation in PEM electrolysis is as the following equation (*3.28*).

$$\Delta\bar{H}_f = \left(\bar{H}_f\right)_{H_2} + \frac{1}{2}\left(\bar{H}_f\right)_{O_2} - \left(\bar{H}_f\right)_{H_2O} \tag{3.28}$$

The molar enthalpy of formation of each substance changes with the reaction temperature and is calculated depending on the molar heat capacity ($\bar{c}_p$). The standard molar enthalpy of formation at ambient temperature is as the following equation (*3.29*).

$$\bar{H}_{T_r} = \bar{H}_{298.15} + \int_{298.15}^{T_r} \bar{c}_p\, dT \tag{3.29}$$

3.4.4 Entropy

Entropy changes result from the electrochemical reactions that happen at the anode and cathode during PEM electrolysis. The anode half-reaction involves the oxidation of water molecules. The water molecules lose electrons during oxidation, turning into protons and oxygen gas. The breaking of chemical bonds and the formation of new bonds contribute to changes in entropy. The cathode half-reaction involves the reduction of protons by gaining electrons to form hydrogen gas. Like the anode reaction, changes in entropy occur due to the breaking and formation of chemical bonds.

The change in entropy ($\Delta\bar{S}$) in PEM electrolysis refers to the change in entropy connected to the formation of products from their elemental forms under standard conditions. The standard entropy change for this reaction can be calculated as the difference between the sum of the standard entropies of the products and the sum of the standard entropies of the reactants as the equation (*3.30*).

$$\Delta\bar{S} = \sum\left(\Delta\bar{S}_f \; of \; products\right) - \sum\left(\Delta\bar{S}_f \; of \; reactants\right) \tag{3.30}$$

For the PEM electrolysis, the primary products are hydrogen gas and oxygen gas and the reactant is water. Therefore, the change in molar entropy in PEM electrolysis is as the following equation (*3.31*).

$$\Delta\bar{S} = \left(\bar{S}_f\right)_{H_2} + \frac{1}{2}\left(\bar{S}_f\right)_{O_2} - \left(\bar{S}_f\right)_{H_2O} \tag{3.31}$$

The molar entropy of each substance changes with the temperature of the reaction and is calculated depending on the molar heat capacity ($\bar{c}_p$). The standard molar entropy at ambient temperature is as the equation (*3.32*).

$$\bar{S}_{T_r} = \bar{S}_{298.15} + \int_{298.15}^{T_r} \frac{1}{T}\bar{c}_p \, dT \tag{3.32}$$

3.4.5 Molar Enthalpy of Formation and Molar Entropy

Table 3.4 Molar enthalpy of formation and molar entropy at 298.1K

	$\bar{H}_{298.15}$ (kJ/mol)	$\bar{S}_{298.15}$ (J/mol.K)
H_2O (liquid)	-285.84	70.05
H_2O (steam)	-241.83	188.83
H_2	0	130.59
O_2	0	205.14

The molar entropy and molar enthalpy of formation values for water, oxygen, and hydrogen at room temperature are listed in Table 3.4.

The molar heat capacity is acquired from the tables of thermodynamics. The molar heat capacity for liquid water is specified as the equation (*3.33*).

$$\bar{c}_p = 75.79\, J.mole^{-1}.K^{-1} \tag{3.33}$$

The molar heat capacity of hydrogen under constant pressure is expressed as the equation (*3.34*).

$$\bar{c}_p = 56.5 - 2.2 \times 10^4 T^{-0.75} + 1.17 \times 10^5 T^{-1} - 5.6 \times 10^5 T^{-1.5} \tag{3.34}$$

And concerning oxygen, the molar heat capacity under constant pressure is provided as the equation (*3.35*).

$$\bar{c}_p = 29.15 + 6.45 \times 10^{-3} T^{-1} - 0.18 \times 10^6 T^{-2} - 1.02 \times 10^{-6} T^{-3} \tag{3.35}$$

3.4.6 Faraday's Laws

The relationship between the amount of chemical change that occurs during electrolysis and the quantity of electrical charge passed through a conducting solution is described by Faraday's laws of electrolysis. These laws are fundamental in understanding electrochemical processes. Faraday's laws can be applied to understand the relationship between the electrical charge passed through the electrolyzer and the amount of hydrogen and oxygen produced in water electrolysis. The stoichiometry of the electrolysis reaction provides the values of n and z (electrochemical valency or number of electrons exchanged per ion in the reaction) to produce hydrogen and oxygen [40]. The equation (*3.36*) gives the relationship between stoichiometry and mass of the substance.

$$m = n.z.F \tag{3.36}$$

where m = mass of the substance deposited or liberated

For hydrogen production, the quantity of electrons exchanged in moles throughout the reaction is 4 and electrochemical valency is 2. For oxygen production, the quantity of electrons that were exchanged during the reaction in moles is 4 and electrochemical valency is 4. The mass of hydrogen and oxygen produced in PEM electrolysis can be calculated in relation to the amount of electricity that passes through the electrolyte using Faraday's laws.

3.4.7 Voltage

In PEM water electrolysis, two voltages are essential for energy computation. They are the reversible cell voltage known as the water electrolysis voltage and the enthalpy voltage, often referred to as thermo-neutral voltage.

3.4.7.1 Reversible Voltage

During the electrolysis process, every molecule of water consumed or hydrogen created involves two electrons traveling through the external circuit. The charge transferred through the external circuit for one mole of hydrogen is expressed by the following equation (*3.37*).

$$Charge\ per\ mole = -2eN_a = -2F \tag{3.37}$$

where Faraday constant (F) = the amount of electric charge carried by one mole of electrons = 96485 C/mol, e = charge of one electron = $1.602\times10_{-19}$ coulombs, N_a = Avogadro's number = 6.022×10^{23}.

An electrochemical reaction's change in molar Gibbs free energy ($\Delta\bar{G}$) is defined as the energy that can be used for external work, minus any work that is done as a result of pressure and volume changes. The movement of electrons across the external circuit is referred to as external work in the electrolyzer. In a lossless system, this external work will align with the electrical work and the formula is as equation (*3.38*).

$$\Delta\bar{G} = nFV_{rev} \tag{3.38}$$

where V_{rev} = voltage of the electrolyzer without losses or reversible potential of the electrolyzer and n = number of moles of electrons per mole of product.

The reversible cell voltage is the lowest required cell voltage for water breakdown and the reversible voltage of the electrolyzer cell is calculated as the equation (*3.39*) [41].

$$V_{rev} = \frac{\Delta\bar{G}}{nF} \tag{3.39}$$

In PEM water electrolysis, the stoichiometry of the electrochemical processes that take place throughout the electrolysis process determines how many moles of electrons there are per mole of product. The primary processes in PEM water electrolysis are the reduction of protons to generate hydrogen gas at the cathode and the oxidation of water at the anode. By examining the half-reactions, four moles of electrons are involved in the reduction of four protons to produce two moles of

hydrogen gas. Similarly, four moles of electrons are released during the oxidation of two moles of water to produce four moles of protons and one mole of oxygen gas. Therefore, the overall reaction results in the net production of two moles of hydrogen gas and one mole of oxygen gas. The value of n is 2 and is the reversible voltage is calculated as the equation (*3.40*).

$$V_{rev} = \frac{\Delta \bar{G}}{2F} \tag{3.40}$$

3.4.7.2 Enthalpy Voltage

The enthalpy of formation represents the energy discharged while a fuel burns, also known as the calorific value. The term lower heating value (LHV) refers to the water in the reaction that is in steam form. It goes by the name net calorific value (NCV) as well. It is known as the higher heating value (HHV) when referring to liquid water. Gross calorific value (GCV) is another name for it. LHV considers the heat released when water vapor is condensed (water in steam form) during combustion. HHV considers the heat released when water vapor remains in the gaseous state during combustion.

The enthalpy voltage which is often referred to as thermo-neutral cell voltage is associated with the heat change in the reaction. When the water splits, a certain amount of entropy is generated. As a result, enthalpy should be used to calculate the potential rather than Gibbs free energy. The enthalpy voltage, which is the lowest energy required for water electrolysis, is therefore connected to the enthalpy change in reaction. The enthalpy voltage is calculated as the equation (*3.41*) [42].

$$V_{TN} = \frac{\Delta \bar{H}}{nF} = \frac{\Delta \bar{H}}{2F} \tag{3.41}$$

where V_{TN} = thermo-neutral voltage or enthalpy voltage

3.4.8 Hydrogen Flow

In the external circuit, two electrons move for each mole of hydrogen produced.

$$Charge\ per\ mole = -2F \tag{3.42}$$

The calculation of hydrogen flow rate in the PEM electrolyzer is based on Faraday's laws of electrolysis. This is determined by the charge carried by one mole of electrons circulating through the external circuit, as expressed in the equation (*3.43*).

$$Total\ charge = -2Fn_{H_2} \tag{3.43}$$

where n_{H_2} = total moles of hydrogen generated

The equation (*3.43*) is divided on both sides by time (t) and its rearranging gives as the equation (*3.44*).

$$\frac{Total\ charge}{t} = -\frac{2Fn_{H_2}}{t} \tag{3.44}$$

The movement of an electric charge via a conductor is known as electric current. The formula for electric current (I) is defined as the rate of flow of electric charge through the conductor which is the ratio of electric charge (Q) to the time during which the charge flows (t) and is expressed as the equation (*3.45*).

$$I = \frac{Q}{t} \tag{3.45}$$

The equation (*3.45*) is taken as the absolute value and substituted with the equation (*3.45*) as the equation (*3.46*).

$$I = \frac{2Fn_{H_2}}{t} \tag{3.46}$$

Hydrogen flow rate is the ratio of total amount of mole of generate hydrogen to the time and is described as the equation (*3.47*).

$$I = 2F \times H_2\ flow \tag{3.47}$$

Therefore, Hydrogen flow is rearranged as the equation (*3.48*).

$$H_2\ flow = \frac{I}{2F}\left(\frac{mole}{s}\right) \tag{3.48}$$

The equation (*3.48*) is multiplied by hydrogen mass in which molar mass of hydrogen is 1.01 g/mol and molecular mass of hydrogen is 2 times of molar mass which is 2.02 g/mol which equals to 2.02×10^{-3} kg/mol and divided by density of hydrogen which is 0.08375 kg/m^3 and it gives the equation (*3.49*).

$$H_2\ flow = \frac{I}{2F} \times \frac{2.02}{0.08375} = 1.246 \times 10^{-7} \times I\ \left(\frac{m^3}{s}\right) \tag{3.49}$$

The above equation is the volumetric hydrogen flow and is changed from m^3/s to ml/min by multiplying 60×10^6 of the equation (*3.50*).

$$H_2\ flow = 7.477 \times I\ \left(\frac{ml}{min}\right) \tag{3.50}$$

3.4.9 Efficiency

Efficiency refers to the effectiveness with which chemical energy is transformed from electrical energy and is then stored as hydrogen gas. There are several types of efficiency relevant to assessing the performance of PEM electrolysis system.

3.4.9.1 Voltage Efficiency

The efficiency with which electrical energy is transformed into chemical energy during the water electrolysis process to produce hydrogen gas is measured by voltage efficiency in PEM water electrolysis. Voltage efficiency is often expressed as a ratio of the theoretical minimum required voltage for electrolysis (reversible cell voltage) to the actual applied voltage. The voltage efficiency (η_{votage}) can be expressed using the equation (*3.51*).

$$\eta_{votage} = \frac{V_{rev}}{V_{actual}} \times 100\ \% \tag{3.51}$$

According to the first law of thermodynamics, it is stated that energy is conserved. Evaluating the transfer of electrical energy to chemical energy yields conversion efficiency. For water electrolysis, the conventional method of calculating efficiency involves considering the higher heating value (HHV) of hydrogen. Since the electrolysis process requires the supply of water in liquid form to the cell, the efficiency is computed using the equation (*3.52*).

$$\eta_{Voltage} = \frac{V_{TN}}{V_{actual}} \times 100\ \% \tag{3.52}$$

3.4.9.2 Faradaic Efficiency

Faradaic is also called as current efficiency. The degree to which electrical current is efficiently used to propel the intended electrochemical reactions that result in the creation of hydrogen gas is known as the faradaic efficiency in PEM water electrolysis. In order to evaluate the flow of electrons to the cathode and anode surfaces via the external circuit and support electrochemical reactions in the electrolytes, such as the hydrogen evolution reaction (HER) and the oxygen evolution reaction (OER), faradaic efficiency is measured. Therefore, the ratio of the experimentally evolved volume of hydrogen during electrolysis to the theoretically calculated volume of hydrogen based on Faraday's principles is known as the faradaic efficiency ($\eta_{Faraday}$) and is expressed as the equation (*3.53*).

$$\eta_{Faraday} = \frac{V_{H_2}(experimental)}{V_{H_2}(theorical)} \times 100\ \% \quad (3.53)$$

The theoretical moles of hydrogen produced are determined based on the supplied electrical charge and the Faraday constant (F) as the equation (*3.54*). The charge of one mole of electrons is represented by the Faraday constant and is approximately 96,485 coulombs per mole [29].

$$Theoretical\ moles\ of\ hydrogen = \frac{Charge\ (coulombs)}{2F} \quad (3.54)$$

3.4.9.3 Overall Efficiency

Overall efficiency provides a comprehensive measure of how effectively the PEM electrolysis system converts electrical energy into usable hydrogen. The overall efficiency represents the combined efficiency of the electrolyzer, including both the electrochemical efficiency and any losses in the supporting systems such as heat losses and electrical losses. Overall efficiency can be computed as voltage efficiency multiplied by current efficiency excluding the losses due to the power consumption as the equation (*3.55*).

$$\eta_{Overall} = \eta_{Voltgae} \times \eta_{Faraday} \quad (3.55)$$

3.4.9.4 Solar to Hydrogen Efficiency

The efficiency of solar-to-hydrogen (STH) conversion is also known as solar hydrogen efficiency. It stands for the efficiency of using solar energy to electrolyze water to create hydrogen. The effectiveness of transforming solar energy into chemical energy stored in hydrogen is known as STH efficiency. It is determined by dividing the amount of hydrogen molecules' Gibbs free energy by the amount of solar energy required to produce hydrogen as the equation (*3.56*) [43].

$$STH = \frac{Energy\ stored\ in\ hydrogen}{Solar\ energy\ input} \times 100\% \quad (3.56)$$

3.5 Irreversibility

Irreversibility is a more accurate term for characterizing inefficiencies in both electrochemical and thermodynamic systems. It is a non-irreversible loss if the energy is recoverable. It is an irreversible loss of energy if it is not possible to regain it. In electrolyzers, irreversibility appears in the form of overpotentials summed to the reversible potential. Overpotentials are additional voltage requirements beyond the

thermodynamic voltage needed for the electrolysis reactions to proceed. In the context of PEM water electrolysis, irreversibility refers to the inherent inefficiencies and losses in the process of producing hydrogen electrochemically from water. While idealized thermodynamic models assume reversible processes, electrolysis systems experience various irreversibilities leading to decreased efficiency and energy consumption. There are three main types of overpotentials.

3.5.1 Activation Overpotential

In electrochemistry, the activation overpotential is a phenomenon that happens when more energy is needed to start and propel electrochemical reactions at the electrodes. It represents the energy barrier that must be overcome to start the reaction and is associated with the kinetic limitations of the electrochemical process. Activation overpotential is a measure of the difficulty in initiating and sustaining the desired electrochemical reaction. Reactions at the electrode surface are happening too slowly, which leads to the activation overpotential. When driving the chemical reaction that causes electrons to transfer to or from the electrode, part of the voltage that is generated is lost. At smaller currents, the current has a greater influence on this overpotential, which is very nonlinear. Activation overpotential can be expressed using Tafel's equation, which relates the overpotential to the exchange current density and the reaction rate constant as the equation (*3.57*).

$$\eta_{act} = \frac{RT}{\alpha F}\ln\left(\frac{i}{i_0}\right) \tag{3.57}$$

where η_{act} = activation overpotential, R = the gas constant (8.314 J/mol.K), α = the charge transfer coefficient (a dimensionless parameter between 0 and 1), i = the actual current density and i_0 = the exchange current density

This equation indicates that activation overpotential is influenced by the ratio of the actual current density to the exchange current density. A higher ratio leads to a larger activation overpotential. The ln function indicates a logarithmic relationship, meaning that small changes in the ratio can lead to significant changes in the activation overpotential. Researchers and engineers use this formula to understand and optimize electrochemical processes, such as in fuel cells and electrolysis, by minimizing activation overpotential for improved efficiency.

3.5.2 Ohmic Overpotential

In electrochemistry, ohmic overpotential is a phenomenon that results from the resistance that icons face while passing through the electrodes and electrolyte. It

represents the voltage drop caused by the electrical resistance within the electrochemical cell. Ohmic overpotential is a significant factor influencing the overall efficiency of an electrochemical process. The formula for calculating ohmic overpotential is derived from Ohm's Law and gives the equation (*3.58*).

$$\eta_{ohm} = IR_{total} \tag{3.58}$$

where η_{ohm} = ohmic overpotential, I = the current passing through the cell and R_{total} = the total resistance of the cell and it is expressed in the equation (*3.59*).

$$R_{total} = R_{electrode} + R_{electrolyte} + R_{interfacial} + R_{external} \tag{3.59}$$

where $R_{electrode}$ = resistance associated with the electrodes, $R_{electrolyte}$ = resistance encountered by ions when they pass through the electrolyte, $R_{interfacial}$ = resistance at the interfaces between the electrodes and the electrolyte and $R_{external}$ = resistance in the external circuit including connectors and conductors outside the electrochemical cell

The equation (*3.58*) indicates that Ohmic overpotential and cell current flow are directly proportional and the total resistance of the system. Higher currents and higher resistances lead to increased ohmic overpotential, which can contribute to energy losses and decreased efficiency in electrochemical processes.

Efforts to minimize ohmic overpotential involve optimizing the design of the electrochemical cell, selecting materials with lower resistivity, and maintaining suitable operating conditions. Enhancing the efficiency of electrochemical devices, including fuel cells and electrolyzers, requires lowering the total resistance inside the cell.

3.5.3 Concentration Overpotential

Concentration overpotential which is also known as mass transport overpotential, is a phenomenon in electrochemistry that arises due to concentration gradients of reactants or products near the electrodes. It represents the additional voltage required to overcome the limitations in the mass transport of species to or from the electrode surfaces. Concentration overpotential is a significant factor influencing the efficiency and kinetics of electrochemical reactions. The Butler-Volmer equation can be used to represent the expression for concentration overpotential. The concentration of reactants or products at the electrode-electrolyte interface is correlated with the concentration overpotential. In the context of the cathodic reaction, it is as the equation (*3.60*).

$$\eta_{conc(cathode)} = \frac{RT}{\alpha_c nF} \ln\left(\frac{C_{H_2}}{C_{0,H_2}}\right) \quad (3.60)$$

where $\eta_{conc(cathode)}$ = concentration overpotential at the cathode, α_c = charge transfer coefficient of the cathode, n = the number of electrons transferred in the electrochemical reaction, C_{H_2} = the actual concentration of hydrogen at the electrode interface and C_{0,H_2} = the standard concentration of hydrogen

This formula shows that the ratio of the reactant concentration at the electrode surface to the concentration of the reactant in the bulk of the electrolyte affects concentration overpotential. The ln function implies a logarithmic relationship, and the overpotential is sensitive to changes in concentration gradients.

CHAPTER 4
RESULTS AND PERFORMANCE ANALYSIS

4.1 Solar Panel Positioning

4.1.1 Sun Path

Sun path is the apparent path that the sun follows in the sky as observed from a specific location on Earth. This path is a result of the rotation of the Earth on its axis and its orbit around the sun. The location of the sun in the sky changes throughout the day and changes with the seasons as a result of the Earth's axis tilt. For solar energy system design, understanding the path of the sun is vital for optimizing the placement and orientation of solar panels. A sun path diagram shows the sun's travel across the sky at a certain place throughout the course of a day or a year. It provides valuable information for architects, urban planners, and designers to understand the sun's movement and its impact on the built environment

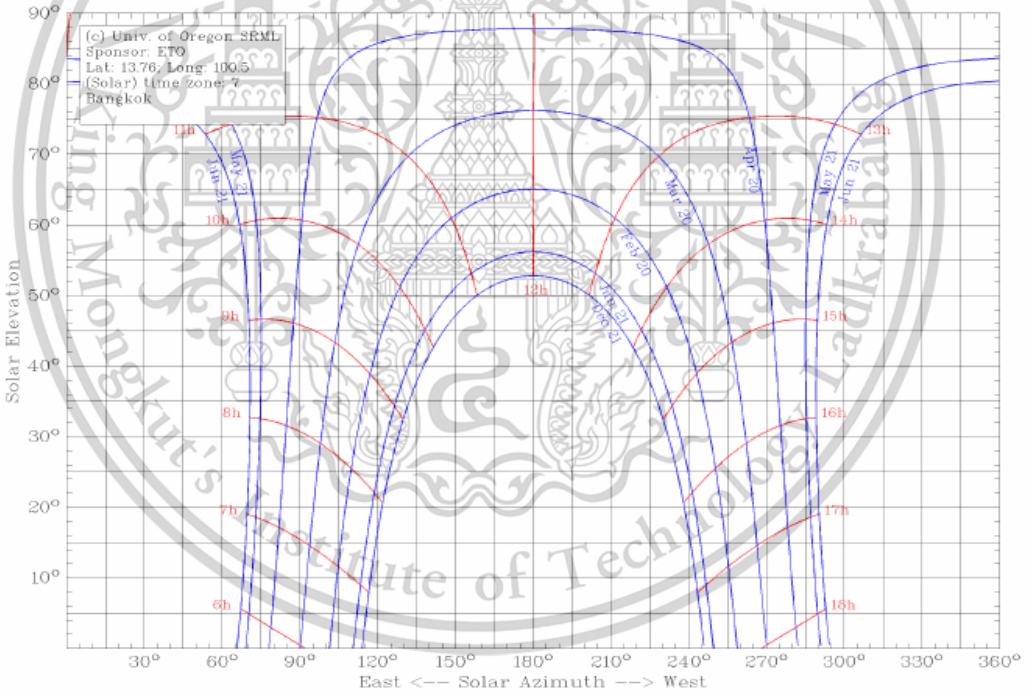

Figure 4.1 Sun path of Bangkok

Figure 4.1 shows the sun path of Bangkok. Solar sun chart program from the solar radiation monitoring laboratory of university of Oregon gives the sun path diagram of Bangkok. X-axis shows the azimuth angle which represents the sun’s position along the horizon measured in degrees from the north and provides information about the sun’s cardinal direction at any given time. The Y-axis shows the altitude angle which

represents the sun's angle above the horizon and indicates the sun's elevation at a specific time. The blue curve shows the sun path from east to west. The red curve gives the local time. The sun path is the longest on June 21 and shortest on December 21. For December 21, the altitude angle is 55 degrees and azimuth angle is 180 degrees north reference at noon.

4.1.2 Sun hour

Sun hour is important in solar energy systems because it provides a measure of the amount of solar energy available at a particular location during a specific period and is crucial for designing and optimizing solar energy systems.

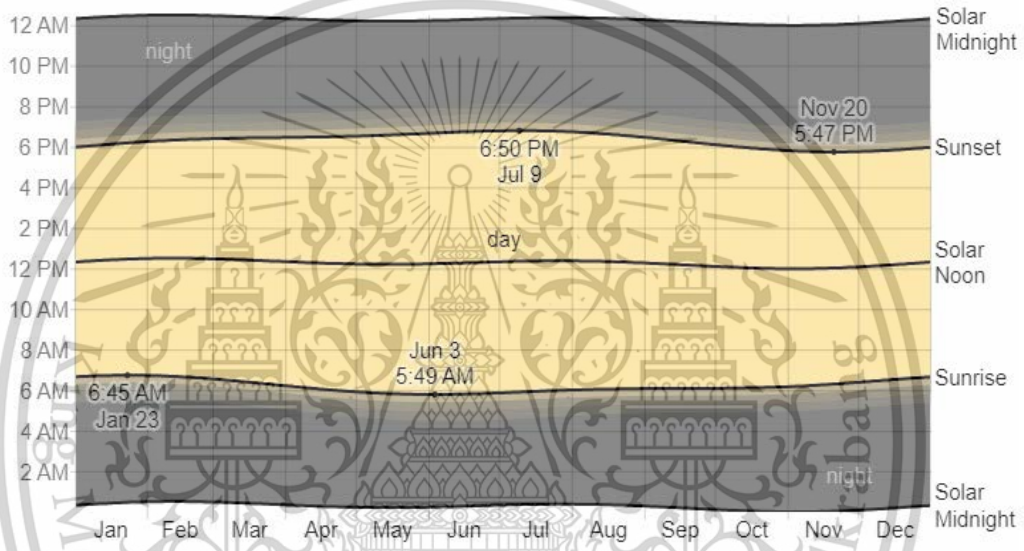

Figure 4.2 Sunrise and sunset with twilight in Bangkok

Figure 4.2 shows the position of the sun in the sky throughout the year for Bangkok. The black lines indicate the solar midnight before, sunrise, solar noon, sunset, and solar midnight after that, in that order. The bars of color that go from yellow to gray represent day, twilight, and night. In June, the sun's path is high in the sky which means that the days are long and the nights are short. In December, the sun's path is low in the sky which means that the days are short and the nights are long. After that, in June the sun rises early and sets late, and in December the sun rises late and sets early.

Table 4.1 Average daylight-saving time for Bangkok

	Jan	Feb	Mar	Apr	Jun	Jul	Aug	Sep	Oct	Nov	Dec
Hours	11.4	11.7	12.1	12.8	12.9	12.8	12.6	12.2	11.8	11.5	11.3

Table 4.1 shows the average daylight-saving time in Bangkok during 2023. Daylight hours refers to the number of hours within a day when natural sunlight is available. Solar energy system harnesses sunlight to generate electricity. The amount of energy that can be produced is directly influenced by the availability of sunlight which is affected by daylight hours. June gives the highest daylight hours of 12.9 hours. Daylight hours are the lowest of 11.3 hours in December.

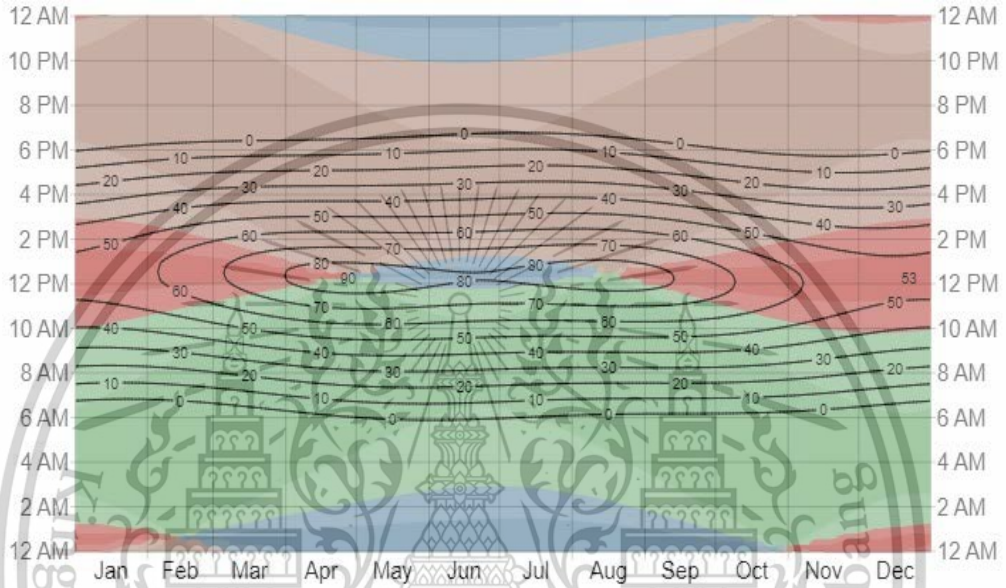

Figure 4.3 Solar elevation and Azimuth in Bangkok

The sun's elevation, or its angle above the horizon and azimuth for each hour of the day, is compactly represented in Figure 4.3. The day of the year is the horizontal axis, while the hour of the day is the vertical axis. The azimuth of the sun at a given time is indicated by the backdrop color for a specific day and hour. Constant sun elevation contours are represented by the black isolines. Lines of constant solar elevation are indicated by the black lines. The sun's azimuth is shown by the background color fills. The inferred intermediate directions (northeast, southeast, southeast, and northwest) are shown by the faintly colored regions at the borders of the cardinal compass points.

This section addresses the total daily incoming shortwave solar radiation that is absorbed by clouds and other atmospheric components, as well as seasonal fluctuations in day length, sun horizon height, and ground surface temperature. UV and visible light radiation are examples of shortwave radiation.

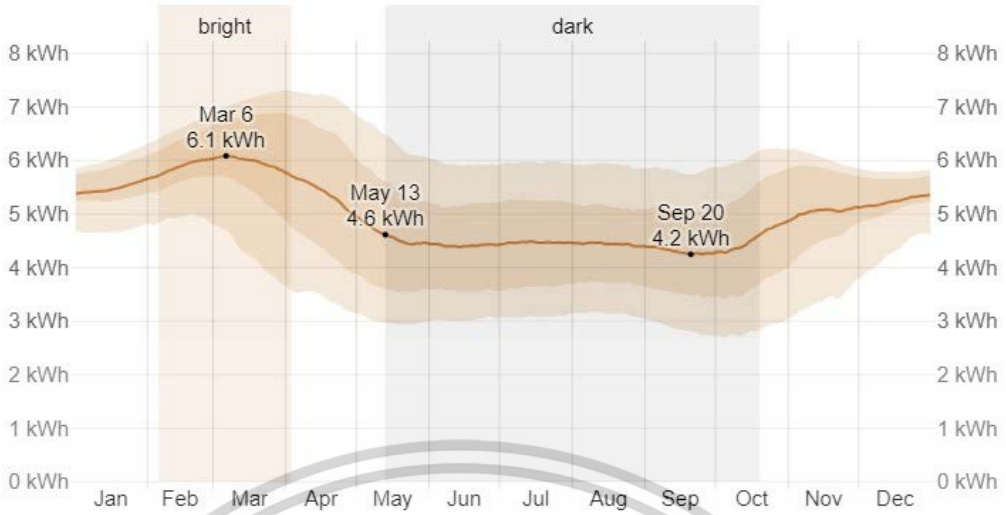

Figure 4.4 Average daily incident shortwave solar energy in Bangkok

There is some seasonal variation in the average daily incident shortwave solar energy throughout the year. From February 5 to April 3, or 1.9 months, is when the year is brightest, with an average daily incident shortwave energy per square meter of more than 5.7 kWh. With an average brightness of 6.0 kWh, March is the brightest month of the year in Bangkok. From May 13 to October 19, or 5.2 months, is the driest time of year, with an average daily incident shortwave energy per square meter of less than 4.6 kWh. September is the darkest month of the year in Bangkok, with an average of 4.3 kWh.

4.1.3 Tilt Angle

Panels are required to track the sun minute by minute because it moves during the day to provide the best results. Regretfully, because of their cost, trackers are typically more expensive for most applications than adding more panels to make up for the difference. Every day at solar noon, when the sun is at its zenith, the angle is displayed by the solar angle calculator. The sun's irradiance reaches its maximum and its power output peaks during solar noon. At solar noon, the sun is due south in the northern hemisphere. As a result, in order to maximize the performance of photovoltaic panels, they should normally be oriented with their faces facing straight south at the ideal angle to allow for the maximum amount of sunshine exposure during this period.

To get the most out of the photovoltaic system, the right angle is crucial. The solar panels are slanted in accordance with the height of the sun in the sky to achieve

optimal performance throughout the summer. The solar panels are tilted toward the winter to maximize their performance during that season in order to boost winter performance.

Table 4.2 gives the optimum tilt of solar panels by month for Bangkok.

Table 4.2 Optimum tilt of solar panels by month for Bangkok

Month	Degree	Month	Degree
January	60	July	92
February	68	August	84
March	76	September	76
April	84	October	68
May	92	November	60
June	100	December	52

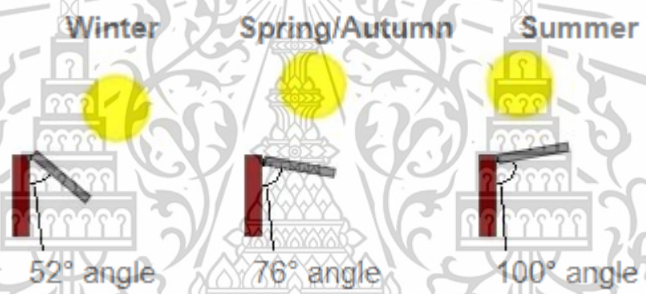

Figure 4.5 Optimum tilt angle from vertical for Bangkok

Figure 4.5 gives the optimal tilt angle of the solar panel from vertical for Bangkok from the solar electricity handbook of 2019 edition. The optimal tilt angle to angle the solar module is as the latitude angle for year-round. Therefore 13.76 degrees is the optimal tilt angle for Bangkok.

4.2 Characteristics of Solar Panel

The I-V and P-V characteristics of the PV module are used in this work under the irradiance of 1000 W/m^2 at 25°C as the following figure.

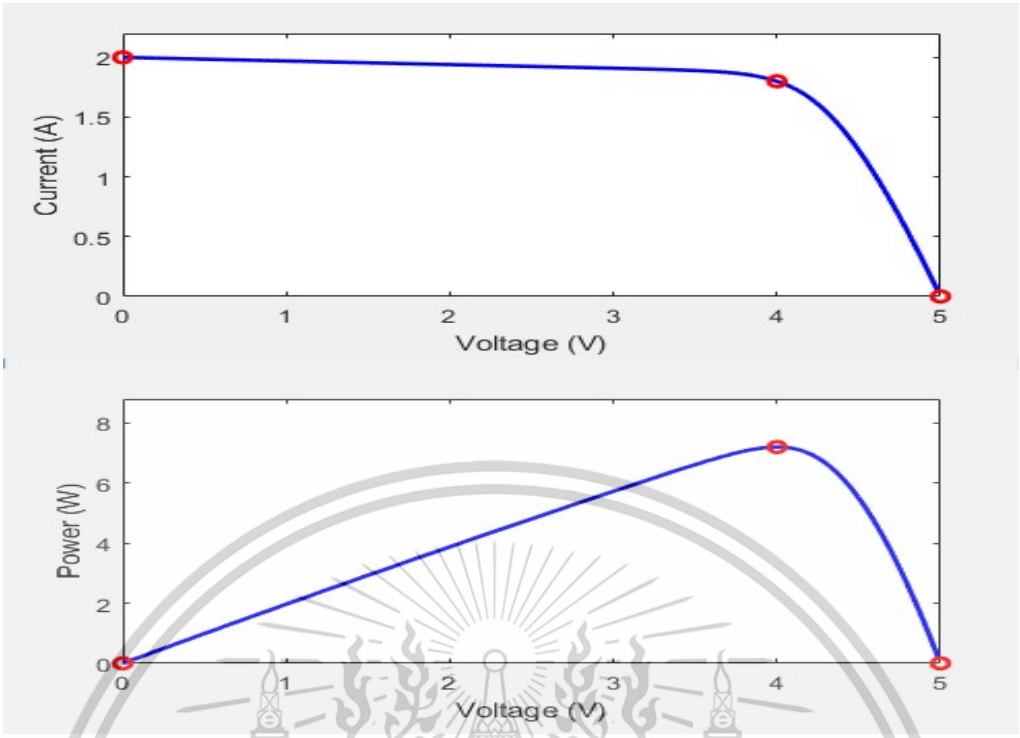

Figure 4.6 I-V and P-V characteristics of PV module at 25°C

Figure 4.6 gives the voltage-current and voltage-power characteristics of a photovoltaic panel. The voltage-current characteristic shows the relationship between the voltage produced by the solar panel and the current that flows through it. At short-circuit point, the voltage across the terminals is 0 V which is short-circuited, and the current is at its maximum 2 A. This short-circuit current (I_{sc}) increases with the irradiance. More sunlight means more protons striking the solar cells leading to higher current. At open-circuit point, the current is 0 A which is open-circuited, and the voltage is at its maximum 5 V. At the maximum power point (MPP), the product of the current 1.8 A and the voltage 4 V is maximum and indicates the highest power output 7.2 W of the solar panel that can deliver. Beyond the MPP, the I-V curve enters the saturation region where further increases in voltage lead to a diminishing return in terms of power output. As the voltage increases, the internal resistance limits the flow of current causing a decrease in power output.

The power-voltage characteristics show the relationship between the power output of the PV panel and the voltage at which it operates. As the voltage increases, the power output initially increases rapidly. This positive correction reflects the direct proportionality between voltage and power in the early stage of the P-V curve. The P-V curve reaches its maximum point at MPP where the product of voltage 4 V and

current 1.8 A is maximum resulting in the highest power output 7.2 W. Beyond the MPP, as the voltage continues to increase, power output starts to decrease. This decrease is primarily due to the impact of the panel's internal resistance. At higher voltages, the internal resistance impedes the flow of current leading to a reduction in power output despite an increase in voltage.

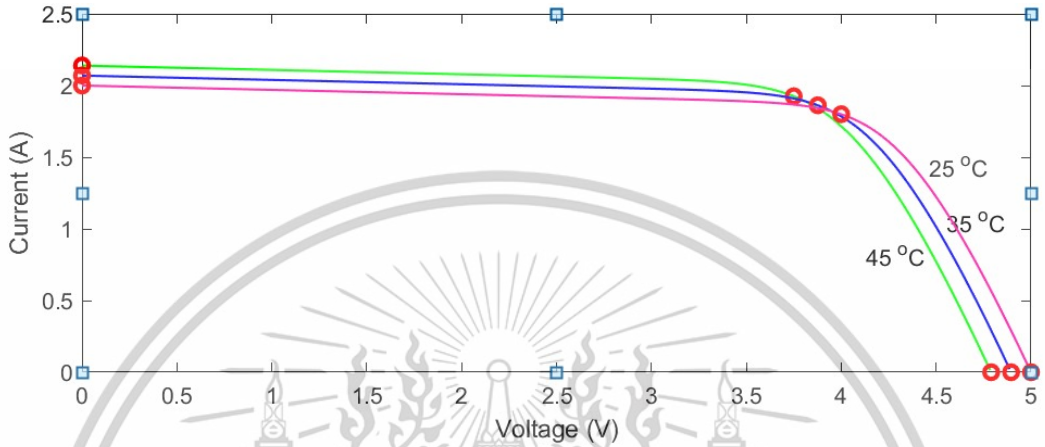

Figure 4.7 I-V characteristics of PV module with temperature change

Figure 4.7 shows the current and voltage curves of a solar panel at different temperatures; 25°C, 35°C, and 45°C at a constant irradiance level of 1000 W/m^2. The curves all share a similar overall profile. Typically, an increase in temperature can lead to a decrease in open-circuit voltage (V_{oc}) and a change in shape off the I-V curve.

The I-V curve starts at the I_{sc} which is maximum current 2 A when the voltage is zero at 25 °C. For 35 °C, I_{sc} slightly increases to 2.075 A due to the rise in temperature leading to the modest shift upward along the current axis. For 45 °C, there is a further increase in I_{sc} to 2.15 A. The increase in temperatures is due to the influence of temperature on semiconductor material used in the solar cells by generating more electron-hole pairs, enhancing mobility of charge carriers, and decreasing internal resistance.

The curve interests the voltage axis at V_{oc} representing the maximum voltage 5 V when no current is drawn. At 25 °C, this voltage is relatively higher compared to higher temperatures. With an increase in temperature to 35 °C, V_{oc} tends to decrease to 4.8 V. For 45°C, there is a further increase in V_{oc} to 4.9 V. This is because higher temperatures can impact the semiconductor material's properties, resulting in a reduction in the built-in potential and, consequently, a lower Voc.

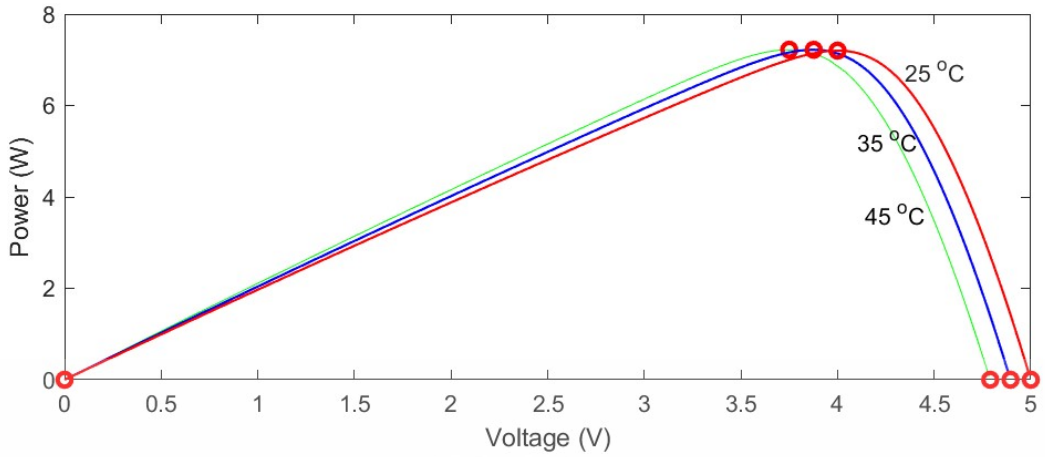

Figure 4.8 P-V characteristics of PV module with temperature change

Figure 4.8 shows the power-voltage characteristics of PV panel at different temperatures at a constant irradiance level of 1000 W/m^2. The P-V curves start from the origin (zero voltage and zero power) and ascend as voltage increases.

At temperature increases, V_{oc} is relatively higher at 25 °C. The panel operates at a higher voltage of 5 V when no current is drawn. For 35 °C, the P-V curve may shift slightly to the left due to the decrease in V_{oc} of 4.9 V. The decrease in V_{oc} results in a decrease in the maximum power point voltage from 4 V to 3.875 V. For 45 °C, the P-V curve continues to shift to the left, indicating a further decrease in V_{oc} of 4.8 V and decrease in the maximum power point voltage to 3.75 V. The I_{sc} might increase due to the rise in temperature. The decrease in V_{oc} and the potential increase in I_{sc} contribute to changes in the shape of the P-V curve, affecting the location of MPP.

4.3 Simulation Results

The simulated subsystems are presented as Figure 4.9, Figure 4.10 and Figure 4.11. The performance had been studied under nominal pressure and temperature. The bulk converter was simulated to achieve the regulation of DC power supply. The selection parameter of the DC-DC buck converter is determined by the output voltage and output current of PV. PV is designed to be output voltage of 5V and output current of 2A. The electrolyzer is designed for voltage 2V and current 1A.

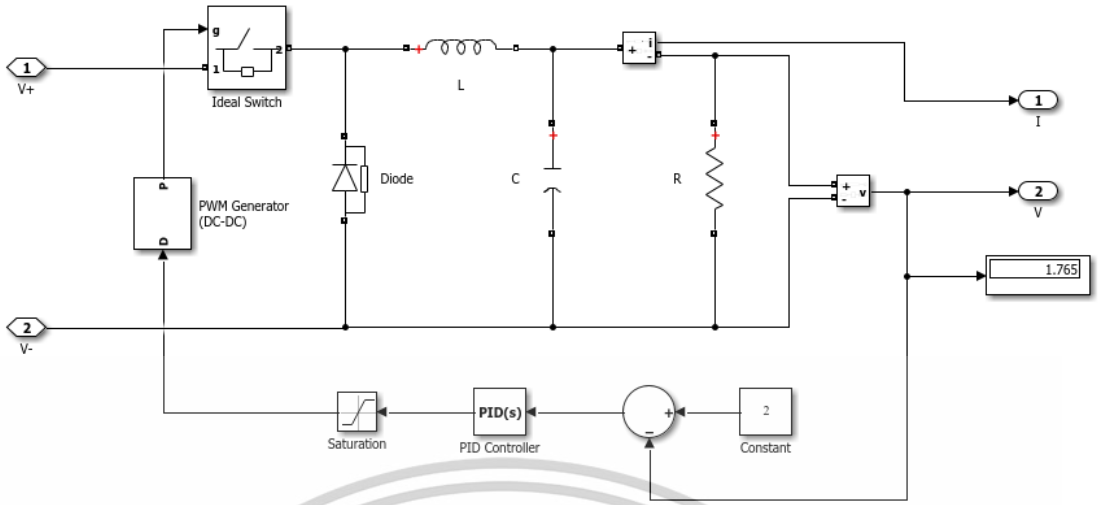

Figure 4.9 Simulation result of bulk convertor

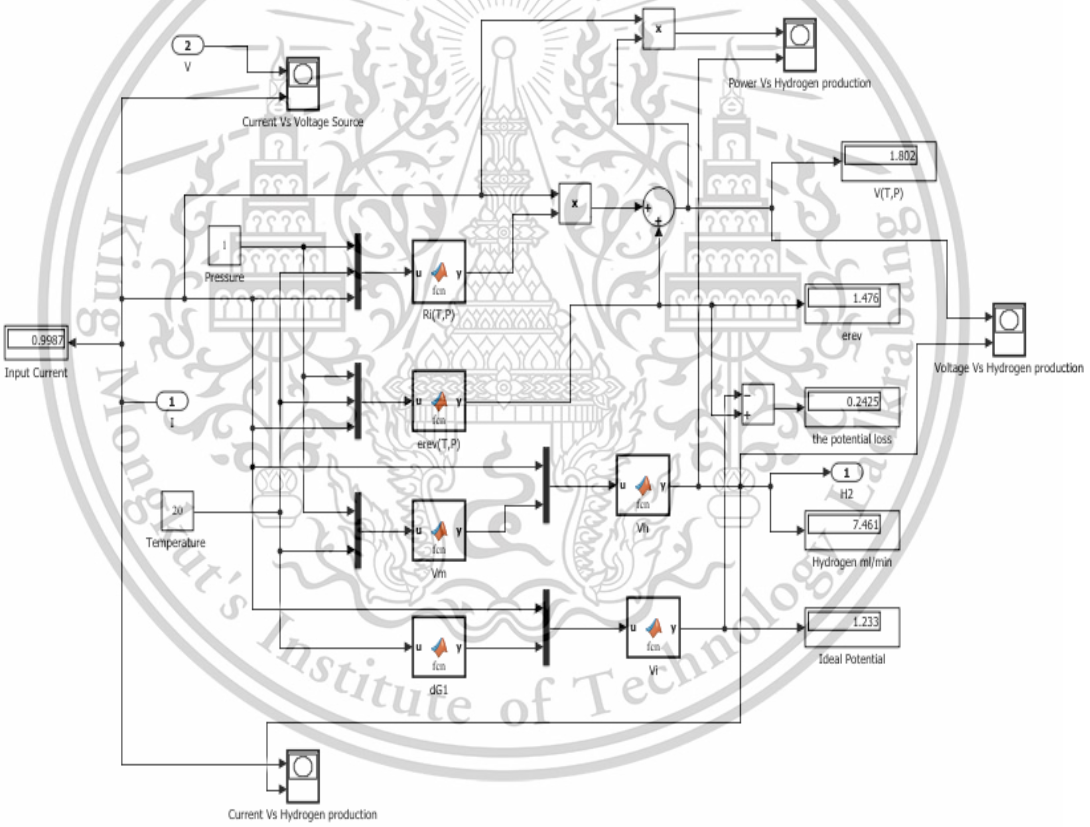

Figure 4.10 Simulation result of PEM electrolyzer

The rate of hydrogen production was achieved by simulating the electrolyzer depending on the current and power at the nominal operation conditions. Some of the equations are developed for steady state conditions. Under nominal conditions,

the value of V_i is determined to be 1.23V. The electrolyzer's resistance is 0.326 ohms and the reversible potential with regard to the ideal voltage is computed to be 1.47V.

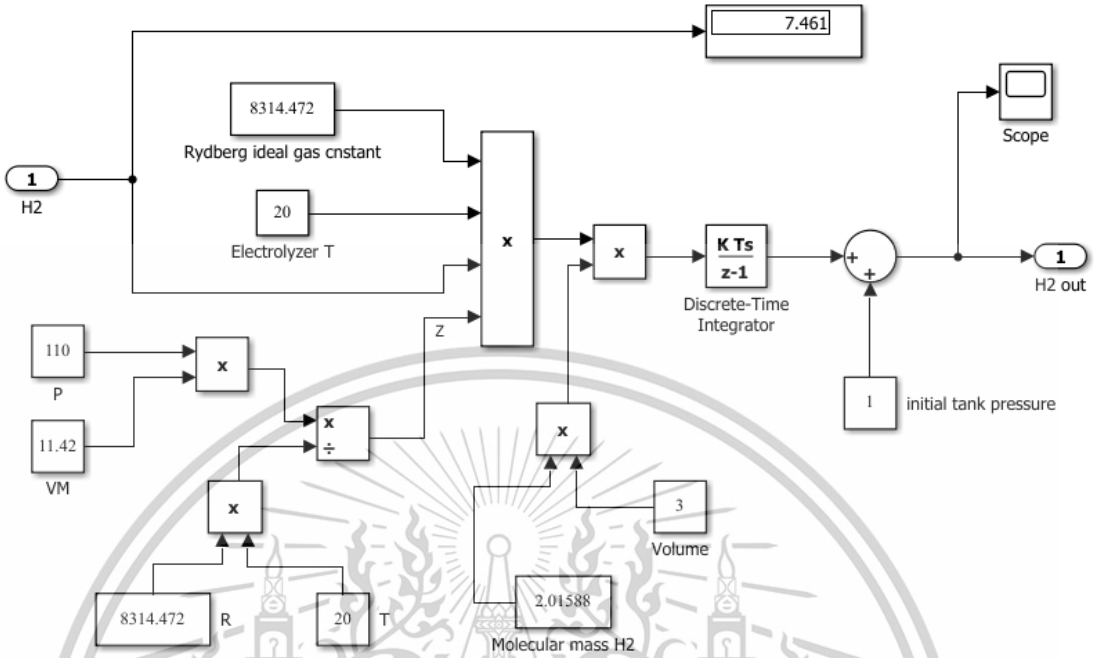

Figure 4.11 Simulation result of Hydrogen storage system

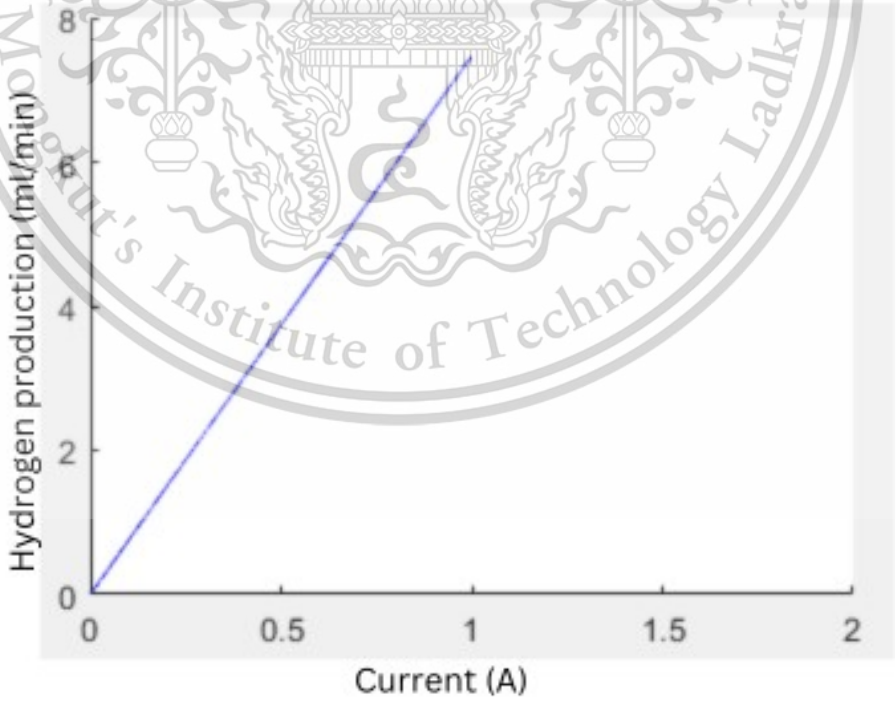

Figure 4.12 Hydrogen production rate with respect to the current flow

Figure 4.12 displays the curve that represents the hydrogen production rates for a range of input currents under nominal operating circumstances. The rate at which hydrogen is produced and the current utilized are linearly related. The amount of hydrogen obtained is 7.6 ml/min.

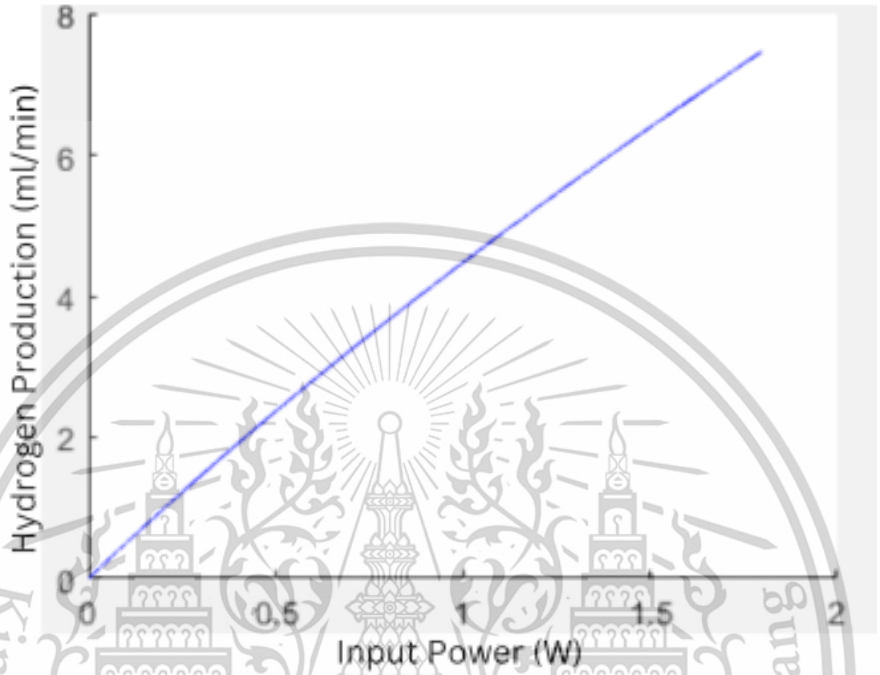

Figure 4.13 Hydrogen production rate with respect to the input power

Figure 4.13 shows the curve that represents the hydrogen generation rates for nominal operating conditions with regard to the input power. The graph indicates that the rate at which hydrogen is produced rises logarithmically with input power.

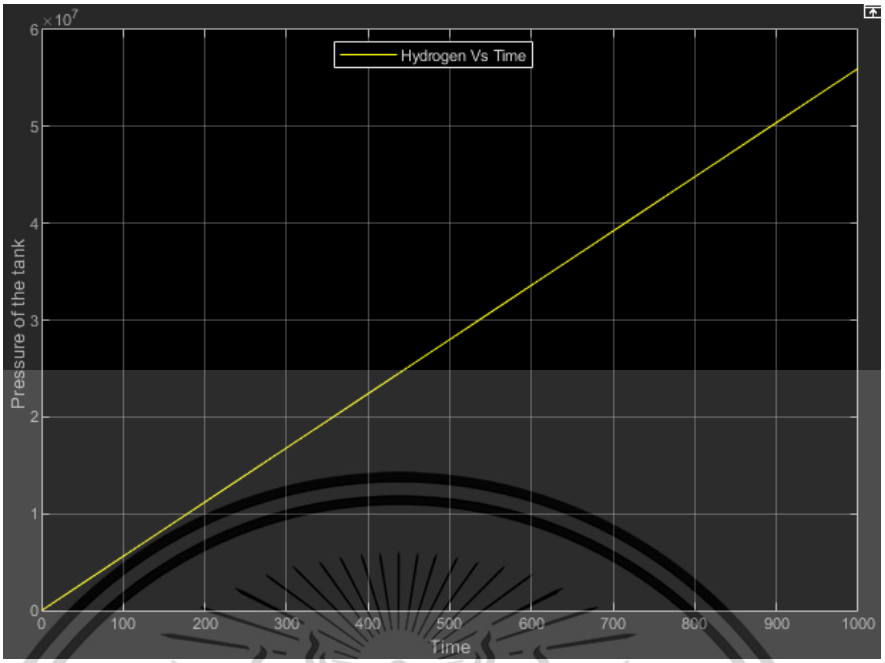

Figure 4.14 The pressure inside the hydrogen tank model

The pressure within the model hydrogen tank is shown in Figure 4.14. The amount of hydrogen is increasing with time.

4.4 Reversible potential

One important measure of the thermodynamic efficiency of the electrochemical process in PEM water electrolysis is the reversible potential. The reversible potential is the standard electrode potential and it is related to the Gibbs free energy change of the electrochemical reaction. It represents the theoretical minimum voltage required to separate water into oxygen and hydrogen at a specific temperature and pressure, based on thermodynamic principles. Temperature has a significant impact on the rates of chemical reactions. Higher temperatures generally increase the reaction rates, which can affect the reversibility of electrochemical processes.

The integrals shown in equation (*3.29*) and equation (*3.32*) are calculated for water temperature from 0˚C to 80˚C with the help of MathCAD software and molar entropy and the molar enthalpy of formation of each substance are obtained. These values are applied in equation (*3.28*) and equation (*3.31*). The results are finally substituted in the equation (*3.26*) to get the molar Gibbs free energy of formation for the temperature range of 0˚C to 80˚C. The reversible potential of the electrolyzer with the DC power supply is obtained by substituting in equation (*3.36*).

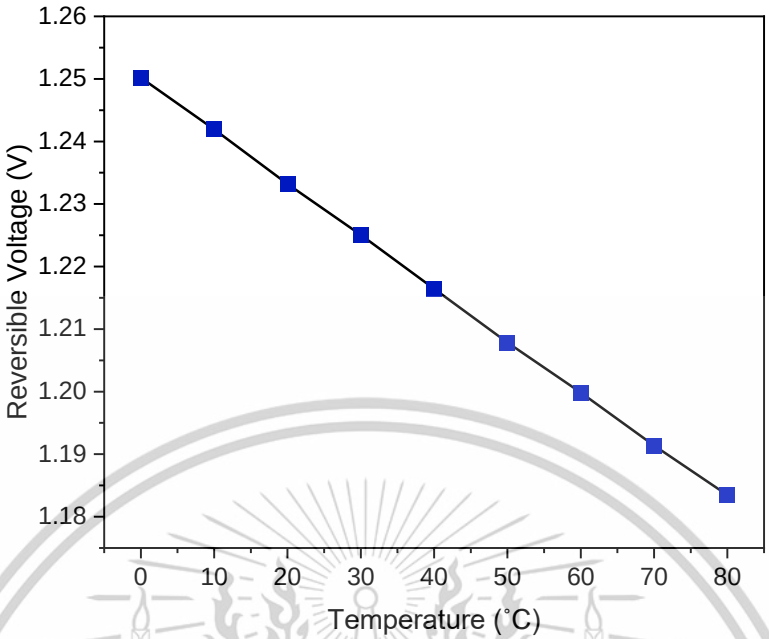

Figure 4.15 Relationship of the reversible voltage and temperature

Figure 4.15 presents the reversible potential related to the temperature which is calculated by the theory. The reversible potential is decreased from 1.25 V to 1.18 V with the temperature increasing from 0°C to 80°C. The reversible voltage is the minimum theoretical voltage required to split water into hydrogen and oxygen at a specific temperature and pressure. As temperature increases, the reversible voltage of PEM water electrolysis decreases. According to this, less electrical energy is required for each unit of hydrogen produced as temperatures rise.

4.5 Cell Voltage

The measured voltage required to drive the water splitting reaction in the real PEM electrolyzer cell. Due to heat, activation, mass transfer, and ohmic losses, the cell voltage is always larger than the reversible voltage.

4.5.1 Influence of Water Temperature

The cell voltage, which directly affects the energy efficiency of PEM water electrolysis, is largely dependent on the temperature of the water. As the reversible voltage decreases with increasing temperature (more favorable thermodynamics), the cell voltage also tends to decrease, but less significantly due to the counteracting effect of increased ohmic and other losses.

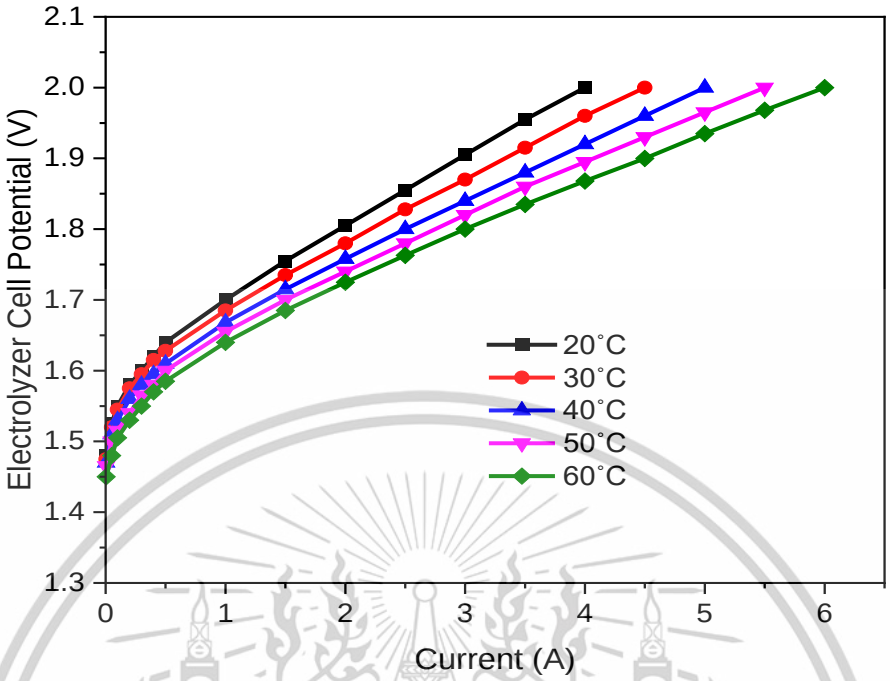

Figure 4.16 Influence of water temperature on the cell voltage

The effect of water temperature on the PEM electrolysis performance is experimentally investigated. Figure 4.16 shows the cell voltage changing with temperature from 20°C and 60°C. The maximum electrical current input value is approximately 5 A. With the use of room temperature water, current 0 A to 4 A is achieved before the cell voltage reaches 2 V. With the higher water temperature, current input 0 A to 5 A is achieved before the cell voltage reaches 2 V. The effect of temperature can be more visible at higher currents.

At higher temperatures, the entropy of the system increases, making the water splitting reaction more favorable and requiring less energy input. And increased temperatures improve the activation energy of the reactions, speeding up the process and reducing the overpotential. While higher temperatures decrease the reversible voltage, other factors must be considered. Higher temperatures can also increase the resistance of the electrolyte membrane, leading to ohmic losses that counteract the gain from a lower reversible voltage. Excessive temperatures can accelerate the degradation of electrodes and other components, reducing lifespan and increasing maintenance costs.

There is an optimal temperature range where the balance between reduced reversible voltage and increased losses is favorable. This range typically lies

between 60°C and 80°C for PEM electrolysis. Beyond the optimal temperature range, losses dominate and the cell voltage starts to increase with temperature.

4.5.2 Influence of Water Flow Rate

The effect of flow rate of water flow on the operating cell voltage is investigated with the water flow rate from 20 ml/min to 60 ml/min. Figure 4.17 shows the influence of water flow rate on cell voltage. With the water flow rate 20 ml/min, operating voltage is 1.93V and the voltage is 2V with the water flow rate 60 ml/min.

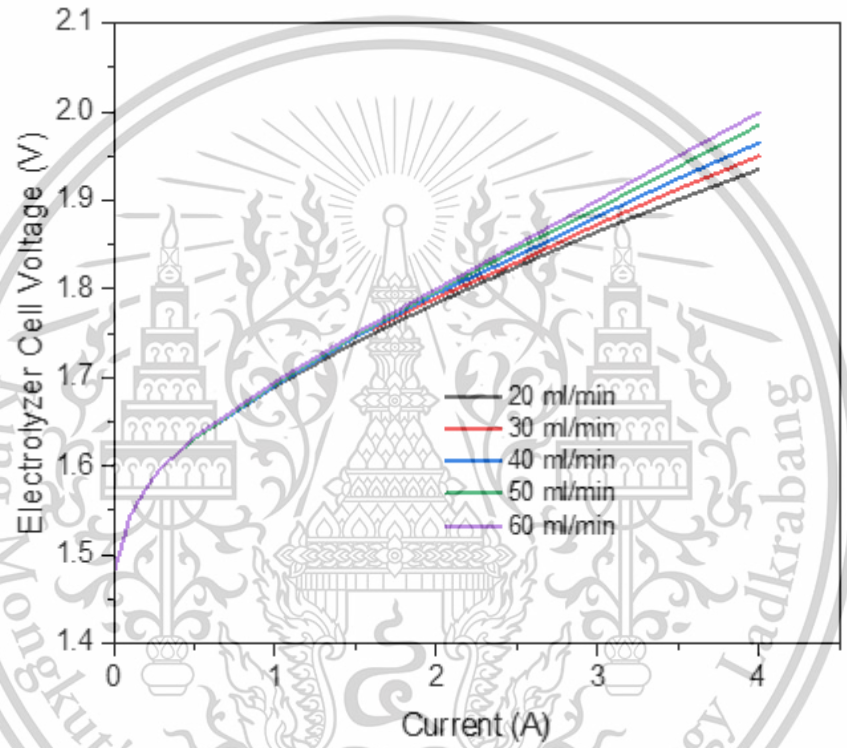

Figure 4.17 Influence of water flow rate on the cell voltage

In PEM water electrolysis, the effect of water flow rate on the actual cell voltage is complicated and depends on a number of variables. Optimizing water flow rate is crucial for efficient PEM water electrolysis operation and minimizing cell voltage. Adequate water flow ensures sufficient reactant supply to the electrodes, preventing mass transport limitations that would increase voltage. Increased flow rates lead to higher pressure drops across the membrane and flow channels, contributing slightly to ohmic losses and raising the cell voltage. Excessive water flow can cause flooding of the gas diffusion layers, hindering oxygen and hydrogen removal and increasing cell voltage. Generally, within a reasonable range, increasing water flow

rate tends to positively influence the cell voltage by preventing mass transport limitations and Improving heat removal, especially at higher current densities.

An optimal water flow rate exists that balances the benefits of sufficient reactant supply and heat removal with the drawbacks of pressure drop and flooding. This optimal rate depends on current density and temperature. Higher current densities require more water for reactant supply and heat removal. At higher temperatures, more water is needed for heat management.

4.6 Hydrogen Flow

Figure 4.18 shows experimental and theoretical hydrogen generation flow within the DC current range of 0.75 A to 4.5 A for the optimal temperature. For room temperature water, the experimental and theoretical hydrogen generation rate are quite similar. Theoretical and actual hydrogen flows are found to closely align over most of the range. The average error percentage is 5% and the maximum error percentage detected at 2.5 A is 7%, suggesting a good agreement between the results of the experiments and theoretical expectations. Furthermore, the experimental results clearly show the expected linear link between hydrogen flow and current.

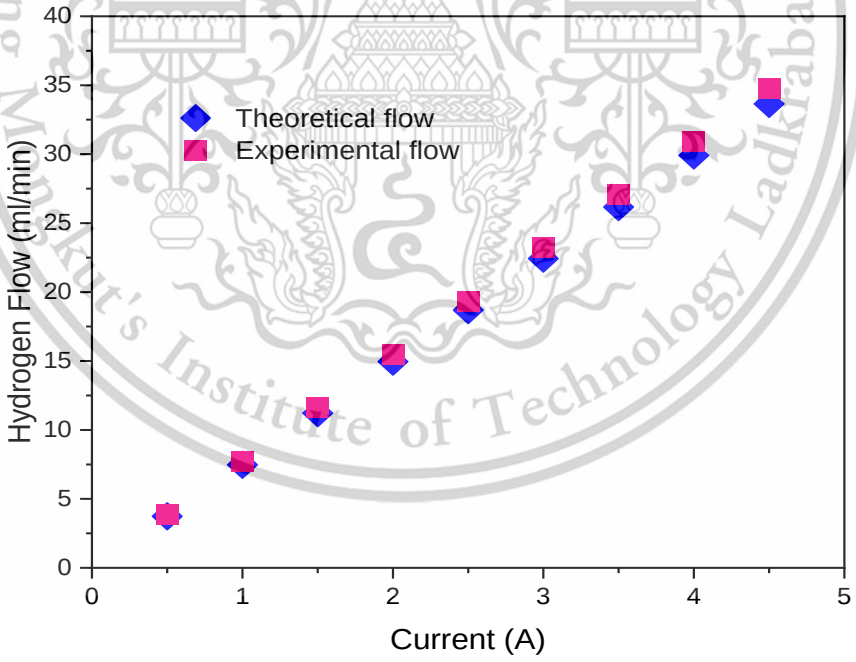

Figure 4.18 Experimental and theoretical hydrogen flow at optimal temperature

Temperature plays a significant role in hydrogen generation through PEM water electrolysis. The relationship between the amount of material generated during electrolysis and the amount of electric charge passed through the electrolyte is governed by Faraday's law. Therefore, the current flowing through the electrolyzer directly relates to the amount of hydrogen produced. Table 4.3 shows the theoretical hydrogen generated with change in temperature from 20°C and 60°C for the current from 1 A to 4 A.

Table 4.3 Theoretical hydrogen production rate

	Hydrogen production rate (ml/min)				
Current (A)	20°C	30°C	40°C	50°C	60°C
1	7.2	7.5	7.7	8.3	8.5
1.5	10.8	11.2	11.6	12.4	12.8
2	14.5	15	15.5	16.5	17
2.5	18.1	18.7	19.4	20.6	21.3
3	21.7	22.4	23.2	24.7	25.5
3.5	25.3	26.2	27	29	30
4	28.9	30	31	33	34

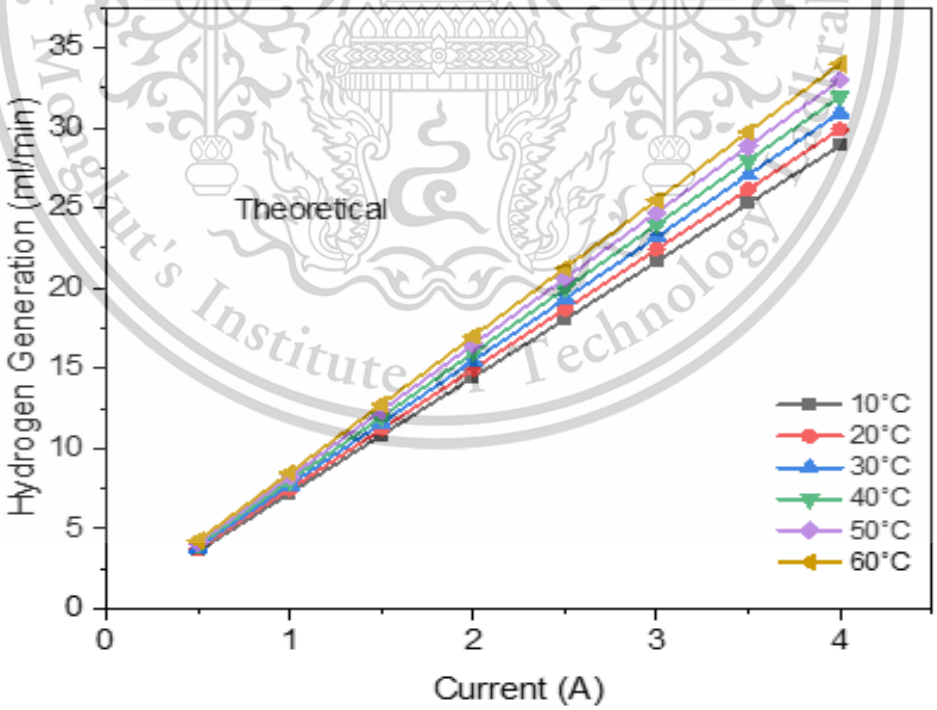

Figure 4.19 Theoretical hydrogen generation with temperature changes

Figure 4.19 shows the theoretical hydrogen generation rate with the effect of water temperature. The theoretical calculation is investigated for the temperature from 20°C to 60°C. There is a direct and linear relationship between current and hydrogen generation rate. This is due to the fact that the quantity of hydrogen generated is directly correlated with the amount of power that flows through the cell, according to Faraday's Law of Electrolysis. In other words, for every 2 moles of electrons transferred (2 Faraday constants), 1 mole of hydrogen is produced. This translates to a linear increase in hydrogen generation rate with increasing current.

Table 4.4 Experimental hydrogen production rate

	Hydrogen production rate (ml/min)				
Current (A)	20°C	30°C	40°C	50°C	60°C
1	7.8	8	8.5	8.7	9
1.5	11.5	12	12.6	13	13.4
2	15.5	16	16.8	17.3	18.1
2.5	19.3	20.2	21.1	21.9	22.7
3	22.9	24	25	26	26.8
3.5	27	28	29	30.3	31.3
4	31	32	33	34.5	35.6

The water displacement method is used to measure the amount of hydrogen. The storage 80 from h-tec education is used for hydrogen storage. Up to 80 milliliters of hydrogen and oxygen can be stored in the Storage 80 gas storage tank. Water from Storage 80 is transferred to the top tank by hydrogen created when the lower tank is filled with distilled water. Table 4.4 shows the experimental hydrogen generated with change in temperature from 20°C and 60°C for the current from 1 A to 4 A.

Figure 4.20 shows the experimental hydrogen generation rate with the effect of water temperature. For the same current, the higher temperatures lead to higher hydrogen generation rates. This is because increased temperature increases the reaction rate of the water splitting process, allowing more hydrogen to be produced at a given time.

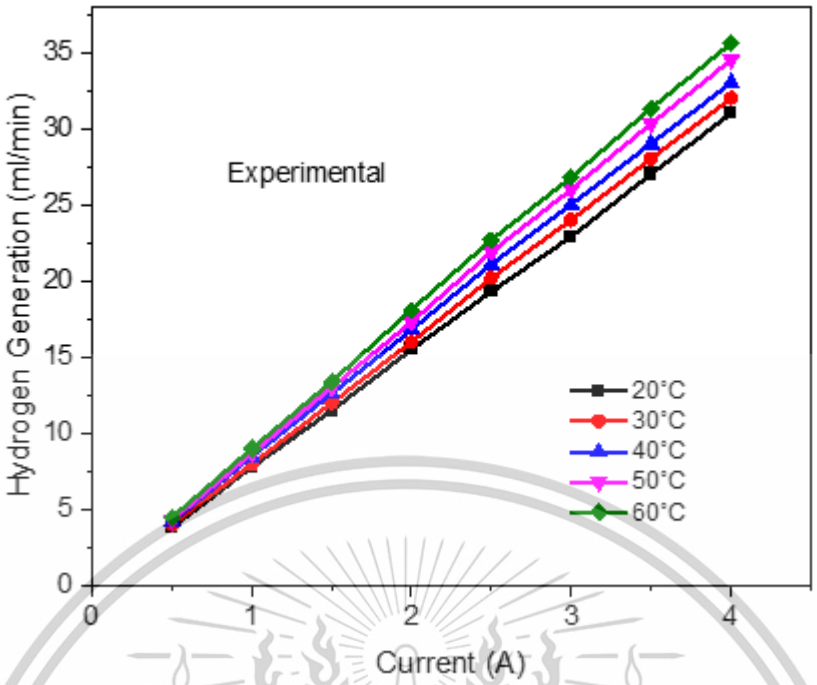

Figure 4.20 Experimental hydrogen generation with temperature changes

A higher current causes a higher rate of hydrogen creation. In general, higher temperatures increase the rate at which hydrogen is generated but this effect has a favorable condition around 50°C - 60°C. The optimal range for PEM water electrolysis is 50°C - 60°C and exceeding the optimal range can degrade the membrane and catalysts, reducing H2 production over time. The specific details of the relationship between these variables can vary depending on the specific PEM electrolyzer system, membrane type, catalyst materials, and operating conditions.

4.7 Efficiency

The enthalpy of formation, also known as calorific value, represents the energy released when a fuel is burned. When water is in steam form, the enthalpy of formation is -241.83 KJ.mole^{-1} at 25 °C and 1 atm and it is referred to as the lower heating value (LHV). It is referred to as LHV when water is included into the reaction in the form of steam. When the water is the liquid form, the enthalpy of formation is -285.84 KJ.mole^{-1} at 25 °C and 1 atm and it is known as the higher heating value (HHV). When the water is involved in the reaction as liquid form, it is called HHV. If the electrolyzer receives all of the electrical energy it needs to produce hydrogen, the reversible potential is calculated as the equation (*3.40*) and the value is 1.25 V for LHV.

During the process of water splitting, there is a generation of entropy. Therefore, it is more appropriate to use enthalpy rather than Gibbs free energy for the calculation

of potential. Thus the enthalpy voltage, which is the lowest energy required for water electrolysis, is connected to the reaction's enthalpy change. The enthalpy voltage is calculated as the equation (*3.41*) and the value is 1.48 V for HHV.

Therefore It makes sense to use the ratio of the enthalpy voltage to compute the voltage efficiency and the actual voltage of the electrolyzer as the equation (*4.1*).

$$\eta_{Voltage} = \frac{1.48}{V_{actual}} \times 100\ \% \tag{4.1}$$

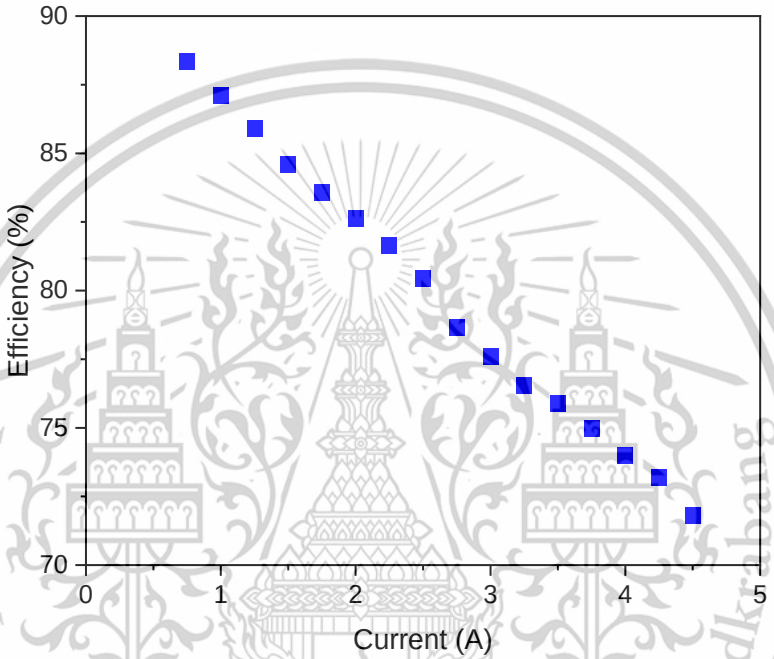

Figure 4.21 Experimental voltage efficiency

Figure 4.21 shows the experimental voltage efficiency calculated by using equation (4.1). At the electrolyzer terminals, the voltage is actually measured. At the electrolyzer terminals, the voltage is actually measured. In the experiment, the actual voltage is measured directly by the programmable power supply. There is a non-linear relationship between current and efficiency. At low current densities, increasing the current leads to a higher efficiency as more hydrogen is produced per unit of energy input. However, for higher current, the efficiency starts to decrease due to several factors.

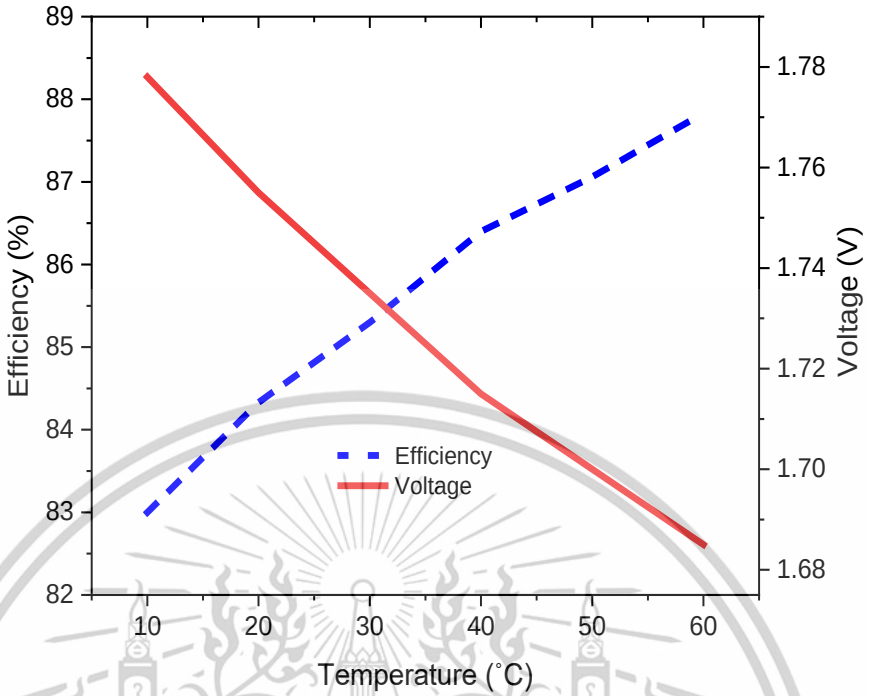

Figure 4.22 Effect of temperature on voltage and efficiency

Figure 4.22 shows the measured efficiency with the effect of water temperature. Efficiency is increased with the temperature increasing because temperatures over a certain point promote electrochemical reactions. The efficiency is measured as 84% at 20˚C and it increases to 88% at 60˚C at 1.5 A. Efficiency can be calculated at any current and the efficiency increases with the higher current densities. Higher temperature typically speed up the water splitting reactions, requiring less voltage to achieve the same hydrogen production rate, leading to initially higher efficiency. Warmer electrolyte generally exhibits lower resistivity, offering less resistance to current flow, potentially requiring slightly lower voltage. Optimizing the operating temperature can enhance the energy efficiency of PEM water electrolysis by minimizing the total energy input required per unit of hydrogen produced. Beyond the optimal temperature range, efficiency starts to decrease due to degradation and mass transportation limitations. Voltage itself does not directly measure efficiency. It represents the electrical energy input per unit charge, not the conversion to hydrogen.

CHAPTER 5
CONCLUSION

The aim of this study was to investigate the nature of hydrogen, electrochemical fundamentals, and intermittent nature of solar energy for hydrogen production. Understanding the properties and behavior of hydrogen at a fundamental level is crucial for harnessing its potential as a clean energy carrier. The exploration of electrochemical principles has provided a foundation for developing efficient and sustainable methods for hydrogen generation, particularly through technologies like water electrolysis. Water electrolysis stands out as a promising method for hydrogen production, offering a sustainable and environmentally friendly approach.

PEM water electrolysis offers distinct advantages, including high efficiency, rapid response times, and flexibility in operation. Its ability to operate at low temperatures and pressures not only enhances safety but also contributes to overall energy efficiency. The deployment of PEM technology aligns with the growing demand for cleaner and more efficient hydrogen production methods. This thesis was conducted with the performance analysis of hydrogen production system through the Polymer Electrolyte Membrane (PEM) water electrolysis system.

Initially, sun path, solar our and tilt angle were employed to determine the solar panel positioning. The analysis indicated that the solar panel would be typically faced due south to get the best performance. The optimal tilt angle to angle the solar module is as the latitude angle for year-round. Therefore 13.76 degrees is the optimal tilt angle for Bangkok. The efficiency and output of solar panels are influenced by various factors, including irradiance levels, temperature, and inherent design features. The dependence on irradiance, particularly at the standard 1000 W/m² level, underscores the importance of considering real-world conditions for accurate assessments. Furthermore, the impact of temperature on solar panel efficiency is a key consideration, with elevated temperatures potentially leading to decreased performance.

The renewable energy system for producing and storing hydrogen has been developed in MALTB/Simulink environment. The utilization of PV solar panels was investigated to capture sunlight whenever available. The generated power from the PV panels is consumed by an electrolyzer, with a DC/DC buck converter employed in the system to control and preserve the current levels that the electrolyzer receives. The error value which is the difference between the desired set point and the measured variable voltage, is monitored by a PID controller. It was considered that all the components of the system to be steady state. The results obtained from the

simulation are nearly close to the experimental results. MATLAB/Simulink supports the simulation environment assisting to integrate the solar driven hydrogen production system.

The modelling of a rebuildable PEM electrolyzer was presented in this work. The reversible potential relating to the temperature and the influences of water temperature and water flow rate on the cell voltage, hydrogen generation rate with the water temperature and efficiency were investigated. The reversible potential plays an important part in determining the overall efficiency and performance of the system. The reversible potential decreases when the temperature increases. Impact of reactant and product pressure also influences the reversible potential of water electrolysis. When the pressure increases, the reversible voltage will increase. The electrolysis operates at the standard temperature and pressure so the effect of pressure is neglected in this experimental work. And the concentration changes can influence the ionic conductivity and affect both the reversible voltage and ohmic losses.

The performance of the electrolyzer is enhanced with the higher operating temperature and it is visible that the voltage is not seriously affected by temperature at lower currents. The temperature of the huge electrolyzer will rise uncontrollably if the water flow rate is too low. The water flow is not an important point to the cell voltage in this experiment. The amount of hydrogen generated is increased with the water temperature increasing. Any current density can be used to compute efficiency, and higher current densities result in higher efficiency. While cell voltage decreases at higher temperatures, efficiency increases.

As for the future works, the development of simulation of more efficient and cost-effective solar photovoltaic system will be investigated to enhance the overall energy efficiency of solar cells.

REFERENCES

[1] “https://www.epa.gov/transportation-air-pollution-and-climate-change/history-reducing-air-pollution-transportation”.

[2] “https://vinfastauto.com/vn_en/benefits-and-barriers-to-full-implementation-of-electric-buses.”

[3] “https://www.transportation.gov/utc/transportation-air-pollution-and-public-health-are-we-doing-right-thing-and-doing-it-right.”

[4] T. Kerekes, E. Koutroulis, D. Séra, R. Teodorescu, and M. Katsanevakis, “An optimization method for designing large PV Plants,” *IEEE J Photovolt*, vol. 3, no. 2, 2013, doi: 10.1109/JPHOTOV.2012.2230684.

[5] H. T. ARAT and M. G. SÜRER, “State of art of hydrogen usage as a fuel on aviation,” *European Mechanical Science*, vol. 2, no. 1, pp. 20–30, Dec. 2017, doi: 10.26701/ems.364286.

[6] “https://corporate.enelx.com/en/stories/2022/02/advantages-of-electric-buses.”

[7] M. L. Luna, “Hydrogen as a Potential Renewable and Secure Source for Energy Supply IoT and renewal energy efficiency View project Hydrogen for sustainability View project”, doi: 10.13140/RG.2.2.26607.38563.

[8] I. Blagojević and S. Mitić, “HYDROGEN AS A VEHICLE FUEL,” *Mobility and Vehicle Mechanics*, vol. 44, no. 2, pp. 37–49, Dec. 2018, doi: 10.24874/mvm.2018.44.02.04.

[9] M. L. Luna, “Hydrogen as a Potential Renewable and Secure Source for Energy Supply IoT and renewal energy efficiency View project Hydrogen for sustainability View project”, doi: 10.13140/RG.2.2.26607.38563.

[10] “https://www.nationalgrid.com/stories/energy-explained/hydrogen-colour-spectrum.”

[11] “https://www.britannica.com/science/hydrogen.”

[12] “https://globalenergyinfrastructure.com/articles/2021/03-march/hydrogen-data-telling-a-story/.”

[13] T. Pregger, D. Graf, W. Krewitt, C. Sattler, M. Roeb, and S. Möller, "Prospects of solar thermal hydrogen production processes," *Int J Hydrogen Energy*, vol. 34, no. 10, 2009, doi: 10.1016/j.ijhydene.2009.03.025.

[14] A. R. da Costa Labanca, "Carbon black and hydrogen production process analysis," *Int J Hydrogen Energy*, vol. 45, no. 47, 2020, doi: 10.1016/j.ijhydene.2020.03.081.

[15] D. Das and T. N. Veziroglu, "Advances in biological hydrogen production processes," *Int J Hydrogen Energy*, vol. 33, no. 21, 2008, doi: 10.1016/j.ijhydene.2008.07.098.

[16] J. D. Holladay, J. Hu, D. L. King, and Y. Wang, "An overview of hydrogen production technologies," *Catalysis Today*, vol. 139, no. 4. pp. 244–260, Jan. 30, 2009. doi: 10.1016/j.cattod.2008.08.039.

[17] P. Nikolaidis and A. Poullikkas, "A comparative overview of hydrogen production processes," *Renewable and Sustainable Energy Reviews*, vol. 67. 2017. doi: 10.1016/j.rser.2016.09.044.

[18] S. Koumi Ngoh and D. Njomo, "An overview of hydrogen gas production from solar energy," *Renewable and Sustainable Energy Reviews*, vol. 16, no. 9. 2012. doi: 10.1016/j.rser.2012.07.027.

[19] S. E. Hosseini and M. A. Wahid, "Hydrogen from solar energy, a clean energy carrier from a sustainable source of energy," *International Journal of Energy Research*, vol. 44, no. 6. 2020. doi: 10.1002/er.4930.

[20] F. Harnisch and M. C. Morejón, "Hydrogen from Water is more than a Fuel: Hydrogenations and Hydrodeoxygenations for a Biobased Economy," *Chemical Record*, vol. 21, no. 9, 2021, doi: 10.1002/tcr.202100034.

[21] H. Idriss, "Hydrogen production from water: past and present," *Current Opinion in Chemical Engineering*, vol. 29. 2020. doi: 10.1016/j.coche.2020.05.009.

[22] S. A. Grigoriev, V. N. Fateev, D. G. Bessarabov, and P. Millet, "Current status, research trends, and challenges in water electrolysis science and technology," *Int J Hydrogen Energy*, vol. 45, no. 49, 2020, doi: 10.1016/j.ijhydene.2020.03.109.

[23] S. Stucki, J. Kepler, and U. Linz, “Hydrogen Production by Water Electrolysis the position is vacant for a Full Professor in Biophysics.”

[24] M. Rashid, M. Khaloofah, A. Mesfer, H. Naseem, M. Danish, and M. K. Al Mesfer, “Hydrogen Production by Water Electrolysis: A Review of Alkaline Water Electrolysis, PEM Water Electrolysis and High Temperature Water Electrolysis Used oil treatment View project King khalid university 370 View project Hydrogen Production by Water Electrolysis: A Review of Alkaline Water Electrolysis, PEM Water Electrolysis and High Temperature Water Electrolysis,” 2015. [Online]. Available: https://www.researchgate.net/publication/273125977

[25] M. D. Merrill, “Water Electrolysis at the Thermodynamic Limit,” *Thesis*, no. January 2007, 2006.

[26] T. Smolinka, H. Bergmann, J. Garche, and M. Kusnezoff, “The history of water electrolysis from its beginnings to the present,” in *Electrochemical Power Sources: Fundamentals, Systems, and Applications Hydrogen Production by Water Electrolysis*, 2021. doi: 10.1016/B978-0-12-819424-9.00010-0.

[27] S. Shiva Kumar and H. Lim, “An overview of water electrolysis technologies for green hydrogen production,” *Energy Reports*, vol. 8. 2022. doi: 10.1016/j.egyr.2022.10.127.

[28] C. Daoudi and T. Bounahmidi, “Overview of alkaline water electrolysis modeling,” *International Journal of Hydrogen Energy*. 2023. doi: 10.1016/j.ijhydene.2023.08.345.

[29] S. Shiva Kumar and V. Himabindu, “Hydrogen production by PEM water electrolysis – A review,” *Materials Science for Energy Technologies*, vol. 2, no. 3. KeAi Communications Co., pp. 442–454, Dec. 01, 2019. doi: 10.1016/j.mset.2019.03.002.

[30] M. F. A. Kamaroddin, N. Sabli, and T. A. T. Abdullah, “Hydrogen Production by Membrane Water Splitting Technologies,” in *Advances in Hydrogen Generation Technologies*, InTech, 2018. doi: 10.5772/intechopen.76727.

[31] M. Carmo, D. L. Fritz, J. Mergel, and D. Stolten, “A comprehensive review on PEM water electrolysis,” *International Journal of Hydrogen Energy*, vol. 38, no. 12. 2013. doi: 10.1016/j.ijhydene.2013.01.151.

[32] T. Wang, X. Cao, and L. Jiao, "PEM water electrolysis for hydrogen production: fundamentals, advances, and prospects," *Carbon Neutrality*, vol. 1, no. 1. 2022. doi: 10.1007/s43979-022-00022-8.

[33] G. Min, S. Choi, and J. Hong, "A review of solid oxide steam-electrolysis cell systems: Thermodynamics and thermal integration," *Applied Energy*, vol. 328. 2022. doi: 10.1016/j.apenergy.2022.120145.

[34] A. Nechache and S. Hody, "Alternative and innovative solid oxide electrolysis cell materials: A short review," *Renewable and Sustainable Energy Reviews*, vol. 149. 2021. doi: 10.1016/j.rser.2021.111322.

[35] "https://www.mapsofworld.com/lat_long/thailand-lat-long.html."

[36] "https://greenpassivesolar.com/passive-solar/scientific-principles/movement-of-the-sun/."

[37] "https://sinovoltaics.com/learning-center/system-design/solar-panel-angle-tilt-calculation/."

[38] J. G. Speight, "Thermodynamics of water," in *Natural Water Remediation*, 2020. doi: 10.1016/b978-0-12-803810-9.00004-8.

[39] H. Wang, W. Li, T. Liu, X. Liu, and X. Hu, "Thermodynamic analysis and optimization of photovoltaic/thermal hybrid hydrogen generation system based on complementary combination of photovoltaic cells and proton exchange membrane electrolyzer," *Energy Convers Manag*, vol. 183, 2019, doi: 10.1016/j.enconman.2018.12.106.

[40] G. D. Wilcox and D. R. Gabe, "Faraday's Laws of Electrolysis," *Transactions of the IMF*, vol. 70, no. 2, 1992, doi: 10.1080/00202967.1992.11870951.

[41] H. Zhang, G. Lin, and J. Chen, "Evaluation and calculation on the efficiency of a water electrolysis system for hydrogen production," *Int J Hydrogen Energy*, vol. 35, no. 20, 2010, doi: 10.1016/j.ijhydene.2010.07.088.

[42] B. Laoun, "Thermodynamics aspect of high-pressure hydrogen production by water electrolysis," 2007.

[43] H. P. C. Buitendach, R. Gouws, C. A. Martinson, C. Minnaar, and D. Bessarabov, "Effect of a ripple current on the efficiency of a PEM electrolyser," *Results in Engineering*, vol. 10, 2021, doi: 10.1016/j.rineng.2021.100216.

APPENDIX A

CONFERENCE PARTICIPATION AND CERTIFICATE

CERTIFICATE

OF PARTICIPATION

in Automotive Aerospace and Marine Engineering Topic with title

Theoretical and Experimental Study of Hydrogen Production by PEM Water Electrolysis

presented by

M. Yusoe, J. Charoensuk, K. Hanamura and C. Saekung

The 12th TSME-International Conference on Mechanical Engineering 2022
13-16 December 2022, Phuket, Thailand

Prof. Dr. Kulachate Pianthong
Honorary Chair
President of Thai Society of Mechanical Engineers (TSME)

Asst. Prof. Dr. Atikorn Wongsatanawarid
Conference Chair
King Mongkut's University of Technology Thonburi (KMUTT)

TSME ICOME 2022
Moving Toward a New Normal with Advanced Research in Mechanical Engineering

APPENDIX B
PUBLICATION

The 12th TSME International Conference on Mechanical Engineering
13th – 16th December 2022
Phuket, Thailand

AME0009

Theoretical and Experimental Study of Hydrogen Production by PEM Water Electrolysis

Myat Yu Soe[1], Jarruwat Charoensuk[2], Katsunori Hanamura[3] and Chaiyuth Saekung[1*]

[1] Department of Automotive Engineering, School of Engineering, King Mongkut's Institute of Technology Ladkrabang, Bangkok, 10520, Thailand
[2] School of Engineering, King Mongkut's Institute of Technology Ladkrabang, Bangkok, 10520, Thailand
[3] School of Engineering, Tokyo Institute of Technology, 152-8550, Japan
[1*] National Energy and Technology Centre (ENTEC), National Science and Technology Development Agency, Pathum Thani, 12120, Thailand

* Corresponding Author: Chaiyuth.sae@entec.or.th

Abstract. This paper aims to investigate the electrochemical fundamentals of hydrogen production by Polymer Electrolyte Membrane (PEM) Water Electrolysis Method and the impact of temperature and flow rate of water feeding on the efficiency of PEM electrolysis. PEM water electrolysis is the electrochemical water splitting into hydrogen and oxygen. The electrolysis is tested by varying water temperature from 20˚C to 60˚C and flow rate of water feeding from 20 ml/min to 60 ml/min. Then, reversible potential of the electrolyzer relating to the temperature is calculated with the help of MathCAD software. The onset potential is decreased with the increase in temperature. Also, the experimental and theoretical hydrogen flow rate via the PEM electrolysis depending on the current and the experimental efficiency are analysed. The efficiency decreases for higher currents. As future work, the solar energy supply to the PEM electrolysis for hydrogen production and the solar to hydrogen efficiency can be modified.

Keywords: Hydrogen, PEM Electrolysis, Efficiency, Temperature

1. Introduction

Today worldwide energy concumption was more and more increasinng due to the growth of human population and the standards of living style. Transportation is one of the essential activities which has the effect the accelerating the economic and social adancement [1]. The main energy source for transport industry is fossil fuels which are hydrocarbon sources made from decomposing plants and animals. Huge amount of greenhouse gases and carbon dioxide are released while the fossil fuels are burned. The use of fossil fuels has caused several negative environmental impacts such as global warming and air pollution [2]. The development of renewable energy is becoming an attrative solution however renewable energies are not suitable in vehicles unlike fossil fuels.

Hydrogen can be mainly used in transport industry as an as an energy for fuel cell vehicles and will be one of the solutions for the storage of renewable energy [3]. Unlike the fossil fules, hydrogen is an energy carrier that can be produced from other energy sources. Hydrogen is one of the most abundant

elements in the universe. It does not exit alone because it easily reacts with other elements. It is the lightest gas and the fastest growing industrial gas [4].

Currently, most of hydrogen is produced from hydrocarbon resources like fossil fuels and the clean technology for hydrogen production is needed. There are many non-fossil fuel based processes like water electrolysis, photocatalysis and thermochemical cycles for hydrogen production. Among them, water electrolysis is an interesting technology for hydrogen production. Electrolyzer is an electrochemical device that converts electrical energy and water into hydrogen and oxygen which can be stored as an energy for later. This electrochemical reaction is also known as electrolysis. Water electrolysis technology can be divided with the type of electrolyte used in the water electrolysis. These are alkaline water electrolysis which is the use of liquid electrolyte, proton exchange membrane electrolysis which is the electrolysis in acidic ionomer environment and solid oxide electrolysis which is the use of solide oxide electrolyte [5-9].

The alkaline electrolysis is the most fully developed technology but it has drawbacks like electrode corrosion, low crossover gas purity, low operating current density, and low operational pressure. Solid oxide electrolyis is on the development stage in the present and it is will able to commercialize soon. PEM electrolysis has many strong points such as compact system design, high gas purity, high current density, high voltage efficiency, easy operation and rapid system response [10-12]. The growing significance of PEM electrolysis mirrors the development of fuel cells and PEM electrolysis can be operated by direct coupling to solar PV panel. A lot of studies conducted connecting electrolyzers and renewable energy sources [11,13-17]. The efficiency of hydrogen production via water electrolysis is quite low and several experimental works are developing for higher efficiency. This present work focuses on the theoretical and experimental reversible voltage, hydrogen generation and efficiency of PEM water electrolysis by changing temperature and water flow rate.

2. Experiment and Methodology

2.1. Electrolyzer setup

The electrolyzer used for experimental work is rebuildable PEM electrolyzer manufactured from the h-tec education. In this electrolyzer, membrane electrode assembly (MEA) is a core component. MEA consists of two electrodes which are cathode and anode and a solid polymer electrolyte membrane which is permeable to protons but which presents a barrier to electrons with catalyst layers applied to both sides. The catalyst loading for this MEA is 2mg/cm^3 of iridium ruthenium oxide ($IrRuO_x$) on the anode side and 0.5 mg/cm^3 of 60% platinum supported on carbon (PtC) on the cathode side. This type of membrane is aslo called catalyst coated membrane (CCM) and it is a backbone of MEA. The electrode area of the electrolyzer is the 16 cm^2 and there is two glass tube for water and gas storage. Each of the two tubes filled with de-ionized water is connected to each side of the two electrodes.

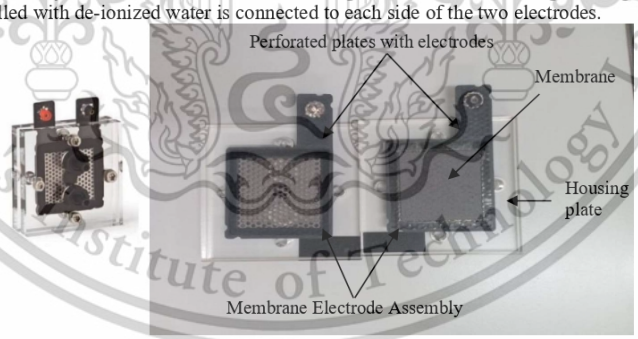

Figure 1. Electrolyzer used in the experiment.

2.2. Electrochemical fundamentals

In this work, de-ionized water is sent to the anode side. The water molecules are oxidized to oxygen gas, hydrogen positively charged ions which is called protons (H^+) and electrons (e^-) on the catalyst surface and the oxidation reaction is occurred. Then H^+ ions moves through the membrane from the anode side to the cathode side On the other hand, the electrons move to the cathode side through the external circuit. At the cathode side, electrons recombine with protons to produce hydrogen gas and the reduction reaction is occurred. The basic equation is as shown below:

$$H_2O(l) + Electrical\ energy \rightarrow H_2(g) + \frac{1}{2} O_2(g)$$

Anode reaction (oxygen evolution reaction); $H_2O(l) \rightarrow \frac{1}{2}O_2(g) + 2H^+ + 2e^-$

Cathode reaction (hydrogen evolution reaction); $2H^+ + 2e^- \rightarrow H_2(g)$

The minimum amount of the enthalpy of reaction is in the form of electrical energy and also the change in Gibbs free energy (△G) to do the extrnal work. This external work is related to the electrons flow through the external circuit. If there is no losse in electrolysis, the minimum cell voltage required to decompose water into hydrogen and oxygen to start the electrolysis is the reversible energy. Gibbs free energy is related to reversible voltage.

$$\Delta G = -nFV_{rev} \quad (1)$$

where n is number of electrons transferred (n=2), F is Faraday's constant (F=96487 C.mol^{-1}) and V_{rev} is reversible voltage [5,6].

And then, the reversible potential of an electrolyzer can be calcultaed by the following equation (2).

$$V_{rev} = -\frac{\Delta G}{2F} \quad (2)$$

△G is temperature (T) dependent and is defined with entalpy change △H and entropy change △S as the equation (3).

$$\Delta G = \Delta H - T\Delta S \quad (3)$$

The equation for standard enthalpy change is calculated with the enthalpy of formation of hydrogen (H_{H_2}), oxygen (H_{O_2}) and water (H_{H_2O}) as below:

$$\Delta H = H_{H_2} + \frac{1}{2} H_{O_2} - H_{H_2O} \quad (4)$$

The equation for standard entropy change is calculated with the molar entropy of hydrogen (S_{H_2}), oxygen (S_{O_2}) and water (S_{H_2O}) as below:

$$\Delta S = S_{H_2} + \frac{1}{2} S_{O_2} - S_{H_2O} \quad (5)$$

The enthalpy of formation and entropy changes with temperature are calculated depending on the molar heat capacity (C_p) and standard enthalpy change and atandatd entropy change as follows:

$$\Delta H_{T_r} = \Delta H_0 + \int_{298.15}^{T_r} C_p dT \quad (6)$$

$$\Delta S_{T_r} = \Delta S_0 + \int_{298.15}^{T_r} \frac{C_p}{T} dT \quad (7)$$

The values of entropy, elthalpy and molar heat capacity are obtained from thermodynamics table [18,19].

Table 1. Enthalpy and Entropy values

	H_0 (J.mol^{-1})	S_0(J.mol^{-1}.K^{-1})
H_2O (liquid)	-28.838	70.05
H_2	0	130.59
O_2	0	205.14

2.3. Hydrogen generation flow

For hydrogen generation in one mole, two numbers of electrons travel through the external circuit and total charge to pass through the circuit is as below:

$$Total\ charge = -2Fn_{H_2} \quad (8)$$

Where n_{H_2} is the total moles of hydrogen generated.

The theoretical hydrogen production rate can be calculated by Faraday's second law based on the ideal gas expression (V_M). Hydrogen generation rate can be calculated by dividing with time and taking the absolute value of the equation (8). And rearranging the equation gives the following equation (9).

$$H_2\ generation = V_M \times \frac{I}{2F} \quad (9)$$

$$V_M = \frac{R(273+T)}{P} \quad (10)$$

Where R is ideal gas constant (0.0821 $atmK^{-1}mol^{-1}$), and P is pressure (1 atm) [1].

There is no effect of temperature and pressure, the equation (10) can be calculated by muliplying by mass of hydrogen (2.02×10^{-3} $kg.mole^{-1}$) and by dividing with density (0.084 $kg.m^{-3}$) and expressed with $ml.min^{-1}$.

$$H_2\ generation = 7.477 \times I \quad (11)$$

2.4. Efficiency

The potential at which the electrolyzer operates adiabatically is the thermoneutral potential. The thermoneutral voltage is higher than the reversible voltage because it contains heat related to the change in entropy of reaction. If all the electrical energy is transformed into hydrogen, the efficiency is calculated with the reversible voltage. The reversible voltage at standard temperature is 1.23V. However, heat is produced during the electrolysis. It is more suitable to calculate with the enthalpy instead of Gibbs free energy for thermoneutral voltage. The thermoneutral voltage at standard temperature is 1.48V [1,10].

The efficiency (η) of the electrolysis is defined as the thermoneutral voltage over the operating voltage and is calculated by the equation (12):

$$\eta = = \frac{V_{TN}}{V} \quad (12)$$

Current efficiency called faradaic efficiency is an important part to determine how many electrons from the external circuit travel to the electrode surface for electrochemical reaction. Therefore, faradaic efficiency is defined as experimentally hydrogen production over theoretically calculated production rate of hydrogen as below:

$$\eta_{faraday} = \frac{Experimental\ measured\ hydrogen}{Theoretical\ calculated\ hydrogen} \quad (13)$$

3. Results and Discussion

3.1. Cell potential

The integrals shown in equation (6) and equation (7) are calculated for T_r from 0°C to 80°C with the help of MathCAD software and the reversible potential of the PEM water electrolysis system with the DC power supply is obtained by substituting the values which are found from equation (5) to equation (2). Figure 3 presents the reversible potential related to the temperature which is calculated by the theory. The reversible potential is decreased from 1.25 V to 1.18 V with the temperature increasing. The effect of pressure of reactants and products also influences on the reversible potential of water electrolysis. When the pressure increases, the revrsible voltage will be increased. The electrolysis operates at the standard temperature and pressure so the effect of pressure is neglected in this expeimental work.

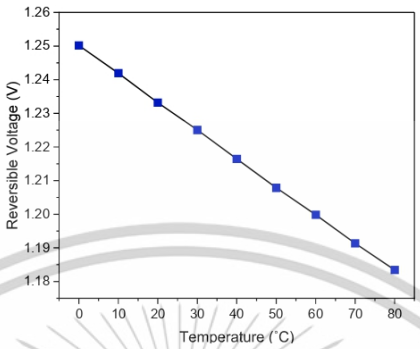

Figure 2. Relationship of the reversible voltage and the temperature.

The effect of water temperature on the PEM electrolysis performance is experimentally investigated. Figure 3(a) shows the cell voltage changing with temperature. The maximum electrical current input value is approximately 5A. With the use of room temperature water, current 0-4 A is achieved before the cell voltage reached 2V. With the higher temperature water, current input 0-5 A is achieved before the cell voltage reached 2V. The effect of temperature can be more visible at higher current.

The effect of flow rate of water flow on the operating cell voltage is investigated with the water flow rate from 20 ml/min to 60 ml/min. Figure 3(b) shows the influence of water flow rate on cell voltage. With the water flow rate 20 ml/min, operating voltage is 1.93V and the voltage is 2V with the water flow rate 60 ml/min.

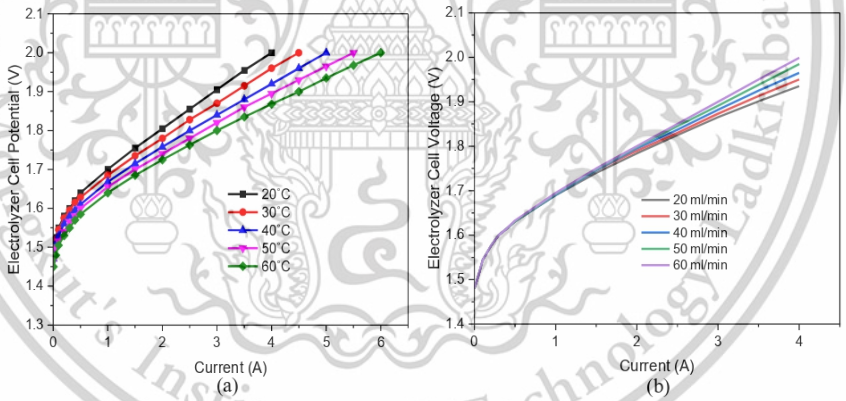

Figure 3. (a) Influence of water temperature and (b) influence of water flow rate on the cell voltage.

3.2. Hydrogen generation rate

The practical amount of hydrogen generated is measured by water displacement method. Figure 4 shows experimental and theoretical hydrogen production with the effect of water temperature. For room

temperature water, the experimental and theoretical hydrogen generation rate are quite similar. The maximum error percentage is 7 % at 2.5 A and the average error percentage is 5 %.

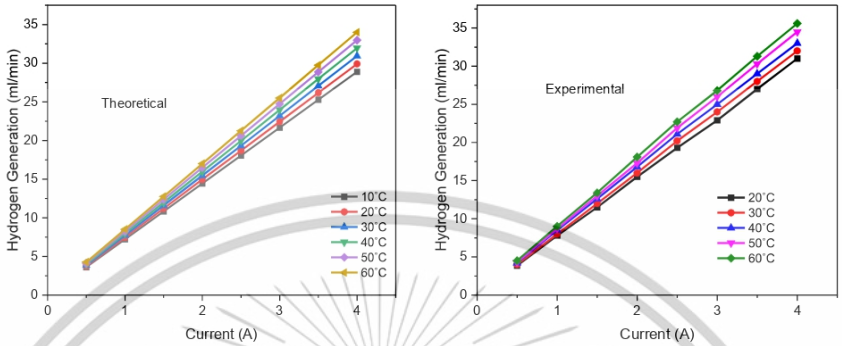

Figure 4. (a) Theoretical and (b) experimental hydrogen generation with water temperature change.

3.3. Efficiency

The voltage efficiency shown in Figure 5(a) is calculated by using equation (12). The efficiency decreases for higher currents as shown in Figure 5 because losses are increases with higher currents. The measured efficiency with the effect of water temperature is as shown in Figure 5(b). Efficiency is increased with the temperature increasing due to the enhanced electrochemical reactions at higher temperatures. The efficiency is measured as 84% at 20°C and it increases to 88% at 60°C at 1.5 A.

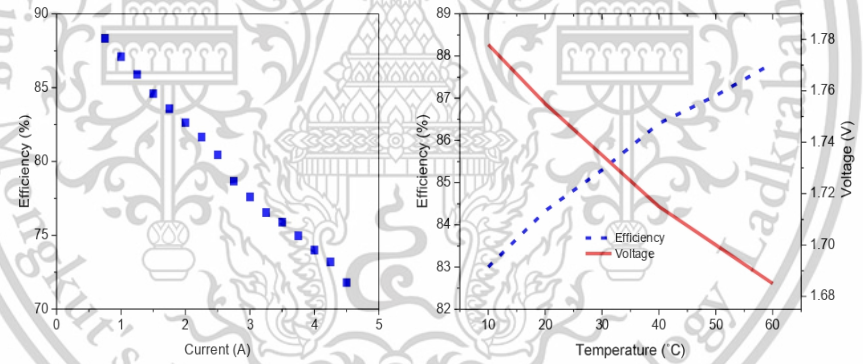

Figure 5. (a) Effect of current and (b) effect of water temperature on the voltage and efficiency.

4. Conclusion

The modelling of a rebuildable PEM electrolyzer was presented in this work. The reversible potential relating to the temperature and the influences of water temperature and water flow rate on the cell voltage, hydrogen generation rate with the water temperature and efficiency were investigated.

1) The reversible potential decreases when the temperature increases.
2) The performance of the electrolyzer is enhanced with the higher operating temperature and it is visible that the voltage is not seriously affected by temperature at lower currents.
3) If the flow rate of water is too low in large electrolyzer, the temperature of the electrolyzer will rise uncontrollably. The water flow rate is not an important point to the cell voltage in this experiment.
4) The amount of hydrogen generation is increased with the water temperature increasing.
5) Efficiency can be calculated at any current and the efficiency is increased with the higher current densities. At higher temperature, the efficiency is increased but the cell voltage is decreased.

Acknowledgments

The authors would like to thank National Science and Technology Development Agency (NSTDA) of Thailand, King Mongkut's Institute of Technology Ladkrabang (KMITL), School of Engineering, Thailand Advanced Institute of Science and Technology and Tokyo Institute of Technology (TAIST-Tokyo Tech).

References

[1] S.S. Kumar and V. Himabindu 2019 *Mater. Sci. Energy Technol.* **2** 442-454
[2] F. Martins, C. Felgueiras, M. Smitkova and N.S. Caetano 2019 *Energies* **12** 964
[3] O. Selamat, F. Becerikli, M.D. Mat and Y. Kaplan 2011 *Int. J. Hydrogen Energy* **36** 11480-11487
[4] M.G. Surer and H.T. Arat 2018 *European Mechanical Science* **2** 20-30
[5] M. Rashid, M. Mesfer, H. Naseem and M. Denish 2015 *IJEAT* ISSN:2249-8958 **4** 80-93
[6] M. Carmo, D.L. Fritz, J. Mergel and D. Stolten 2013 *Int. J. of Hydrogen Energy* **38** 4901-4934
[7] B. Yodwong, D. Guilbert, M. Phattanasak, W. Kaewmanee, M. Hinaje and G. Vitale 2020 *J. of Carbon Research MDPI* 10.3390/c6020029 hal-02569824
[8] B. Kiran and Y. Ramana 2015 *Int. J. Mech. Eng. and Computer* **3** ISSN 2320-6349
[9] B. Lee, K. Park, and H. Kim 2013 *Int. J. Electrochem. Sci.* **8** 235-248
[10] Y. Yin, X. Wang, J. Zhang, X. Shangguan and Y. Qin 2018 *Int. J. Energy Res.* 1-13
[11] N.A. Burton, R.V. Padilla, A. Rose and H. Habibullah 2021 *Renewable and Sustainable Energy* Reviews **135** 20255
[12] S.P.S. Badwal, S. Giddey and F.T. Giacchi 2006 *Ionics* **12** pp. 7-14
[13] Y.K. Sanusi, G.R. Fajinmi and E. Babatunde 2015 *The Pacific J. of Sci. and Techmol.* **12** 176-180
[14] A. Shiroudi, M.S. Deleuze and S.A. Mousavifar 2017 *Int. J. of Ambient Energy* **38** 40-249
[15] W. Pirom and A. Srisiriwat 2022 iEECON 53204.2022.9741687
[16] N. Chennouf, N. Settou, B. Negrou, K. Bouziane and D. Dokkar 2012 *Energy Procedia* **18** 1280-1288
[17] N. Naseri, S.E. Hani, A. Aghmadi, H. Mediouni, I. Aboudrar and M. Benbouzid 2019 IEEE 4549-4554
[18] P. Millet, N Mebmba, S. Gridoriev, A. Aukauloo and C. Etievant 2018 *Int. J. Ionic* **24** 3113-3121
[19] A. Tijani, A. Rahim, and M. Hisam 2015 *J. Teknologi* **75** 65-69
[20] M. Bananno, K. Muller, B. Bensmann, R. Rauschenbach, P. Peach and S. Thiele 2021 *J. of the Electrochem. Sci.* **168** 094504
[21] K.W. Harrison, E.H. Pacheco, M. Mann, and H. Salehfar 2006 *J. Fuel Cell Sci. Technol.* vol 3 p 220-223
[22] A.T. Marshall, S. Sunde, M. Tsypkin and R. Tunold 2007 *Int. J. Hydrogen Energy* **32** 2320-2324
[23] A. Tijani and A. Rahim 2016 *Int. Conf. on System-integrated Intelligence* **26** p 419-427
[24] Meng Ni, M.K.H. Leung, and D.Y.C. Leung 2008 *Energy Conver. and Management* **49** 2748-2756

AUTHOR BIOGRAPHY

NAME	Ms. Myat Yu Soe
DATE OF BIRTH	2 May, 1996

EDUCATION RECORD

BACHELOR'S DEGREE	Bachelor of Engineering (Electrical Power) Mandalay Technological University, Myanmar, 2018
MASTER'S DEGREE	Master of Engineering (Automotive and Advanced Transportation Engineering) King Mongkut's University of Technology, Ladkrabang, 2024
SCHOLARSHIP	TAIST-Tokyo Tech scholarship Master's degree in automotive and advanced Transportation Engineering 2021-2024 Founded by National Science and Technology Development Agency (NSTDA, Thailand), Tokyo Institute of Technology (Tokyo-Tech, Japan) and King Mongkut's University of Technology Ladkrabang (KMITL, Thailand)
EMPOLYMENT RECORD	Assistant Engineer Zenith Power Company Limited, Myanmar July 2018 - January 2020 Site Engineer Aerial Mandalay Construction Group, Myanmar January 2020 – July 2020

PUBLICATION

International Conference Proceeding	Myat Yu Soe, Jarruwat Charoensuk, Katsunori Hanamura and Chaiyuth Saekung "Theoretical and Experimental Study of Hydrogen Production by PEM Water Electrolysis", 12th TSME International Conference on Mechanical Engineering Proceedings, 2022.